UNIVERSITY OF CALIFORNIA SAN DIEGO

Microbiome Dynamics and Pathogen-Driven Impacts in Marine Mollusks: Insights from Oysters and White Abalone

A Dissertation submitted in partial satisfaction of the requirements
for the degree Doctor of Philosophy

in

Marine Biology

by

Emily Kunselman

Committee in charge:

Jack Gilbert, Chair
Eric Allen
Sara Jackrel
Lisa Zeigler

2024

The Dissertation of Emily Kunselman is approved, and it is acceptable in quality and form for publication on microfilm and electronically.

University of California San Diego

2024

TABLE OF CONTENTS

LIST OF FIGURES

LIST OF TABLES

ACKNOWLEDGEMENTS

Chapter 1, in full, is a reprint of the material as it appears in American Society for Microbiology, Microbiology Spectrum. Emily Kunselman, Jeremiah J. Minich, Micah Horwith, Jack A. Gilbert, Eric E. Allen. Pineridge Press, 2022. The dissertation author was the primary investigator and author of this paper. Thank you to Laura H. Spencer for providing the oyster spat used in this study. Thank you to the Ryan Kelly lab for allowing me to use their lab space for dissection of oysters and extractions. Thank you to the Washington Department of Natural Resources for supplying extraction kits. This project was supported by the US National Science Foundation grant OCE1837116 to E.E.A. and funding from the Aquatic Assessment and Monitoring Team at the Washington State Department of Natural Resources.

Chapter 2, in full, has been submitted for publication at the Applied Microbiology International Journal of Sustainable Microbiology as of April 15th, 2024. Emily Kunselman, Daysi Manrique, Colleen Burge, Sarah Allard, Zachary Daniel, Guillaume Mitta, Bruno Petton, Jack A. Gilbert. Temperature and microbe mediated impacts of the San Diego Bay ostreid herpesvirus (OsHV-1) microvariant on juvenile Pacific oysters. The dissertation author was the primary investigator and author of this paper. Thank you to the Hog Island Oyster Company for donating the oysters used in this study. Thank you to Darren de Silva at the USDA Pacific Oyster Genome Selection Project (POGS) for preparing and sending the algal cultures used in this study. Thank you to the UCSD Microbiome Core for quality library preparation and sequencing to generate the 16S rRNA amplicon data analyzed in this study. This research was funded by the American Malacological Society, Conchologists of America and the Western Society of Malacologists.

Chapter 3.1, in full, has been accepted for publication by ASM Microbial Resource Announcements. Emily Kunselman, Sarah Allard, Colleen Burge, Blythe Marshman, Alyssa Frederick, Jack Gilbert. Metagenome-assembled genome of Withering Syndrome causative agent, '*Candidatus* Xenohaliotis californiensis', from endangered white abalone (*Haliotis sorenseni*). 2024. The dissertation author was the primary researcher and author of this paper. This work was funded in part through contract P1970003 from CDFW to UC Davis, through a federal NOAA Section 6 Grant NA19NMF4720103 to CDFW. All work with white abalone was performed under the Endangered Species Act (ESA) permit for white abalone (Invertebrate Enhancement Permit 14344-2R) held by UC Davis.

Chapter 3.2 is in preparation for submission to the Animal Microbiome Journal. Emily Kunselman, Blythe Marshman, Chelsey Souza, James Moore, Colleen Burge, Sarah Allard, Jack A. Gilbert. Abalone Withering Syndrome: The cascading microbial impacts of one bacterial invader. The dissertation author was the primary researcher and author of this paper. This work was funded through contract P1970003 from CDFW to UC Davis, through a federal NOAA Section 6 Grant NA19NMF4720103 to CDFW. Thank you to the UC Davis Bodega Marine Laboratory White Abalone Captive Breeding Program and the California Department of Fish and Wildlife Shellfish Health Laboratory for providing facilities and resources to support this study. All work with white abalone was performed under the Endangered Species Act (ESA) permit for white abalone (Invertebrate Enhancement Permit 14344-2R) held by UC Davis.

I would like to acknowledge Professor Gilbert for his support as the chair of my committee and Dr. Sarah Allard for her guidance throughout my program. Their encouragement and feedback were essential, and I value the time and effort they devoted toward my success.

VITA

2019 Bachelor of Science in Marine Biology, University of California San Diego

2024 Doctor of Philosophy in Marine Biology, University of California San Diego, Scripps Institution of Oceanography

PUBLICATIONS

Kunselman E, Wiggin K, Diner RE, Gilbert JA, Allard SM. 2024. Microbial threats and sustainable solutions for molluscan aquaculture. Sustainable Microbiology, qvae002, https://doi.org/10.1093/sumbio/qvae002

ABSTRACT OF THE DISSERTATION

Microbiome Dynamics and Pathogen-Driven Impacts in Marine Mollusks: Insights from Oysters and White Abalone

by

Emily Kunselman

Doctor of Philosophy in Marine Biology

University of California San Diego, 2024

Jack Gilbert, Chair

Marine ecosystems are facing various threats, from population declines to diseases that impact their overall health. My dissertation investigates the complex interplay between microbiomes, pathogens, and environmental conditions in three distinct marine organisms: Olympia oysters (*Ostrea lurida*) in the Puget Sound, Pacific oysters (*Crassostrea gigas*) in San Diego Bay exposed to OsHV-1 SDB µvar, and white abalone (*Haliotis sorenseni*) afflicted by Abalone Withering Syndrome. The goal of combining and comparing these systems is to

elucidate the crucial role of microbiota in understanding ecosystem and host health, including microbes' response to environmental variables and their interaction with pathogens.

The first chapter focuses on the Olympia oyster, a native species in the Puget Sound that has experienced a substantial population crash. To assess the impact of eelgrass habitat and geographical location on oyster microbiomes, Olympia oysters from a single parental family were deployed at multiple sites, both within and outside eelgrass (*Zostera marina*) beds. Using 16S rRNA gene amplicon sequencing, I demonstrate that gut-associated bacteria differ significantly from the surrounding environment. Regional differences in gut microbiota are associated with the oyster survival rates at different sites after two months of field exposure. However, eelgrass habitat does not influence microbiome diversity significantly. This research highlights the importance of understanding the specific bacterial dynamics associated with oyster physiology and survival rates in the Puget Sound.

In the second chapter, I explore the OsHV-1 SDB µvar, a virus threatening oyster aquaculture globally, with a focus on its microvariant in San Diego Bay. The study investigates the influence of temperature on OsHV-1 SDB µvar infectivity. All microvariants of this virus exhibit limited replication and are unable to induce oyster mortality at lower water temperatures. Through experimental infections of hatchery-raised oysters at temperatures ranging from 15 to 24°C, I found that no oysters died at 15°C but most exposed oysters died above 18°C. The infection took hold faster at 21 and 24°C compared to 18°C. As oysters are often immunocompromised by this viral infection, I also chose to focus on the potential contribution of secondary bacterial infections to the disease. The microbiome of healthy, sick and dead oysters was compared using 16S rRNA gene amplicon sequencing to determine how the microbiome is disrupted by infection and which bacteria may be responsible for further progression of the

disease. There is a clear shift in microbiome composition and decreases in evenness following infection with OsHV-1 SDB µvar.

The third chapter centers on Abalone Withering Syndrome, characterized by the intracellular parasite Candidatus *Xenohaliotis californiensus* (Ca*Xc*) which disrupts gut morphology leading to starvation and possible death. Investigating the microbiome in endangered white abalone exposed to Ca*Xc* over an 11-month period reveals dynamic variations in the fecal microbiome and its distinctiveness from the internal tissue microbiomes. Ca*Xc* exposure notably impacts the anterior region of the digestive tract more than the distal tissues and feces, sometimes representing up to 99% relative abundance in the post esophagus samples. This comprehensive analysis incorporates qPCR to quantify pathogen loads over time and feces and in internal tissues. The pathogen is detected after 5 months of exposure and is most abundant in the post-esophagus tissue. The samples with the highest relative abundance of the pathogen were also shotgun sequenced to generate whole genome assemblies of bacteria. This led to the novel assembly of a 90% complete genome for CaXc, which is deposited in a public database. To pair these data with a more holistic understanding of the impact of this pathogen, RNA sequencing data was analyzed for differential gene expression patterns between exposed and unexposed abalone. While functional annotation and prediction was poor on the de novo assembled transcriptome, clear differences exist in gene-level response to CaXc between post esophagus and digestive gland tissue.

Introduction
OYSTER AND ABALONE MICROBIOMES: DRIVERS, DISTURBANCES AND KNOWLEDGE GAPS.

The dynamic interaction between mollusks and their microbiome remains understudied Thus far, research has demonstrated the importance of tissue type, genetics, age, diet and other external environmental variables in determining the composition and structure of the oyster microbiome. Disturbance to the microbiome is complex, with both the physical environmental variables and pathogens causing drastic shifts in the mollusk microbiome that may be equated with dysbiosis. This poses a risk to mollusks due to the potential protective and nutritional benefits of the microbiome. Presented here is review of the existing literature on oyster and abalone microbiomes to preface subsequent chapters which delve deeper into some of these topics.

Intro

Research aimed at elucidating the composition and function of the microbial communities associated with oysters is becoming more prevalent (Figure 1). Published studies cover a wide breadth of research topics, such as characterizing the impact of internal and external environmental factors on the microbiome. Some common assumptions are that the oyster microbiome consists of both resident and transient members [1–3]. Resident members include those that are possibly co-evolved with the host and distinct from the surrounding environment. Transient members exist because of the constant exposure of the oyster tissue to the surrounding seawater community. Transient bacteria are those that come and go with environmental change, meaning they may be sampled at any given time point just by chance. Many studies will try to remove transient bacteria to better understand the interaction between resident bacteria and the

host [2,3]. Some studies also refer to these resident bacteria as “core” microbiota because they are ubiquitous across oysters, even if at low relative abundance, and potentially hold functional roles [4–6]. Core or resident bacteria are most likely to be conserved across individuals. However, when disturbance occurs, the oyster microbiome can shift completely from its original state [7].

Similar tends are found between the oyster and abalone microbiomes. Although abalone are marine snails and oysters are marine bivalves, the factors that drive their microbiomes and some of the resident bacteria within them are highly conserved.

This review will focus on the common bacteria associated with oysters and abalone and how their proportional abundance is influenced by environmental and host disturbance. Some speculation regarding the potential role these bacteria play in the health of mollusks is touched on. This background information is foundational for the experiments laid out in this dissertation and the conclusions derived from those experiments. Special consideration will be given to the oyster microbiome, with comparisons to abalone to demonstrate how these patterns can be extrapolated to other mollusk species.

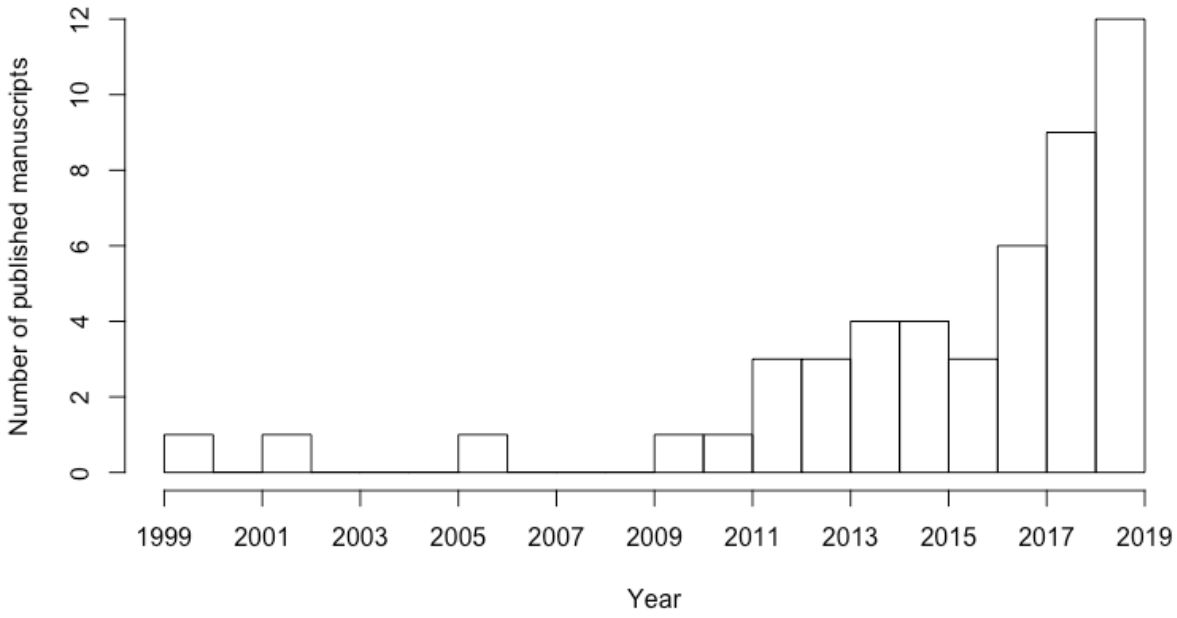

Figure 1. The number of papers published relating to the oyster microbiome each year from 1999 to 2019.

Factors that influence the composition and structure of the oyster and abalone microbiome

The mollusk microbiome is shaped by many factors. The factors that govern microbial abundance and composition are both internal and external to the oyster or abalone. Each tissue hosts its own unique microbial community, but this community is impacted by both the environment and the host's genetic background.

Tissue

Tissue is an important factor to consider in microbiome studies because the bacterial communities are adapted to each tissue's unique environment. Many studies combine the entire adult tissue homogenate for microbiome analysis, but this provides little information on host-microbial associations [8–10]. In order to better understand the relationship between a microbiome and the host, tissue specific resolution should be implemented in all studies that

hope to gain new insight on the oyster associated microbiota. The digesta, gill and hemolymph have been studied for their respective microbial communities.

The microbiome of oyster digestive tissues is difficult to analyze but demonstrates common characteristics across studies. One key component of the oyster digestive tract is its incredibly selective environment, due to digestive enzymes and low oxygen. This can lead to high [11,12] or low [13,14] richness, which is the number of unique operational taxonomic units (OTUs; often equated to species level taxonomy) found in a specific sample. While the environment of the digestive tract may limit the number of bacteria that can grow, polysaccharides in the oyster gut mucus that are not successfully removed during DNA extraction may inhibit PCR amplification and result in false estimation of gut bacterial diversity [11,15]. In many cases, there is evidence that a single bacterial taxon dominates the gut-associated community by relative abundance [15]. Mollicutes, and specifically the genus *Mycoplasma*, is often among the most prevalent taxa in the gut of more than one oyster genus [2,6,11,13]. Mycoplasma are also very common in abalone gut microbiomes and may contribute to mollusk digestion [16–19]. Burkholderiales are also commonly identified in the gut of juvenile and adult Pacific oysters (*Crassostrea gigas*) in regions across the world [11,20]. These common groups found in oysters despite genera-level differences and geographic barriers suggest the presence of "core" members or functional groups within the oyster gut microbiome. These groups may have more to offer to the host than is currently known.

The gill also shares common bacterial groups across studies and could be the most diverse and active site within the oyster. Spirochaetes tend to be more abundant in oyster gills than any other tissue in both *C. gigas* and *Pinctada margaritifera* [6,11]. *Endozoicomonas* are found in the gills of oysters from French Polynesia to the Mediterranean [6,21]. The gill of the

oyster consistently interacts with the surrounding water because it is the site of filter feeding. The similarities in dominant taxa seen across species and regions suggest selection for specific bacterial groups. The gill is characterized by high bacterial diversity [14]. There are frequently high quantities of bacterial DNA extracted from the gill compared to the digestive tract tissues [11,15]. One study used DAPI staining to illuminate bacterial DNA within the oyster gill [14]. The bacteria they found were of various morphologies, validating the diversity observed by 16S amplicon sequencing [14]. Furthermore, this study used Fluorescence In Situ Hybridization (FISH) to validate the taxonomic groups of bacteria in the oyster gill [14]. FISH uses short DNA fragments analogous to those from a specific group of bacteria but incorporates fluorescently labeled nucleotides into the sequence. The probes, or fluorescently labeled nucleotide strands, will bind to the complement strand in the target bacteria's DNA and fluoresce under a confocal microscope. A bright signal was seen for different bacterial groups in the gill, but not as strong in the gut [14]. This may suggest a more active group of bacteria in the oyster's gill than its gut, despite numerous core bacteria identified in both tissues.

The hemolymph is another unique region of the oyster and the bacteria found in the hemolymph could be an indicator of oyster health. The hemolymph of the oyster is analogous to blood, but oysters have an open circulatory system. Their circulatory fluid is passed through sinuses and cavities which interact with other tissues. Bacterial richness in hemolymph also varies across studies [6,13]. In some cases, the hemolymph community is abundant in few taxa, such as Chromatiaceae and Rhodobacteraceae in *C. gigas*. In other *C. gigas*, the community is a diverse assemblage of *Arcobacter*, Flavobacteria, *Psychrilyobacter*, Oceanospirillaceae, Vibrionaceae, and Spirochaetes [13]. In either case, no clear similarities have shown up across studies. Interestingly, *Psychrilyobacter* and *Vibrio* are also considered core abalone microbiota,

but are found dominant in the gastrointestinal tract [18,19]. The hemolymph may be an axis between the seawater and other tissues, as seen by the transfer of *Vibrio* from the hemolymph into solid tissue [13]. Healthy oysters often have *Vibrio* in their hemolymph, but oysters found with high relative abundances of *Vibrio* in hard tissues are likely diseased [13]. This demonstrates the hemolymph as an important region for immune defense and predictor of oyster health.

While the gut, gill and hemolymph are the most studied regions in the oyster, the gonad, mantle, and adductor muscle have also been analyzed. The oyster gonad and mantle show lower alpha diversity than other tissues, with alpha diversity referring to the average diversity seen within the specific tissue across individuals [6,11]. Gonads may be dominated by Endozoicimonaceae [6]. The mantle is dominated by Spirochaetes for *C. gigas* in Australia [11]. Compared to the gut and hemolymph, the adductor muscle of the oyster has high alpha diversity and is most compositionally similar to the gill [15]. Overall, these tissues are understudied and may yield new information on the colonization of the oyster microbiome.

The microbiome of various abalone tissues has been characterized, including digestive gland, intestine and gills [16–19,22–26], but there is a lack of studies comparing abalone tissue types directly. Therefore, more research must be done to compare tissue microbiomes for multiple species to further elucidate how microbial structure and function may depend on tissue properties.

Host Age and Genetics

The oyster microbiome has various external forces acting on it, but there is host specificity in the oyster microbiome attributed to genetic background. The maintenance of a

portion of bacteria within one oyster population suggests some host-specific control over their microbiome [27]. Even when oysters encounter an entirely new environment than their place of origin, their microbiome is not completely changed. This trend holds true of other species of oysters, such as *Crassostrea gigas*. In the Wadden Sea, oysters from Northern and Southern populations were translocated to the opposite region and still maintained a portion of their microbiome from the original population for over a month [28]. The microbiome of oysters from the host environment showed significant dissimilarity from the newly transplanted oysters [28]. There is evidence from multiple studies that genetic differentiation among oysters can lead to differences in microbiome composition. In fact, microbiome differentiation correlates with host genetic distance across the gills of *C. gigas* [7]. Additionally, the more closely related the hosts are by comparison of satellite markers, the more taxa they share [7]. However, once these unrelated oysters undergo heat shock treatment in the lab, their host-associated differentiation disappears [7]. Extreme stress may result in a loss of these co-adapted groups. Another case of host differentiation results from oysters that are continually bred for OsHV-1 resistance. OsHV-1 (ostreid herpesvirus) is frequently associated with severe mortality outbreaks [29]. Breeding for resistance tries to eliminate massive mortalities that cause huge economic losses for the aquaculture industry. Oysters that have high resistance to OsHV-1 due to selective breeding show dissimilarity in the muscle microbiome compared to oysters with naturally low resistance to the virus [5]. Specific bacteria are differentially abundant across resistance groups [5]. The natural populations with low resistance show an elevated proportion of *Pseudomonas* and *Vibrio,* and a reduced proportion of *Tenacibaculum* and *Dokdonia* compared to the selectively bred oysters [5]. This demonstrates that breeding for resistance to OsHV-1 not only improves the host's ability to defend itself from the virus, but also carries over microbial associates which may

offer additional protection. The genetic divergence of oyster populations affects the bacteria that are associated with them and leads to variability between individuals.

Abalone genetics are also important when studying their microbiome. Different species of abalone may respond in contrasting ways to environmental interventions [16]. The differences in microbiome composition between species may be due to the depth at which different abalone species reside or specialized diets [17].

Another important factor often overlooked in abalone and oyster microbiome studies, likely due to time constraints and long development periods, is age or life stage. With respect to oysters, various studies have sampled larvae, juveniles and adult oysters to compare bacterial composition and diversity [20,30,31]. The microbiome resembles the surrounding water in early life stages but then becomes more specialized in adults [30,31]. Studies have speculated that this may also be a factor influencing abalone microbiomes, but the transition of the microbiome with age has not been directly tracked [18].

External Environment

The biogeography of the oyster microbiome may be influenced by a complex interaction of geographic and environmental features. Geographic separation of different study sites yields very different transient bacterial communities within oysters. Across different water masses, the influence of the external environment on the microbiome composition is evident. For example, invasive oysters from the Red Sea into the Mediterranean retained a small portion of core microbiota, but the transient community changed: it is made up of bacteria more adapted to the new surrounding environment [27]. Another example is in Australia, where there are clear differences in oyster-associated microbiomes between wave dominated and tide dominated

estuaries [11]. The tide dominated estuaries experience more ocean flushing which has led to higher bacterial diversity in the oysters [11]. However, Spirochataceae is a conserved taxa in all estuaries, demonstrating the influential yet limited importance of the external environment in dictating bacterial composition [11]. Even at small spatial scales, such as from low to high intertidal zones, oyster gut microbiota significantly diverge and are greatly influenced by the environmental fluctuations of their habitat [2].

There are specific environmental factors that have been directly associated with variation in the oyster microbiome, including oxygen concentrations and temperature fluctuations associated with seasons. Under low oxygen conditions, gut richness actually increases, suggesting the adaptation of gut microbiota to a hypoxic environment [32]. Seasonal studies are primarily split into summer and winter, where high and low temperatures influence relative abundances. The winter is characterized by lower bacterial richness, including culturable bacteria [4,10,21,27,33,34]. Oceanospirillales were found to be enriched in the winter [27], but otherwise bacterial community diversity decreases in colder months. In summer months, oysters tend to have higher bacterial richness [10,21,27,33]. Bacteria enriched in the summertime include Enterobacteriaceae, *Synechococcus*, Spirochaetes and especially *Vibri*o [27,33,35]. While *Vibri*o are frequently associated with warmer temperatures, one study found species differentiation across seasons. *Vibrio splendidus* were dominant in warmer months while *Vibrio harveyi* were more prevalent in colder months [34]. Furthermore, the diversity of carbon substrates used by oyster-associated bacteria was higher in summer compared to winter [4,31]. Oysters may be more active in the summer than in the winter, explaining the variation in their corresponding microbiome activity. Returning to the study in the Mediterranean, the comparison between the Red Sea and Mediterranean demonstrates a clear relationship between oyster microbiomes and

temperature fluctuation (17, 18). The Red Sea maintains a far more stable temperature than the Mediterranean, which may translate to the greater shift seen in the microbiome of oysters in the Mediterranean Sea through seasons (17, 18). Other than temperature, seasonal changes in microbiome have also been attributed to changes in rainfall (10).

The type of food available to and selected by oysters is another external factor that impacts the microbiome. Oyster gut microbiomes respond rapidly (within a week) to changing food sources from one algal stock to another (34). The composition of the microbiome is significantly different based on which algae the oysters are fed (34).

Abalone microbiomes are also prone to the impact of temperature and other external variables. Temperature impacts both alpha and beta diversity in the abalone microbiome, with moderate temperatures enabling the highest bacterial diversity [16]. Additionally, diet can impact gut microbiota of abalone because abalone are able to feed on various algae species and this may promote specialized species of bacteria which degrade those algae [16]. However, In additional to temperature and algae, other variables may change seasonally and contribute to shifts observed in the abalone microbiome over time [18,19]. Temperature of the environment and type of food available in a given region are both important drivers of the abalone microbiome, but there are likely additional factors yet to be explored.

Environmental influences are hard to disentangle into specific variables, such as temperature, oxygen, pH, salinity or even food availability. This emphasizes the importance of controlling for and recording environmental conditions in mollusk microbiome studies. Research on the oyster microbiome may benefit from more controlled lab experiments to assess the individual impact of each environmental variable on the microbiome.

Factors that Disturb the Microbiome

Oysters are filter-feeders and in constant contact with their external environment. Because of this, the oyster microbiome is greatly affected by external changes, especially those that would induce stress on the oyster's physiology. Both oysters and abalone may encounter a variety of stressors in their lifetime, some of which they are better equipped to deal with than others. Mollusks must survive predation, seasonal changes in the environment, variation in oxygen and salinity levels, pollution and even human induced-changes to their habitat. Currently, temperature stress, translocation and pathogen invasion are the only documented disturbances that have a negative impact on the microbiome. These types of stressors induce internal disruptions in the microbiome and decrease diversity.

Temperature Stress

Ocean warming is a big concern for oyster aquaculture, and heat waves are already leading to mass mortality events (Personal communication with Dennis Peterson of San Diego Bay Aquaculture). The disruption of the microbiome by temperature stress rather than impact on the oyster itself, is likely leading to significant mortality [8]. The oyster microbiome diverges from the ambient state under high temperatures, with negative consequences [7,8,36]. Steep temperature increase over a period of days can lead to decreases in bacterial alpha diversity, including in the gill and hemolymph, and allow for opportunists to proliferate [7]. *Vibrio* species are the most common pathogens detected under high temperature stress [8,36]. In some cases, these *Vibrio*, such as *V. harveyi* and *V. fortis* in *Crassostrea gigas*, stem directly from the original bacterial population of the oysters' tissues [8]. This shows that bacteria do not have to be newly introduced to turn pathogenic. *Arcobacter* also tends to increase in abundance in response

to heat stress [8] and has been previously identified as an opportunistic pathogen to oysters [9]. Normally oysters and abalone will encounter heat stress in summer months, and seasonal differences in the microbiome have already been demonstrated for both mollusks [10,18,21,27,33]. One study sampled oysters during the winter and exposed them to heat stress [7]. In contrast to other studies, *Vibrio* were rarely detected but *Mycoplasma* and *Planctomycetales* increased in relative abundance following the heat stress [7]. This may be due to seasonal differences in the background composition of the oyster microbiome. Overall, higher temperatures are an imminent threat to the oyster microbiome and survival.

Translocation

Oyster translocation is another applicable stress, considering most commercial production involves moving post-larval spat from hatcheries to grow-out fields, where oysters experience an extremely different environment from where they were raised. Oysters that are either in rearing tanks or lab conditions generally have lower evenness in their microbiome [13]. Once they are moved to the field, they are not well suited to deal with their surrounding environment. More research should be done in this area to understand how host-microbial interactions are affected by moving them from rearing tanks to wild conditions. Adult oysters can experience similar stress from translocation. Oysters that were translocated from the southern Wadden Sea in Northern Europe to the northern Wadden Sea harbored greater proportions of *Vibrio* [13]. Proliferation of *Vibrio* demonstrates a disturbed microbiome state and host stress. Most studies look at how the microbiome is structured after a disturbance, but it is also important to understand how the microbiome may affect susceptibility of the oyster to infection and mortality.

Pathogens

Pathogen invasion presents a challenge to the oyster's immune system as well as its microbiota because pathogens can outcompete resident bacteria. Oyster pathogens consist of known invaders to the system as well as proliferation of opportunistic species within the oyster microbiome when there is increased stress on the oyster. When one population of oysters is challenged with a pathogen, they tend to share similar microbiome features and lose natural inter-individual variability [37]. *Vibrio* species are most frequently documented as oyster and abalone pathogens and a common suspect for mass mortality episodes [9,37,38]. For example*, V. harveyi* and other *Vibrio* species were at higher abundances in oyster tissue during a disease outbreak in Australia [37]. *Vibrio aestuarianus* is another known oyster pathogen which has resulted in decreased microbial diversity in *Crassostrea gigas* [9]. Diversity decreases because of the proliferation of *Vibrio* and other opportunists, such as *Arcobacter* [9]. This shift in microbial evenness suggests a cascading effect of polymicrobial disease in oysters that are disrupted with pathogens. Once the oyster begins to die, they have no defense against their bacterial invaders and bacteria such as *Paludibacter* show up to take advantage of the wasting tissue [37]. The oyster herpesvirus, OsHV-1, is another pathogen of concern for oyster populations [37,39]. Oysters infected with OsHV-1 are often found with elevated abundances of *Vibrio*, suggesting a weakening of the host control over their microbiome [9,39]. While *Vibrio* and OsHV-1 are frequently detected in *C. gigas* populations, Sydney rock oysters (*Saccostrea glomerata*) are faced with a protozoan parasite, *Marteilia sydneyi* [40]. A study looking at *S. glomerata* infected with *Marteilia sydneyi* found one dominant OTU in the gut which was closely related to the Rickettsiales-like prokaryote that causes abalone withering syndrome [40]. These oysters ceased

feeding, which may have allowed the proliferation of one bacterium [40]. All of the above pathogens have been associated with decreased diversity in the microbiome. While specific pathogens (bacteria, virus or protozoa) are often blamed for mass mortality of oysters, the shifts in the microbiome associated with many of these diseases may also be a factor in the eventual demise.

Abalone are susceptible to many other pathogens, including viruses and intracellular pathogens [38]. The intracellular pathogen (*Candidatus* Xenohaliotis Californiensis) known to impact digestive tissue and cause withering syndrome in abalone also causes significant microbiome disruption [41,42]. Similar to oyster diseases, this pathogen leads to a decrease in microbiome diversity [42]. Although *Candidatus* Xenohaliotis Californiensis is a known pathogen, its presence alone does not confirm the withering syndrome disease, as this bacterium can be found in perfectly healthy abalone in low stress conditions [17]. In many cases, it is difficult to distinguish between pathogenic and beneficial microbes based on composition and relative abundances alone [18].

Protective Functions of the Microbiome

Pathogens can lead to major shifts in the oyster microbiome, but there is growing evidence for pathogen inhibition ability by certain oyster-associated bacteria. In two different culture-dependent studies*, Pseudoalteromonas* isolated from the *Crassostrea gigas* hemolymph displayed antibacterial activity against *Vibrio* [43,44]. *Pseuodoalteromonas* is able to inhibit the growth of *Vibrio* without negatively impacting the oyster's hemocyte viability [43]. Certain nonpathogenic species of *Vibrio* are also seen to exhibit antibacterial activity against primarily Gram negative bacteria [44]. Antimicrobial peptides have also been isolated from the

hemolymph of the oysters where the *Pseudoalteromonas* and *Vibrio* were isolated [44]. Bacteriocin-Like Inhibitory Substances are produced directly from these *Pseuodalteromonas* [44]. Since these studies came out in the early 2010s, no more have looked directly at pathogen inhibition by oyster-associated microbiota, despite this evidence that certain members of the microbiome may offer protection against pathogenic bacteria. There is speculation about the oyster's ability to select for bacteria in the gills that may be used for antimicrobial activity and enzyme production [6]. It has been suggested that simply having a diverse microbiome helps prevent pathogen proliferation by enhancing competition [12]. Indirect evidence of pathogen protection includes the differentiation between microbiomes of OsHV-1 resistant and non-resistant groups [5,39]. Specific bacterial groups, such as *Winogradskyella* and *Bradyrhizobiaceae* are more present in oysters with higher resistance to OsHV-1, but their true function is unknown [5]. Oysters certainly have the potential to host bacteria that will help defend them from pathogens. Probiotic studies have shown the suppression of pathogenic *Vibrio* in the oyster by *Bacillus pumilis* and *Streptomyces* supplements [30,45]. The treatment with *Streptomyces* increases oyster microbiome diversity and promotes the growth of *Bacteriovorax*, a bacteria which preys on gram negative bacteria, like *Vibrio* [30]. The oyster microbiome, especially in the hemolymph, has potential to benefit the host by preventing pathogen proliferation.

Abalone also benefit from probiotics and their natural microbial inhabitants. Two *Shewanella* species administered to abalone as probiotics led to enhanced immunity and pathogen resistance [46]. Microbiota within the abalone digestive tract may be contributing important digestive enzymes for the breakdown of complex algal polysaccharides [25,47]. Higher microbiome diversity has been correlated with higher feed efficiency in Pacific abalone

[25]. However, multiple mechanisms may be at play to lead to increased efficiency of digestion, including both direct enzyme production by bacteria and indirect protection of the intestine and its function through bacterial defenses [25]. While less studied in oysters, gut associated bacteria maybe be similarly important for oyster digestion and growth.

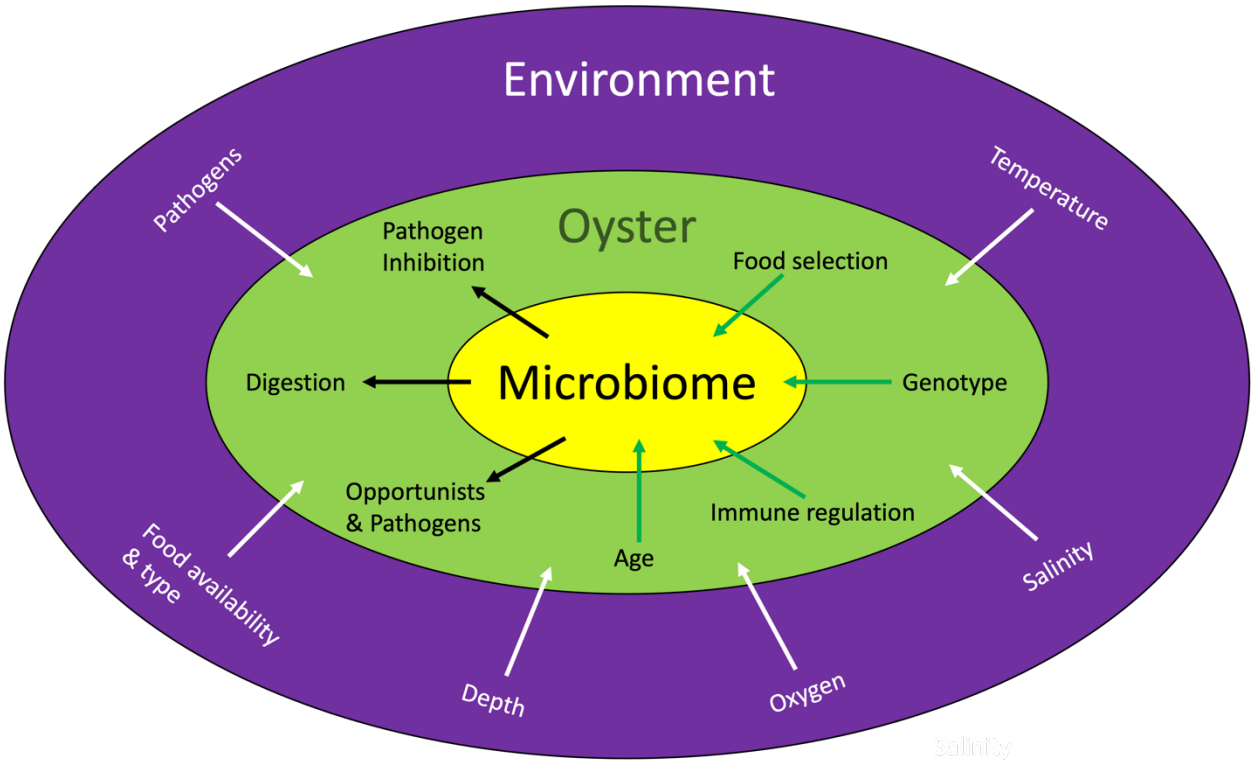

Figure 2. Summary of the interaction between the environment, oyster host and its microbiome. Arrows going from the environment sphere into the oyster sphere are environmental interactions with the oyster that impact its microbiome. Arrows going from the oyster into the microbiome sphere are host factors that impact their microbiome. The arrows that point back out from the microbiome into the oyster are potential services or risks from the microbiome to its oyster host.

Conclusion

Compositional data on the oyster and abalone microbiomes show similar trends across mollusk types. Each tissue likely harbors a select community of microbes. Across environments and genotypes, these communities diverge. The mollusk microbiome is most impacted by

pathogens and external stress. Disease state is especially of interest with regard to microbial dynamics and associations. While the bacteria in mollusk microbiomes may offer some benefits, such as pathogen inhibition and aid in digestion, the activity is largely undescribed. This dissertation will explore various environmental influences on the oyster and abalone microbiota and pathobiota.

Chapter 1 VARIATION IN SURVIVAL AND GUT MICROBIOME COMPOSITION OF HATCHERY-GROWN NATIVE OYSTERS AT VARIOUS LOCATIONS WITHIN THE PUGET SOUND

Abstract

The Olympia oyster (*Ostrea lurid*a) of the Puget Sound suffered a dramatic population crash, but restoration efforts hope to revive this native species. One overlooked variable in the process of assessing ecosystem health is association of bacteria with marine organisms and the environments they occupy. Oyster microbiomes are known to differ significantly between species, tissue type, and the habitat in which they are found. The goals of this study were to determine the impact of field site and habitat on the oyster microbiome and to identify core oyster-associated bacteria in the Puget Sound. Olympia oysters from one parental family were deployed at four sites in the Puget Sound both inside and outside of eelgrass (*Zostera marina*) beds. Using 16S rRNA gene amplicon sequencing of the oyster gut, shell, and surrounding seawater and sediment, we demonstrate that gut-associated bacteria are distinct from the surrounding environment and vary by field site. Furthermore, regional differences in the gut microbiota are associated with the survival rates of oysters at each site after 2 months of field exposure. However, habitat type had no influence on microbiome diversity. Further work is needed to identify the specific bacterial dynamics that are associated with oyster physiology and survival rates.

Importance

This is the first exploration of the microbial colonizers of the Olympia oyster, a native oyster species to the West Coast, which is a focus of restoration efforts. The patterns of differential microbial colonization by location reveal microscale characteristics of potential

restoration sites which are not typically considered. These microbial dynamics can provide a more holistic perspective on the factors that may influence oyster performance.

Introduction

Invertebrate microbiology research is increasingly important in the face of environmental and anthropogenic change. Olympia oyster (*Ostrea lurida*) populations declined across their native range on the west coast of the United States due to overharvesting by humans in the late 1900s [48]. The loss of the Olympia oysters poses a threat to ecosystem services, as oysters create structured habitat and filter surrounding water [48]. Recovery of these valuable services could be achieved through restoration efforts. To improve restoration outcomes, it is essential to identify where juvenile oysters will survive and grow successfully. Environmental and host-associated microbiota can impact settlement and growth in marine invertebrates [49–51] but the impact of microbial communities on the survival and growth of Olympia oysters in particular is unknown. Here, we explore the connection between Olympia oyster performance and associated microbiota through a field experiment in Puget Sound, Washington (USA).

Temperature, dissolved oxygen, salinity, and carbonate chemistry can limit oyster growth, metabolism, and survival [52–54] and may therefore limit restoration success. Alone or in tandem, environmental conditions can stress oysters and make them more susceptible to disease [52,55]. Environmental stress can alter diversity and composition of oyster microbiomes, either as a result of bacterial response to the changing environment, or to the host's changing gene expression [36,56,57]. A core microbiota has been demonstrated for oysters [1,11,20], but microbiota also vary significantly depending on environmental conditions and on the geographic location of the host [1,11,32,33,36,56]. A disturbance of the oyster microbiome may have consequences for host health due to the direct and indirect benefits of bacteria. Metabolism and

enzyme production by bacteria in the gut improves digestion and provides additional nutrients to the host [58]. Studies have shown that bacteria may prime the immune system and protect against pathogens [59]. Some bacteria may have the ability to regulate oxidative stress through production of antioxidants [60]. Finally, the oyster microbiome can indirectly benefit the host through production of antimicrobial peptides, which may limit growth of pathogens [43].

In this study, we evaluated the microbial diversity associated with the native Olympia oyster by comparing environmental and host-associated microbiota to identify differences across field sites and habitats and connections with oyster performance. The study aimed to: (i) characterize core or consistent members of the Olympia oyster microbiome, independent of other factors; and (ii) assess the extent of microbial variation across space. Methodologically, oysters were outplanted from a hatchery to field sites either inside or outside of eelgrass beds, left in place for 2 months, and then dissected and processed for bacterial community analysis. The field sites and habitats were further characterized by physicochemical parameters and assessment of the environmental microbiome.

Materials and Methods

Sampling. Juvenile Olympia oysters (~1 year old) were collected from the hatchery at the Kenneth K. Chew. Center for Shellfish Research in Manchester (WA, USA) and distributed to four field sites throughout Puget Sound in June of 2018 and retrieved 2 months later in August 2018 (Fig. 3). All oysters used were from a common genetic background (a subpopulation of Fidalgo Bay oysters) and were raised in the same hatchery conditions. At each of the four field sites, one PVC mesh oyster cage was deployed in the center of a patch of eelgrass (*Zostera marina*) habitat and another cage was deployed in the center of a patch of unvegetated habitat. The 1-cm mesh-size cages were intended to exclude predators while allowing circulation. Each

cage was anchored to a PVC post and contained 10 oysters upon deployment. A “patch” of eelgrass habitat was defined as an area at least 6 m in diameter with at least 60 shoots per square meter, and a “patch” of unvegetated habitat was defined as an area at least 6 m in diameter with no eelgrass present. The centroid of all patches was located at a tidal elevation between 20.3 m and 21 m MLLW. Cages were cleaned of biofouling organisms and debris every 2 weeks during the deployment.

Upon retrieval, three water samples and three sediment samples were taken from the area around each oyster cage (n = 6 water and 6 sediment samples per site). At Case Inlet, only three water samples were taken (n = 2 inside eelgrass beds and n = 1 outside eelgrass) due to a shortage of bottles in the field. Water samples were collected within 3 m of each oyster cage on an ebbing tide, when the water column was approximately 1 m deep. Samples were collected in acid-washed Nalgene bottles with mesh filters over the opening. The bottle was dipped below the surface of the water while wearing gloves and kept underwater until nearly full. Sediment samples were collected in 15 mL Falcon tubes by opening the tubes at the top of the sediment, sweeping the tube opening across the top 1 in. of sediment and then pouring out excess water before capping. Oyster cages were then retrieved and transported to the laboratory within 1.5 to 2 h in cool, dark and dry conditions.

In the laboratory at the University of Washington, oyster shells were lightly scrubbed with sterile toothbrushes to remove mud and left to dry for a few minutes. Biofilm samples were collected from three oysters in each cage by swabbing back and forth across the entirety of the shell surface on one side. Swab tips were removed, placed in individual 1.5 mL vials, immediately frozen in a dry ice bath, and then stored at -80°C. Shell length was recorded for all oysters after swabbing to prevent cross contamination. Living oysters were then shucked using a

sterile scalpel. Complete stomach and digestive tissue were removed using a newly sterilized scalpel blade, flash frozen, and then stored at -80°C. For each oyster cage, survival was recorded as the proportion of living oysters remaining out of 10.

Sediment samples were stored at -80°C upon arrival at the laboratory, and water samples were filtered over 0.2 mm-pore size cellulose filters using vacuum filtration. The filters were folded and dropped into Powerbead tubes from the Qiagen DNeasy Powersoil Kit and stored at -80°C.

Environmental data collection. PME miniDOT sensors (for temperature and dissolved oxygen data) and Odyssey conductivity loggers (for salinity data) were deployed alongside oyster cages in eelgrass habitat and in unvegetated habitat at each site. Instruments logged at 10-min intervals from early June 2018 to late August 2018. Measurements collected when the predicted tidal elevation was lower than 0 m MLLW were excluded to eliminate data collected during immersion. Dissolved oxygen data were adjusted based on salinity and reported in $mg*L^{-1}$. To assess relative differences between habitats and between field sites, temperature and dissolved oxygen data from the 24 h immediately prior to collection were analyzed. A permutational two-way ANOVA for repeated measurements was run to account for repeated measures from the same sensors at the same sites over time (51). This data did not follow a normal distribution, and therefore the permutational ANOVA approach was used. The interaction between site and habitat was also explored when assessing differences in the environmental data.

DNA extraction, amplification, and sequencing. Following the Earth Microbiome Project protocols, DNA was extracted from all sample types using the single tube Qiagen DNeasy Powersoil Kit. Single tube extractions, although more time-consuming, reduce the

amount of well-to-well contamination [61]. Extracted DNA was shipped over dry ice to Scripps Institution of Oceanography and stored at -20°C. DNA was amplified following the 16S rRNA gene Illumina amplicon protocol provided by the Earth Microbiome Project [62]. Primers 515F and 806R were used to target the V4 region of the 16S rRNA gene and sequenced on the Illumina MiSeq platform to produce 250 bp forward and reverse reads.

Sequence analysis. Resulting sequence data were uploaded to Qiita [63] (Qiita ID 12079) and demultiplexed, trimmed to 150 bp and erroneous sequences were removed using the Deblur workflow positive filter [64]. The deblur final table was exported to Qiime2 [65] and used for all subsequent analyses. Alpha diversity across sample types was assessed by Shannon diversity index [66], which measures richness and evenness within given sample types (Fig. 4). Significance of alpha diversity across groups was conducted with a Kruskal-Wallis test. Beta diversity was analyzed via Bray Curtis [67], weighted and unweighted UniFrac [68,69], and Qiime2's DEICODE RPCA [70] method with a sampling depth of 1,920. A sampling depth of 1,920 was chosen based on rarefaction curves, which are displayed in the supplementary data (Data Set F). The number of observed ASVs started to plateau around 2,000 sequences, but in order to retain one feature which had 1,922 sequences, the sampling depth used was 1,920. Phylogenetic tree derivation for UniFrac was performed using an insertion tree with the fragment insertion sepp function in Qiime2 [71]. PERMANOVA tests for all beta diversity metrics were run in Qiime2 [72]. RPCA was chosen for presentation because this method does not use pseudocounts and is therefore termed a more robust version of the Aitchison's distance metric (Fig. 4). Taxonomy was assigned in Qiime2 against the Silva database v.138 [73,74]. The biom table and taxonomy was downloaded from Qiime2 and reconstructed in R using the program Qiime2R. The taxonomy bar plots and heat maps were generated in R (Fig. 5), alongside the

alpha diversity boxplot in Fig. 4. All samples that were retained through the Deblur workflow are presented in the taxonomy plots in Fig. 5. The heatmap encompasses sediment, water, biofilm, and oyster gut samples, while the bar plot was generated using only oyster gut samples. RPCA analysis was conducted once again, but after filtering out all sediment, seawater, and shell biofilm samples to include oyster gut samples only. The purpose of this was to further investigate the differences within oysters across field sites (Fig. 6). For oyster gut samples, DEICODE RPCA beta diversity analysis was performed at a sampling depth of 1,000 because the alpha diversity started to plateau at a lower sequencing depth compared to other sample types (Data Set F). This depth allowed one additional gut sample to be retained in the analysis. Songbird differential abundance analysis was then performed to rank the differentials of every ASV across field sites [75].

Results

Oyster survival was highest at Case Inlet and Fidalgo Bay and lowest at Skokomish and Port Gamble (Fig. 3A). Difference in survival is significant between Port Gamble and Case Inlet (proportion test, P = 0.0336). Mean survival in eelgrass beds across all sites (mean = 77.5 +/- 20.6%) was slightly higher than that of unvegetated habitat (mean = 67.5 +/- 22.2%), but this trend is not consistent across all sites and is not significant (two-way t test, P = 0.533). Alpha and beta diversity analyses were conducted on habitat type (eelgrass habitat versus unvegetated habitat) with considerations for nestedness. For alpha diversity, an ANOVA was run on habitat type and showed no interactions with geographic location or sample type (Data Set A2), although assumptions of normal distribution were violated to test this effect. For beta diversity, adonis was run on habitat type, which was nested within each site and across sample types (Data Set B2). Overall, no significant differences in alpha diversity or beta diversity among all samples

were observed between habitats (Shannon ANOVA, F = 0.002, P = 0.962; Unweighted UniFrac Adonis, F = 1.257, P = 0.123). For this reason, habitat type was not considered for subsequent analyses.

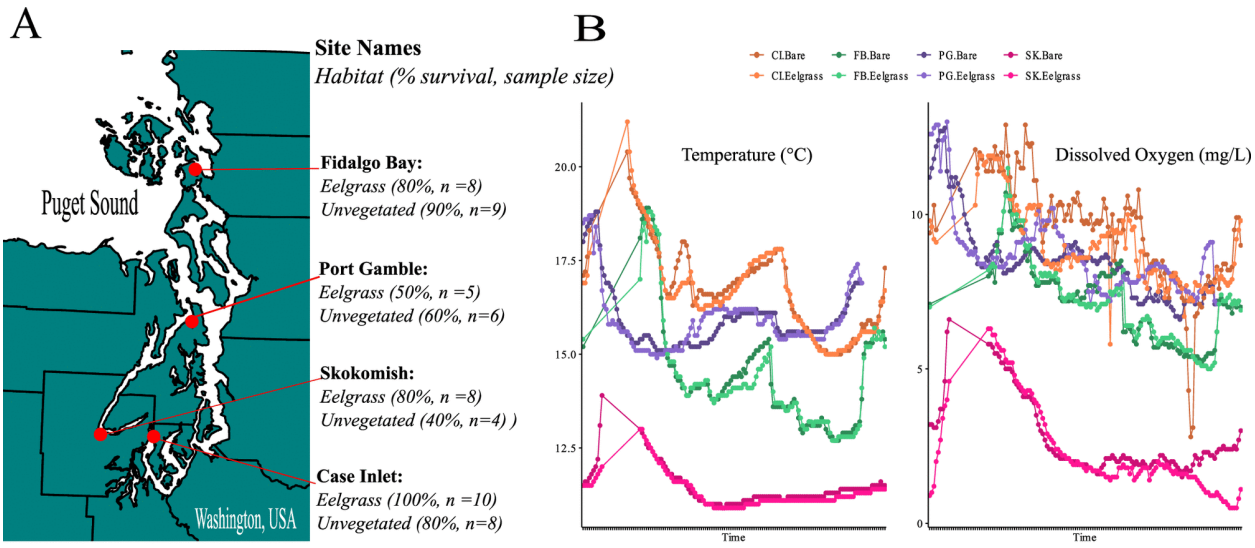

Figure 3. Overview of study site characteristics. (A) Juvenile oyster survival rates across four field sites and two types of habitats in Washington State, USA (20 oysters initially deployed at each site). (B) Temperature and dissolved oxygen measurements at each site, for both habitats, plotted over the 24-h period prior to sampling.

Temperature was significantly different across the sites but did not vary between eelgrass and unvegetated habitat (PERMANOVA by site, F = 411.478, P = 0.0002, PERMANOVA by habitat, F = 0.33596, P = 0.5626, Data Set D2). Dissolved oxygen also varied significantly across site but not between habitats (PERMANOVA by site, F = 258.9586, P = 0.0002, PERMANOVA by habitat, F = 0.9197, P = 0.3266, Data Set D1). There were no interactions between site and habitat when comparing temperature or dissolved oxygen. These data were plotted by site and habitat and the Skokomish site showed the lowest values overall for both temperature and dissolved oxygen (Fig. 3B).

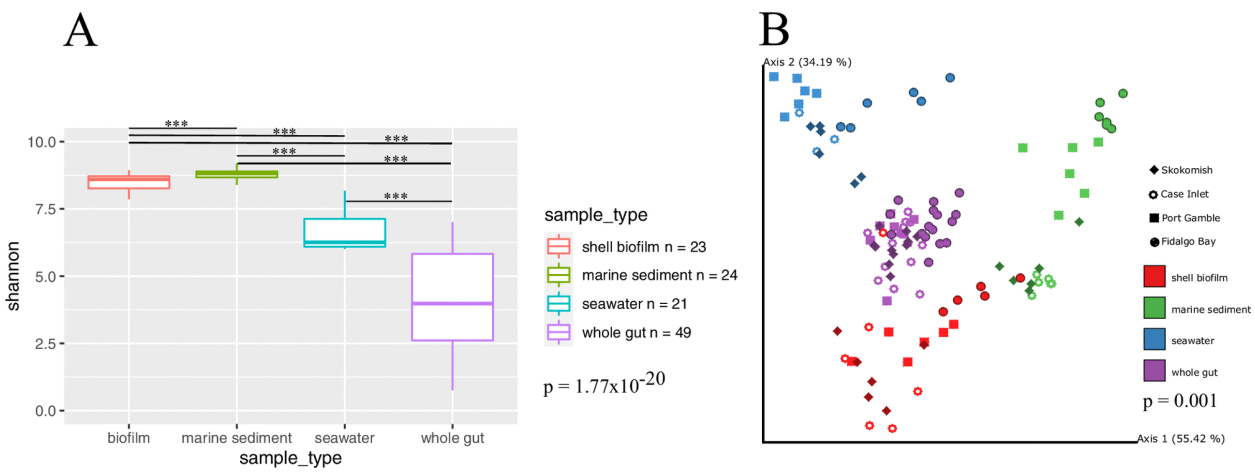

Figure 4. Alpha (A) and beta (B) diversity across sample types: seawater and sediment (n = 3 per cage), oyster gut (n varies by cage due to differences in survival) and shell biofilm (n = 3 per cage). (A) Shannon Diversity Index used to calculate alpha diversity by sample type. Significance of pairwise comparisons is indicated by ***, which implies adjusted $P < 0.001$. (B) Robust Aitchison Principal Components Analysis plot demonstrating distance between sample types. Within each sample type grouping, different shapes are used to differentiate which study site the sample comes from. The RPCA metric was used to calculate the dissimilarity matrix and define top explanatory axes.

Alpha diversity (Shannon's index) was significantly different (Kruskal-Wallis, H = 95.084, P =1.77 x 10^{-20}) between sample types (Fig. 4A, Data Set A1). All pairwise comparisons between groups were significant, indicating that sediment samples host the highest diversity, followed by biofilm, seawater, and oyster gut (Fig. 4A, Data Set A1). While oyster gut samples were found to host the lowest diversity of bacteria, they also manifest the greatest range in alpha diversity, suggesting that some samples were higher in richness and evenness than others (Fig. 4A). Robust Aitchison principal component analysis (RPCA) analysis of beta diversity concluded that sample types varied significantly from one another in composition PERMANOVA, F = 123.43, P = 0.001; Fig. 4B, (Data Set B1). Pairwise comparisons in beta diversity between sample types show that they all are significantly different in composition (Data Set B1). As a reference, gut samples were closest in similarity to the biofilm samples (mean

distance = 1.67, P < 0.001), followed by sediment samples (mean distance = 2.13, P < 0.001), and furthest in distance from seawater samples (mean distance = 2.28, P < 0.001).

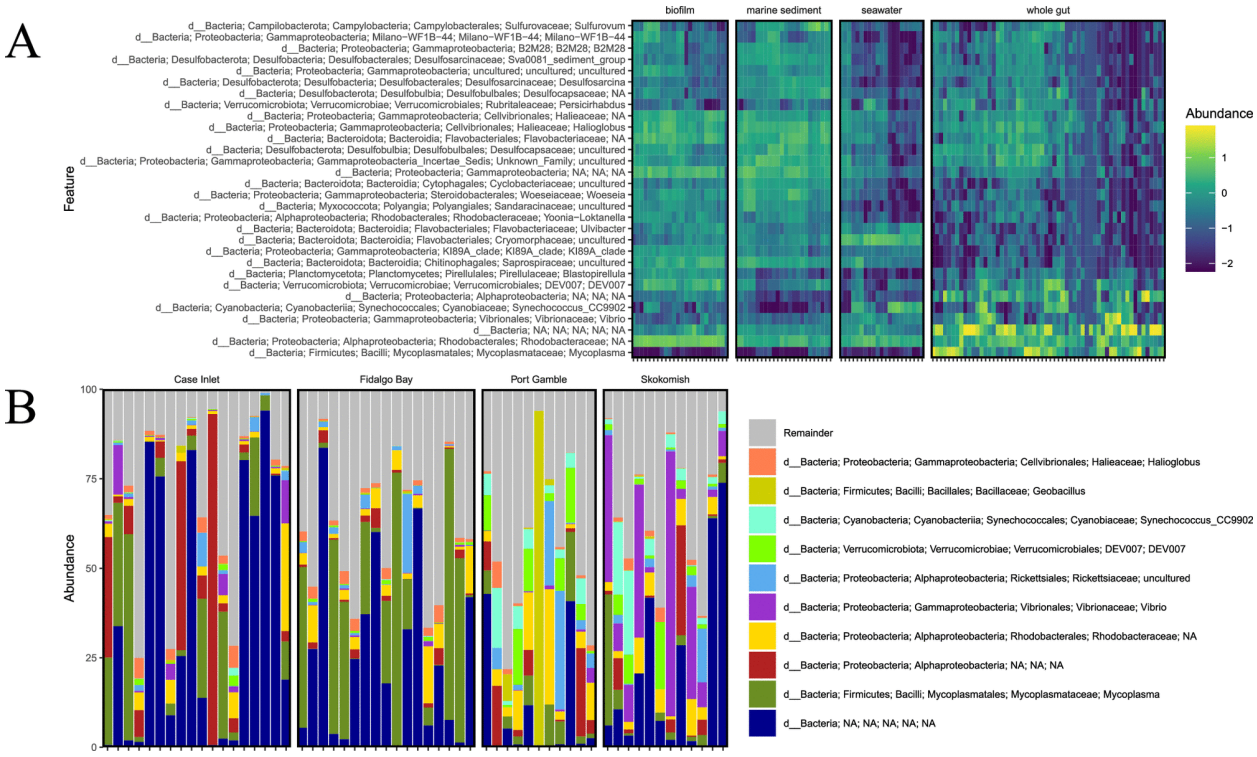

Figure 5. Taxonomic composition assigned by comparison to the Silva database to identify bacterial groups across sample types. (A) Heat map comparing relative abundances of taxa across sample types. The scale assigns a positive number to taxa which comprise a large majority of their sample composition while negative numbers are assigned to taxa which comprise a minority of the sample or are completely absent. Abundances are not absolute, but rather the relative percentage unique to each sample showing patterns in the over or under representation of key taxa. (B) Taxa bar plot displaying relative abundances of major bacterial groups within oyster gut samples. The bar plot is separated by study sites after finding significant differences in the beta diversity of gut samples between different sites.

Taxonomic alignment of bacteria amplicon sequence variants (ASVs) reveals relative abundances of key taxa groups within each sample type (Fig. 5A). Taxonomic assignment of ASVs identified across samples demonstrates that *Mycoplasma* sp. dominates the oyster gut samples compared to any other sample type, which mostly lack *Mycoplasma* spp. (Fig. 5A). A large proportion of gut samples contain an unidentified ASV in relatively high abundance. This

ASV was blasted against the NCBI 16S rRNA gene database to assess the nature of this sequence. The ASV was found to be only 87% similar to the closest match, which is *Nitrosomonas marina*. When placed in a phylogenetic tree, the ASV falls within a large group of Proteobacteria. This ASV was not filtered out of the data set during mitochondrial and chloroplast sequence exclusion and insertion tree placement, therefore, it is unlikely to be a eukaryotic sequence.

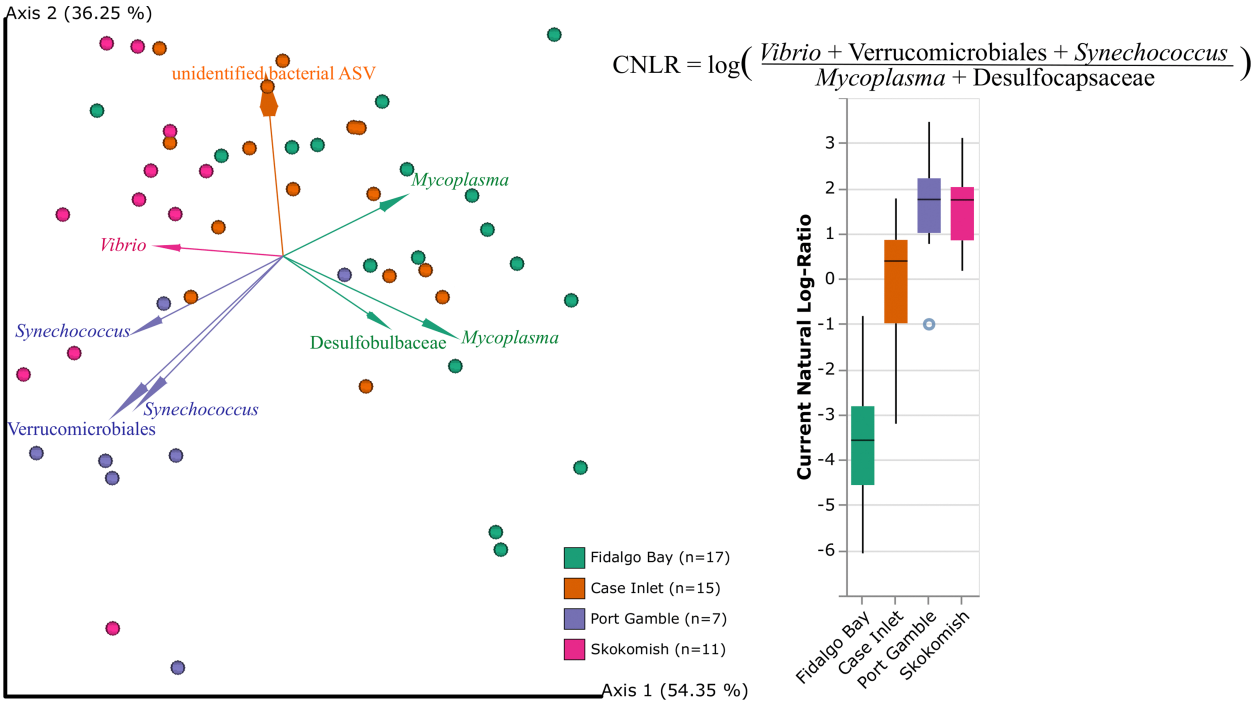

Figure 6. Variance in the oyster gut microbiota between sites. (Left) RPCA plot with only oyster gut samples. The dots are color coded by geographic location (site) within the Puget Sound and the arrows are colored by groups of bacterial ASVs found across samples which drive separation of that site. The RPCA biplot displays arrows which demonstrate the top 8 features associated with dissimilarity between samples. The visual association of these arrows with specific study sites informed the taxonomic groups to use for the differential abundance analysis ratios displayed in the box plot on the right. (Right) Ratio of differential abundances generated by Songbird analysis with Vibrio, Verrucomicrobiales, and Synechococcus aligned ASVs as the numerator and Mycoplasma and Desulfocapsaceae aligned ASVs as the denominator.

Although alpha diversity within the oyster gut samples did not significantly vary across sites (Kruskal-Wallis, H = 5.01, P = 0.17, Data Set E), beta diversity did significantly vary across

sites (PERMANOVA on RPCA distance matrix, F = 10.6534, P = 0.001; Fig. 6, Data Set B3). DEICODE biplots were used to identify ASVs driving differences across sites. One ASV (pink *Vibrio* arrow, Fig. 6) appeared to drive separation of the Skokomish samples. This ASV was inspected closer by searching related sequences in the NCBI nucleotide blast database. Multiple species were 100% similar to this sequence, but the top hits were *Vibrio toranzoniae*, *Vibrio crassostreae*, and *Vibrio kanaloae*. Using Qurro, a visualization tool for the differentials generated by Songbird (21), ratios of the driving taxa were generated for the boxplot in Fig. 6 and values were organized by site. DEICODE and Songbird differentials can both be viewed in Qurro, but Songbird models are trained on metadata variables of interest and therefore the predictive accuracy of the model is directly related to the metadata variables included in the model's formula. The Songbird model that was generated with a formula of field site outperformed the null model with a Q2 score, which is similar in concept to an R^2 value, of 0.17. For the ratio, groups of ASVs assigned to *Vibrio*, *Synechococcus*, and Verrucomicrobiales were clustered because they were heavily associated with oysters in the Port Gamble and Skokomish sites. ASVs assigned to *Mycoplasma* and Desulfocapsaceae were clustered because they appeared to drive the separation of the Fidalgo Bay oyster samples from other gut samples. Seven samples were dropped from the Qurro visualization because zeros were present in the log-ratio, implying that these ASVs were not actually detected in those samples. The comparison of relative abundances of a single taxon across samples can be misleading because its value within each sample depends on the abundance of all other taxa within that sample. To avoid this issue, one taxon is chosen as a reference and differentials of the other taxa are compared to this reference. This allows inference of the taxa's true change in relative abundance from one site to the next. *Mycoplasma* spp. were chosen as the reference because this group is found in the

majority of gut samples, allowing for a consistent comparison of other groups from one site to the next. The "identify core features" command was used to identify ASVs present in over 75% of gut samples, one of which was a *Mycoplasma* ASV. After the differentials of specific taxa are grouped into the ratio, with the reference group in the denominator, the natural log is taken, and these values are plotted in Fig. 6.

Mycoplasma and Desulfocapsaceae ASVs were at greater proportions in the samples at Fidalgo Bay than *Vibrio*, Verrucomicrobiales, and *Synechococcus* ASVs. Port Gamble and Skokomish demonstrated the opposite trend: *Vibrio*, Verrucomicrobiales, and *Synechococcus* ASVs were at a greater proportion than *Mycoplasma* and Desulfocapsaceae ASVs. Case Inlet represents a middle ground, where the ratio fluctuates around 0 to show that these specific ASVs were overall fairly equal in abundance for the group of samples from this site. While this ratio does not come from absolute abundances and therefore, we cannot define the midpoint of the x axis, the use of reference points from the differential abundance analysis confirms the observation that these taxa explain variation between sites. The natural log ratio values were imported into R and run through a Kruskal Wallis nonparametric analysis of variance test and found to be significantly different across sites ($H = 33.243$, $P = 2.86 \times 10^{-7}$, Data Set C1). A post hoc Dunn test was also run to confirm the specific differences across sites, and all were significantly different from one another except Port Gamble and Skokomish (Data Set C1). This can be seen in Fig. 6 as the boxplots heavily overlap between these sites. Additional tests were performed on the log ratios to determine whether environmental variables also drove differences in these key taxa. Linear models were created to test the correlation between the log ratios of the above taxa and the mean values for temperature or dissolved oxygen over the 24 h prior to collection for each site and habitat. Neither of these linear models showed significant

correlations of environmental conditions with the oyster-associated bacteria (linear regression correlation and P values: $R^2_{temperature}$ = 20.009721, $p_{temperature}$ = 0.4709; R^2_{DO} = 0.02157, p_{DO} = 0.1557).

In summary, Port Gamble and Skokomish experienced the highest overall mortality and highest fraction of *Vibrio*, Verrucomicrobiales, and *Synechococcus*.

Discussion

Olympia oysters in Puget Sound are a focal species for conservation and restoration science, due to the dramatic decline in population numbers from historical overfishing and failure of recovery efforts [48,76]. This field study found differences in Olympia oyster survival and microbiome between field sites, suggesting that some locations in Puget Sound may be more amenable to restoration than others. Temperature and dissolved oxygen were also significantly different across field sites. Upon further inspection, these variables only changed across sites and not between habitat types within those sites. There were also no differences within microbiome communities across the different habitats and no association between eelgrass habitat and oyster survival. The distance between eelgrass and unvegetated habitat at each site was minimal compared to geographic separation of the sites and leads to the conclusion that site characteristics were more impactful than microscale habitat changes.

Microbial communities showed significant variation across sample types: seawater, marine sediment, oyster shell biofilm, and oyster gut. The gut of the oyster hosted the lowest diversity of bacteria, which has been demonstrated previously in comparison to the surrounding water and sediment [2,77]. Beta diversity analysis suggests that the gut microbiome was significantly different from the microbiome found on the shell or in surrounding seawater. There are some shared ASVs between the gut and the surrounding environment, but these are primarily

transient bacteria and the degree to which these bacteria are functional within the oyster gut is unclear. In another study, the biofilm of the shell of live and dead oysters was compared and found not to vary, suggesting that the shell microbiome is not controlled in the same way as the internal oyster tissue microbiota [77]. Previous studies have demonstrated that the community of bacteria within the gut tends to be more controlled by the host itself than surrounding environmental variables [12]. The ASVs unique to the oyster gut were, in fact, the most prevalent groups in the gut, creating a specialized microbial community. The oyster gut microbiome is hypothesized to break down polysaccharides and produce amino acids and vitamins, likely aiding in host digestion and nutrient absorption [6].

The most abundant bacteria within the oyster gut cannot be predicted by the environmental bacterial community or physical variables. In this study, *Mycoplasma* and an unidentified bacterial group made up a high percentage of the total community and were found in over 75% of oyster gut samples. *Mycoplasma* is a genus of the Mollicutes class and have been found in high proportions in various oyster species across a broad geographic range [1,2,77]. One study demonstrated that *Mycoplasma* are likely relying on the oyster to provide certain compounds [78]. The other highly abundant ASV in the oyster gut did not align to any known bacterial subgroups, which suggests some potential novelty in the microbiota of oysters. *Synechococcus* were also found in many of the oyster gut samples, and along with other cyanobacteria are frequently observed in the oyster gut [35,79], but are likely sourced from the environment as they are also found frequently and in high proportions in seawater [79]. While it is difficult to tease apart resident versus transient and active versus inactive microbial populations from amplicon sequencing data, the groups identified here come to play an important role in further analysis.

Variation in gut microbiome composition by sites is largely driven by the balance of a few key taxa. Site-specific characteristics, such as temperature, salinity, and dissolved oxygen, may influence the abundances of these key taxa. In fact, many studies show significant dissimilarity in the internal oyster microbiome across growing locations [1,20,28]. However, there is little evidence to suggest the gut bacteria originate solely from the environment [80]. Some studies see far less variation in the microbiome across sites [33], but this could depend on how closely the sites are linked. The microbiome responds strongly to the food ingested by the oysters, and the type of food available is likely to change across habitats [81]. In the case of this study, the variation can be summarized by the ratio of small groups of taxa across the sites. A higher ratio of *Vibrio*, Verrucomicrobiales, and *Synechococcus* in oyster gut microbiomes are responsible for the separation of Port Gamble and Skokomish from the other sites. Fidalgo Bay and Case Inlet, on the other hand, host more of the bacteria that are thought to be core to the oyster's gut tissue, particularly *Mycoplasma* spp. [1,4,9,78]. A previous study on Pacific oysters in the Hood Canal, Washington identifies Tenericutes (the phylum *Mycoplasma* belongs to) and *Vibrio* in their samples, which matches the Hood Canal sites used in this study, Port Gamble and Skokomish [82]. While *Vibrio* may be a common constituent of the oyster microbiome and are frequently non-pathogenic [83], they generally make up only a small percentage of the total community. In the case of Skokomish, *Vibrio* makes up a larger percentage than expected for a healthy oyster (Fig. 5). Port Gamble and Skokomish oysters also held a higher proportion of *Synechococcus* in their gut. *Synechococcus* could be a transient member of the community from filter-feeding, but previous studies also demonstrate its successful colonization of oyster tissue [35,84]. The overrepresentation of this taxa in Port Gamble and Skokomish oysters could indicate higher filtering activity than the oysters at Fidalgo Bay and Case Inlet or an increase in

Synechococcus in the water column. The connection of Port Gamble and Skokomish by the Hood Canal supports the hypothesis that these sites experienced the same Synechococcus bloom.

The groups of bacteria which drive differences across sites also fluctuate similarly with respect to survival rate. Ratios of bacteria from Port Gamble and Skokomish were not statistically different from one another and these sites had the lowest survival rates (55% and 60%, respectively). Previous studies focused on stressed oysters suggest that proportions of *Vibrio* similar to those observed in our study are a sign of infection [13]. Furthermore, the specific *Vibrio* sequence that is overrepresented in Skokomish aligns with species which have been reported as fish or shellfish pathogens, including *Vibrio toranzoniae*, *Vibrio crassostreae*, and *Vibrio kanaloae* [85,86]. On the contrary, *Mycoplasma* is characterized as a core member of the oyster gut in this study and associated with higher survival. One study found that *Mycoplasma* actually increased in proportion in the gills of disturbed oysters [7], but as they are normally identified in the gut, this could be a sign of inappropriate translocation from the gut to more distal tissues, suggesting physiological disturbance. Therefore, the high prevalence of gut-associated *Mycoplasma* in our study is unlikely to be a sign of disturbance. In more recent years, research has explored the role of the microbiome in responding to viral or parasitic infections of oysters. Microbiome composition could be used to predict oyster mortality following exposure to OsHV-1, the ostreid herpesvirus [87]. Susceptibility of oysters to infections could be dictated by their microbiome composition, stressing the importance of characterizing bacterial dynamics at oyster restoration sites. Oysters can also experience a loss of core bacteria following infection, such as the decreased abundance of Mollicutes in oysters infected with the parasite *Perkinsus marinus* [78]. In this study, the reduced presence of *Mycoplasma* in the Skokomish samples could be explained by the increase in *Vibrio*, which may indicate some type of infection. The

type of infection cannot be determined, as there are no records of *Vibrio* species causing disease in Olympia oysters. In anoxic conditions, the oyster microbiome may respond to host stress and shift toward an opportunist-dominated community, leading to mortality of the host, even if it had the physiological capacity to withstand the anoxic conditions [57]. Oysters at Skokomish were collected after a period of very low oxygen compared to the other sites, suggesting a stressful environment for the oysters and a likely cause for the dominance of potentially opportunistic *Vibrio* species in the gut microbiome at this site. While the microbiomes of dying oysters could not be captured in this study, the patterns between survival rate and bacterial differentials suggest a potential role of these bacteria in oyster mortality, which should be further tested.

Bacterial dynamics are important to consider when monitoring ecosystem health. A diverse set of microorganisms are better equipped to handle disturbance and outcompete invaders [12]. Looking at the sites observed in this study, Fidalgo Bay varied greatly from Port Gamble and Skokomish, which are connected by the Hood Canal. The Fidalgo Bay oysters fared better than the Hood Canal oysters, which could predict higher likelihood of recruitment success and survival at Fidalgo Bay, compared with other sites. In fact, Fidalgo Bay restoration efforts have been very successful and native oyster populations grew from about 50,000 oysters in 2002 to almost 5 million in 2016 [88]. Environmental conditions also varied in the time leading up to oyster collection, which could influence microbial communities in the environment and within the oyster. However, the environmental data failed to fully explain the variation in key bacterial taxa driving the differences across sites. There is no explanation yet as to why the bacterial communities varied so much or how to evaluate an optimal microbiome. Other variables that were not assessed in this study can also cause variation in the microbiome, such as estuary morphology [11], non-bacterial disease causing agents [5,39,89], and pollutants [90]; it is

possible that these other unknown variables may be linked to the oyster gut microbiota differences, and may be driving mortality rates. Transcriptional activity can also vary along environmental gradients and provide more insight about the behavior of bacteria within the oyster [91]. While this type of data was not collected for this study, it will be an important factor to evaluate in the future.

As with any microbiome study, there are limitations in amplicon sequencing and deriving conclusions from a single time point of environmental data and tissues. Amplicon sequencing has biases in many steps of the process, from the initial subsampling of tissue to PCR primer bias. Bacterial proportions were not absolute, which prevents us from declaring that specific ASVs were increased or decreased from one sample to the next. However, future studies should aim for targeted quantification of the bacteria identified in this and other oyster microbiome studies or attempt to normalize ASV abundances with quantitative PCR of the total bacterial community [80]. Moreover, microbiome data was only collected for one time point in the late summer. A time series of samples or an early sampling point for comparison may have revealed how the oyster microbiome initially responded to field conditions and how it changed over time. Temperature and dissolved oxygen variables were explored over the 24 h prior to collection, but the time of mortality for any lost oysters was unknown, meaning it was not possible to test association between these environmental conditions and mortality. Furthermore, it was not possible to statistically test correlation between survival rate and microbiome because the time of mortality for oysters at each site was unknown and microbiome of dying oysters was not captured. Additional constraints required all oysters to be held in one cage per site and habitat, which could lead to batch effects within the cages. Additionally, triplicate sediment and seawater samples were taken within close proximity of one another in order to investigate those

communities closest to the oysters, but this likely led to higher similarity among the individual clusters and did not show a true range of alpha or beta diversity across the entire site. Considering such limitations, future field sampling efforts such as this should attempt to limit random and fixed effects as much as possible and collect widely dispersed samples to capture the full range of variation.

Conclusion

Oyster microbiomes have the potential to change because of their environment and/or host biology. This study demonstrated that while Olympia oyster gut microbiomes varied greatly by field site, the gut hosts a microbiome distinct from the surrounding environment. The microbial community was also associated with the survival rates, suggesting a connection between bacterial composition in the gut and oyster performance. These outcomes have implications for restoration management of the native Olympia oyster in the Puget Sound, providing critical insight into the bacterial dynamics faced by oysters recruiting to these sites. Furthermore, this study takes one step toward developing microbiome analysis as a diagnostic tool, which could use oyster gut samples to determine whether a given population is under stress.

Data availability

Sequence data generated in this project are deposited in the EBI-ENA database and NCBI BioProject database under (accession no. PRJEB49367) and made available through Qiita (Study ID: 12079). Processed data files and scripts for Qiime2 and R are available in the GitHub Repository (https://github.com/ekunselman/OlympiaOysterMicrobes).

Acknowledgements

Chapter 1, in full, is a reprint of the material as it appears in American Society for Microbiology, Microbiology Spectrum. Emily Kunselman, Jeremiah J. Minich, Micah Horwith, Jack A. Gilbert, Eric E. Allen. Pineridge Press, 2022. The dissertation author was the primary investigator and author of this paper. Thank you to Laura H. Spencer for providing the oyster spat used in this study. Thank you to the Ryan Kelly lab for allowing me to use their lab space for dissection of oysters and extractions. Thank you to the Washington Department of Natural Resources for supplying extraction kits. This project was supported by the US National Science Foundation grant OCE1837116 to E.E.A. and funding from the Aquatic Assessment and Monitoring Team at the Washington State Department of Natural Resources.

Chapter 2 TEMPERATURE AND MICROBE MEDIATED IMPACTS OF THE SAN DIEGO BAY OSTREID HERPESVIRUS (OSHV-1) MICROVARIANT ON JUVENILE PACIFIC OYSTERS

Abstract:

The ostreid herpesvirus (OsHV-1) was recently detected in San Diego Bay for the first time in farmed juvenile oysters. Due to the virus' ability to cause mass mortality (50 to 100%), it is important to determine the factors that promote infection as well as the consequences of infection. Here we assess the role of temperature in controlling OsHV-1 induced mortality. Oysters were exposed to the San Diego Bay microvariant of OsHV-1 at 4 different temperatures (15, 18, 21, and 24°C). While OsHV-1 was able to replicate in oyster tissues at all temperatures, it did not induce mortality at 15°C, only at the higher temperatures. Additionally, we examined oyster tissue-associated bacterial response to OsHV-1 infection. As shown previously, bacterial richness increased following OsHV-1 exposure, and then decreased as the oysters became sick and died. Four bacterial taxa linked to the San Diego Bay microvariant infection, including *Arcobacter*, *Vibrio*, *Amphritea*, and *Pseudoalteromonas*, were the same as those shown for other microvariant infections in other studies from globally distributed oysters, suggesting a similar spectrum of co-infection irrespective of geography and microvariant type. The significant shift in the bacterial community following exposure suggests a weakening of the host defenses as a result of OsHV-1 infection, which potentially leads to adverse opportunistic bacterial infection.

Sustainability Statement:

The temperature threshold of OsHV-1 microvariant from San Diego Bay is critical information for management of the virus. With global ocean temperatures rising, the likelihood of OsHV-1-induced mortality outbreaks may increase. Microbial sequencing also further elucidated the presence of genus-specific bacterial activity in association with OsHV-1, which

may be critical in disease progression and potential targets for combatting oyster disease. The impacts that OsHV-1 has on oyster aquaculture affect both food security (UN Sustainable Development Goal 2) and ocean sustainability (UN Sustainable Development Goal 14) because growth of aquaculture is essential to address seafood demand but disease outbreaks can cause negative consequences to both food supply and the health of the environment around those outbreaks.

Introduction:

The Ostreid herpesvirus (OsHV-1) is a pathogen that plagues aquaculture industries around the world, namely in France, Italy, Ireland, New Zealand, Australia and the West Coast of the United States [29,92–101]. Microvariants of OsHV-1 (µVar) have developed which carry several sequence variations compared to the reference genome published by Davison et al 2005 [102]. Microvariants of OsHV-1 are highly virulent and lead to mass mortality events on oyster farms [94,97,98,103]. Herpesvirus particles are seen in microscopy across various tissues, including adductor muscle, mantle and digestive gland, and specifically target oyster immune cells called hemocytes which may act as a vehicle transporting the viral particles to different tissues [89,104,105]. The virus attaches to host cells to invade them and replicate within [106]. Inhibition of apoptosis is frequently found in susceptible oysters and may be caused by viral reprogramming in favor of its own proliferation [89,104,107,108]. OsHV-1 may be detected and quantified, both DNA copies and mRNA expression levels, with quantitative PCR [94,109–112]. Controlled laboratory studies have shown that OsHV-1 may be transmitted by filtered viral homogenate into naïve oysters through intramuscular injection, bath exposure with tissue homogenates or bath exposure using shed virus [89,105,110]. The virus is also spread through

cohabitation, suggesting inter-oyster transmission on farms and in natural populations during outbreaks [89,113].

OsHV-1 virulence is exacerbated by increasing temperatures. In fact, certain microvariants of OsHV-1 are incapable of inducing mortality below certain temperatures. An Australian microvariant was only found to induce mortality above 14°C [114]. Other microvariants, such as the French microvariant, have greatly reduced replication and almost no oyster mortality at lower temperatures such as 13°C [115]. As temperatures are increased, OsHV-1 induced mortality can increase up to 57% [116], 84% [114], 89.8% [113] or even 100% [52]. The most optimal range for most OsHV-1 microvariants appears to be between 16 and 26°C [52,113–117]. Optimal growth and function temperature for Pacific oysters is typically around 20°C [118]. Higher temperatures may interfere with antiviral gene expression and cause differential response to OsHV-1, leading to higher likelihood of mortality [119].

In San Diego Bay, temperatures vary from 15°C in winter to more than 22°C in summer (NOAA National Data Buoy Center). High temperatures reach to 25°C in San Diego Bay. The first detection of an OsHV-1 microvariant in San Diego Bay occurred in 2018 in farmed triploid juvenile oysters [94]. The detection of high OsHV-1 copy numbers in October of 2018 coincided with 99% spat mortality [94]. This is a microvariant of OsHV-1 which is highly virulent, similar to French and Australian microvariants (Kachmar et al in press). There have since been ongoing sentinel studies to monitor the spread of the OsHV-1 microvariant, which is more similar to the French, Australian and Chinese microvariants than to the Tomales Bay, California OsHV-1 variant [94]. OsHV-1 San Diego Bay microvariant has since been detected during a mass mortality of small juvenile oysters in San Diego Bay in 2020 (Evans et al. submitted). The mitigation of this virus can be successful with selective breeding programs, informed planting

times to avoid vulnerable periods based on age, temperature and other environmental factors, appropriate stocking density and limiting oyster transfer from one location to another [110,120–124]. Currently, a single oyster nursery exists in San Diego Bay, and the current management strategy is to allow commercial production of oysters only in times when the temperature is <20 °C, while sentinel oysters remain to better understand when outbreaks occur.

In addition to temperature, microbes may also play an important role in OsHV-1 infection. The ability of OsHV-1 to impair host immune defense offers the opportunity for opportunistic microbiota to also invade and colonize the oyster. Oysters launch a predominantly antibacterial response at later stages of infection, hinting at the likelihood of secondary bacterial co-infections associated with viral infection [107]. This is further demonstrated by drastic shifts in microbiome community composition and bacterial accumulation with associated tissue damage upon histological examination of infected oysters [89]. A specific group of opportunistic bacteria is conserved across many OsHV-1 infectious environments, including *Arcobacter*, *Pseudoalteromonas*, *Amphritea*, *Marinomonas*, and *Marinobacterium* [89,117,125,126]. It is also likely that *Vibrio* species contribute to disease and further its progression after initial infection with OsHV-1 [87,89,125,127,128]. Some bacteria may be co-infectors, while others may take advantage of both the host's immunocompromised state and resources produced by other bacteria, such as siderophores [127].

As a result of the limited known detections in San Diego Bay, it is difficult to narrow down an optimal temperature range for the OsHV-1 San Diego Bay microvariant. Therefore, the first goal of this study is to assess the temperature threshold of this microvariant in naïve oysters without prior exposure to OsHV-1. This was conducted through bath exposure to OsHV-1 in experimental aquaria under four different temperatures (15, 18, 21, and 24°C) and monitoring

mortality for 14 days after exposure. To explore microbial community dynamics after OsHV-1 exposure, another bath exposure was performed at 21°C and oysters were visually assessed and categorized into different disease states (alive, sick or dead). The microbial patterns in community diversity across disease states and key bacterial players after exposure were compared with other studies to reinforce the theory that a common group of OsHV-1-associated bacteria are conserved across both geographic regions and across different microvariant infections. Finally, to assess the magnitude of bacterial impact on OsHV-1 disease, an antibiotic treatment was applied to half of the tanks in all temperatures but failed to reduce mortality. This study has critical implications for OsHV-1 management in San Diego Bay, revealing a tight linkage between temperature and mortality, as well as demonstrating the ability for opportunistic and potentially detrimental bacteria to emerge during viral outbreaks.

Methods:

Oyster Infection Trials:

Due to handling of a deadly oyster virus, the experimental room used for infection was an enclosed, climate-controlled room with no flow-through seawater. Waterproof lab boots were worn at all times when in the room and a 10% bleach bath was prepared in a mat outside of the room for washing the boots after working in the room. Lab coats and boots worn inside the room did not leave the area and were reserved strictly for use in this room. All trash that was accumulated from the experiment was disposed of in double-bagged biohazardous trash bags for off-campus autoclaving. All sharps, including needles and scalpels, were disposed of in biohazardous sharps containers. Drop cloths were placed over tanks to control possible aerosolization of the virus, therefore keeping a barrier between controls and OsHV-1 as a measure of contamination prevention. At the end of the experiment, all containers and materials

which were in contact with oysters or OsHV-1 were soaked in 10% bleach for 30 minutes or sprayed with 10% bleach before rinsing and drying. All protocols were reviewed by the state of California and the facility inspected prior to the start of experiments.

Oyster Infection Experiment #1 - Mortality:

Juvenile oysters (9 mm or 24 mm in length) were shipped on ice from an oyster farm in Humboldt Bay, California to Scripps Institution of Oceanography. Oysters had only been exposed to Humboldt Bay water, where OsHV-1 has never been detected (Burge CA, unpublished data, Elston RA unpublished data). All seawater used was from the Scripps Institution of Oceanography pier inlet, was at 35 ppt and was 0.2 micron-filtered prior to use. Immediately upon arrival, oysters were rinsed briefly with freshwater to clean off sediment and placed into tanks at 15 or 17℃. Oysters were split into either "donor" or "recipient" tanks. Water with OsHV-1 present would later be transferred from donor oyster to recipient oyster tanks. The two donor tanks were 39 Liter Sterilite containers with 100 oysters (24 mm length) each starting at 17℃. Recipient tanks were split into two sides: OsHV-1 exposure or Control (Figure 7). Each side had 4 water baths to allow for the final acclimation of oysters to 4 different temperatures (Figure 7). The recipient tanks were 1 Liter lidded containers with a hole in the lid for an airline. 10 oysters (9mm length) were placed in each of these recipient tanks and 4 tanks were placed into each water bath (Figure 7). One water bath on each side (both Control and OsHV-1 exposed) was kept at room temperature, which was 15℃, while all other water baths were started at 17 ℃ by using water heaters. Starting one day after the arrival of the oysters, the temperature in the water baths and the donor tanks was increased 1℃ per day until the water reached the desired temperature. Donor tanks were increased to 21℃, while recipient tanks were made to be

15, 18, 21 and 24℃ (Figure 7). Temperature loggers were placed in the recipient tank water baths at 21℃ to monitor true water temperature fluctuation.

Water in every tank was changed completely every 2 days. All seawater used in the experiment was bleached at 10% before being disposed of down the sink drain. Oysters were fed *ad libitum* every day during the acclimation period. A mix of algae containing 50% *Chaetoceros muelleri*, 5% *Tetraselmis* sp., 20% *Tisochrysis lutea* and 25% *Nannochloropsis oculata* was boiled at 100℃ for 1 minute to kill exogenous bacteria before being fed to oysters.

Once all tanks had reached their target water temperatures (21℃ for donor oysters or 15, 18, 21 and 24℃ for recipient oysters), the donor oysters were placed into an epsom salt bath at 50 g/L overnight to relax their adductor muscle. These donor oysters were injected with 100 uL of OsHV-1 homogenate with a total of $1x10^6$ copies using a 27-gauge needle injected directly into the adductor muscle. The homogenate used was a secondary pass from the original homogenate (Burge et al 2021) prepared previously and cryopreserved at -80 C (Kachmar et al in press). After waiting for 10 minutes oysters were placed back into the 39 Liter containers with filtered seawater at 21℃ for 48 hours. After 48 hours, a water sample was collected from each donor tank, extracted using the Zymo Quick-DNA Miniprep Plus Kit following the Biological Fluids and Cells Protocol and the concentration of OsHV-1 copies was quantified using qPCR (see full description below). The quantification of virus in the water in each tank was deemed sufficient for exposure ($>1x10^5$ copies/mL). The water in the two donor tanks was mixed and another sample was taken to determine the final viral concentration in the water ($4.05x10^6$ copies/mL). 500 mL of the seawater carrying the virus was added to each recipient tank for every temperature on the OsHV-1 exposure side, dosing each set of 10 oysters with $2.03x10^9$ copies of OsHV-1. For oysters on the control side, tank water was changed with just filtered seawater.

For each temperature and condition (OsHV-1 exposed or control), there were four tanks with 10 oysters each (n = 32 tanks, n = 320 oysters). Two replicate tanks received antibiotics while the other two replicates did not (Figure 7). Starting with the first day of exposure and continuing at each water change, Chloramphenicol at a final concentration of 10 mg/L [57], Ampicillin at a final concentration of 1 mg/L, and Streptomycin at a final concentration of 0.1 mg/mL [8] were added to the seawater immediately before adding the seawater to the antibiotic-treated tanks. Control tank water did not receive any additives. A follow-up experiment was conducted to validate the lack of difference in mortality between antibiotic and non-antibiotic treated oysters at 18℃. All conditions were replicated, except 20 oysters were used per antibiotic treatment in an OsHV-1 exposure condition, and 10 oysters were used per treatment in the control tanks.

Oysters from all conditions were fed boiled algae immediately after virus exposure and 24 hours after virus exposure to ensure filtering of the virus but were starved for the remainder of the experiment. Every day, oysters were monitored for mortality. Starting with the control side, tanks were lifted from the water bath, tapped to confirm that live oysters would close, and investigated further if any oysters remained gaping open. Any oysters that remained open were touched lightly with a pair of tweezers. If oysters did not close after this, they were deemed dead and removed from the tank. The tissue of the dead oysters was immediately removed from the shell, weighed, and stored in DNA/RNA shield solution (Zymo Research). Once mortality leveled out, with less than 3 oyster deaths per day for 4 days, the experiment was terminated and tissue from all remaining live oysters was dissected and preserved in DNA/RNA shield.

Oyster tissue was homogenized in the DNA/RNA shield solution for 30 seconds using the soft tissue tips with the Omni Tissue Homogenizer tool (Omni International). Then, 500 uL

of homogenate was used for DNA extraction with the Zymo Quick-DNA Miniprep Plus Kit following the Solid Tissues Protocol. This kit included a Proteinase K digestion for 1 hour. The extracted DNA template was stored at -20℃ until use for qPCR.

Oyster Infection Experiment #2 - Microbiome:

A replicate experiment was conducted at 21℃ to collect oyster tissue samples from control and exposed oysters (alive, sick/moribund and dead) for microbiome characterization and comparison (Figure 7). Oysters from the nursery in Humboldt Bay were shipped to the climate-controlled room and placed in filtered seawater at 17℃. The temperature of the seawater increased 1℃/day until it reached 21℃. Water was changed every 2 days and oysters were fed boiled algae. Once oysters reached 21℃, 10 oysters were dissected, weighed and stored in DNA/RNA shield solution. Then, over 100 donor oysters were relaxed with an epsom salt bath overnight and injected with 100 uL of $1x10^6$ total copies of OsHV-1 homogenate. After 48 hours, a water sample from the tank was collected, extracted and run through qPCR. The water contained $1.41x10^6$ copies/mL of OsHV-1. 500 mL of this virus water was added to each of 6 recipient tanks with 10 oysters per tank. After 4 days, 10 dead oysters and 2 sick oysters were collected from the tanks overall. Dead oysters failed to close after touching them with sterile tweezers, while sick oysters closed slowly and only after the tweezers touched their shells directly. After 5 days, 8 more sick oysters and 10 live oysters were collected from the tanks overall and the experiment was terminated. Live oysters closed immediately after tapping the outside of their tank.

Oyster tissue was homogenized in the DNA/RNA shield solution for 30 seconds using the soft tissue tips with the Omni Tissue Homogenizer tool and stowed at -20℃. Then, 500 uL of homogenate was sent for DNA extraction at the UCSD Microbiome Core using the Applied

Biosystems MagMax Ultra Nucleic Acid Isolation Kit. A portion of extracted DNA template was returned from the Microbiome Core and viral quantification was performed via qPCR.

qPCR:

Tank water and all oyster tissue samples were run through a quantitative PCR reaction to determine if OsHV-1 was present and at what concentration. Methods were adapted from Burge et al 2020, Burge et al 2021, and Agnew et al 2020 [94,109,110]. Each qPCR reaction well was prepared with 10 uL of Agilent Brilliant III Ultra-Fast SYBR QPCR master mix, 0.8 uL of each 10 uM OsHV-1 primer (ORF100 Forward and Reverse), 0.5 uL of BSA, 5.9 uL of molecular grade sterile H_2O and 2 uL of DNA template. All samples were run in triplicate. A standard curve and negative extraction and qPCR controls were included in every run. The standard curve was prepared using a synthetic gBlock strand of the OsHV-1 ORF100 region in a dilution series from $2x10^7$ copies down to 20 copies/uL. Thermocycler conditions included one cycle of 20 seconds at 95℃, followed by 40 cycles of 3 seconds at 95 ℃ and 30 seconds at 60℃, and finished with a melt curve profile of 95℃ for 15 seconds, 60℃ for 15 seconds and a ramp up to 95℃ held for 15 seconds. OsHV-1 copy number in unknown oyster and water samples was derived from the standard curve equation for that plate and averaged across the 3 replicates. Specificity of the amplified template was confirmed by comparing the melt curve of samples to that of the gBlock positive controls.

Microbiome Sequencing:

Control (n=10), live (n=10), sick (n=10) and dead (n=10) oyster microbial community libraries were prepared and sequenced by the Microbiome Core and the Institute for Genomic Medicine at UCSD. Library preparation was conducted by the UCSD Microbiome Core using the KAPA Hyper Plus Kit (Roche Diagnostics, USA). The protocol for library preparation and

sequencing is based on the Earth Microbiome Project, which uses primers 515F/806R to target the V4 region of the 16S rRNA gene in bacteria [62,129]. Sequencing was conducted by the UCSD IGM Genomics Center on the Illumina MiSeq platform with paired-end 250 base pair cycles.

Analysis

Oyster Infection Experiment #1 - Mortality:

During the 14-day period following OsHV-1 exposure, oysters were monitored every day for mortality. If an oyster was found dead, it was recorded as a "1", along with its temperature, exposure condition (control vs. OsHV-1 Exposed), antibiotic treatment (yes or no), and the days since exposure for when it was found dead. Each mortality was recorded as an individual data point. At the end of the experiment, any remaining live oysters across all variables were recorded individually as "0". The data on mortality was tracked in this way to perform a survival analysis using the Kaplan-Meier estimate [130]. In R, the Kaplan Meier survival estimate was computed with the function *survfit()* from the package *survival* [131,132]. Then, the step function plots were created using *ggsurvplot()* from the *survminer* package. Finally, a log rank test was conducted with the *survdiff()* function in the *survival* package to determine whether mortality varied significantly across conditions.

All oyster tissue was collected from this experiment and all tissue was assessed for OsHV-1 viral load. Quantitative PCR data for all OsHV-1 exposed oysters was normalized by weight of tissue in grams, because samples were collected in a standardized volume. The log of the normalized copy numbers by temperature and mortality status (live vs. dead) were visualized with violin plots. Kruskall Wallis tests were used to determine whether OsHV-1 copy number varied between live and dead oysters and across temperatures.

Oyster Infection Experiment #2 - Microbiome:

Sequencing reads from the control, alive, sick and dead oyster samples were demultiplexed with Qiime2 [65]. DADA2 from Qiime2 v2020.6 was used to denoise the data and produce a feature abundance table of Amplicon Sequence Variants [133]. Reads were truncated at 224 base pairs on the forward reads and 200 base pairs on the reverse reads based on sequence quality plots. Taxonomic classification of reads was conducted with the Qiime2 pre-trained classifier from Greengenes2 v2022.10 [134]. 'Unassigned' taxa were filtered out of the feature abundance table. A phylogenetic tree was constructed using the SEPP fragment insertion method [71]. The DADA2 ASV abundance table, Greengenes2 taxonomy file, and phylogenetic tree were imported into R as a phyloseq object. Phyloseq was used to calculate Richness, Evenness, Shannon's, and Simpson's alpha diversity [135]. Kruskal Wallis tests with pairwise Dunn's test were used to determine statistical significance between groups. An alpha correlation test was run to determine strength of linear correlation between evenness and viral load. Richness values were plotted against evenness values as proposed by Gauthier and Derome [136]. A distance matrix was calculated with unweighted UniFrac using the Phyloseq package and plotted with Principal Coordinates Analysis [68,69]. Adonis tests were run on unweighted UniFrac distances to determine significance of both disease state and viral load in altering microbial composition. Hierarchical clustering was conducted with the unweighted UniFrac distance matrix and hclust using the complete linkage method. The tree was cut into its primary 5 clusters. Differential abundance analysis was conducted with ANCOM-BC, which corrects the bias from uneven sampling fractions across samples, uses a log-linear regression, and conducts multiple pairwise comparisons all while controlling the multi-direction false discovery rate [137]. ANCOM-BC is robust to the sparse matrices used in microbiome data and adaptive to

structural versus sampling zeros. The disease state of the oyster sample was used as the fixed formula for ANCOM-BC with an initial prevalence cutoff of 10% and Holm p-value adjustment. Pairwise comparisons were conducted against the control samples (before OsHV-1 exposure) as the reference. An adjusted p-value of less than 0.05 was used as the cutoff for significantly different taxa, which were agglomerated at the genus level. Finally, Random Forest analysis with *randomForest()* [138] package and function in R was performed to assess the ability to predict disease state and OsHV-1 exposure status based on the microbial composition and abundance data. A prevalence cutoff of 10% for each sample set was used again to remove rare taxa. Out of bag error rate was calculated for two comparisons: Alive versus Dead oysters and Control ("Before") vs. Alive & Sick ("After") oysters. The top 20 ASVs that were most important for predicting condition in either comparison were selected based on the greatest mean decrease in GINI coefficient, which equates to the ASVs improving predictive capabilities at a given node in the decision tree.

Results:

Oyster Infection Experiment #1 - Mortality:

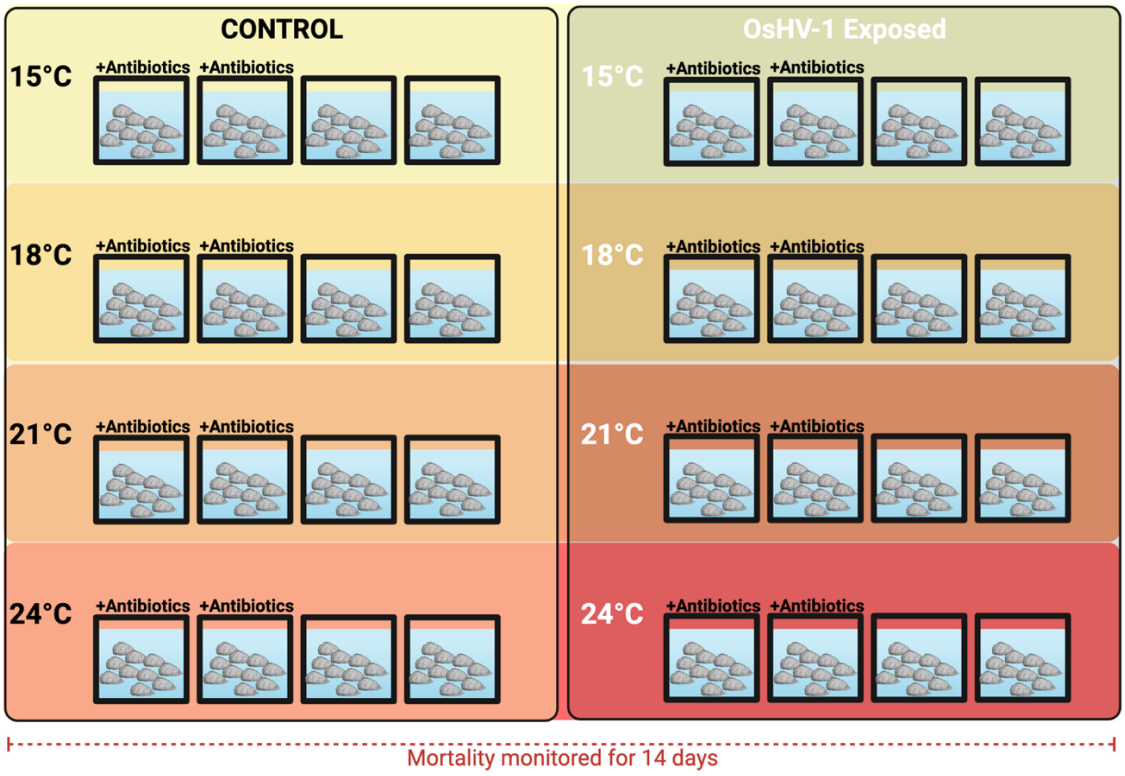

Oyster Infection Experiment #2 - Microbiome:

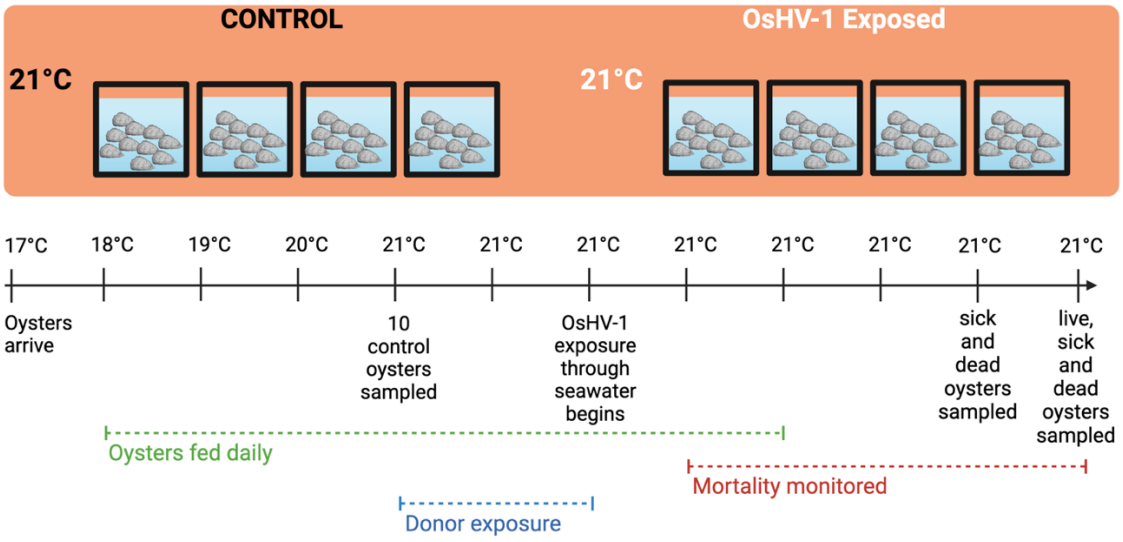

Figure 7. Experiment schematic. Top panel is showcasing mortality experiment setup while bottom panel is showing microbiome experiment setup. A highly similar timeline as shown in the bottom panel was used for both experiments, with the exception that mortality was monitored for longer in the first experiment and oysters were not sampled until they died, or the experiment was ended at 14 days post exposure.

Oyster Infection Experiment #1 - Mortality:

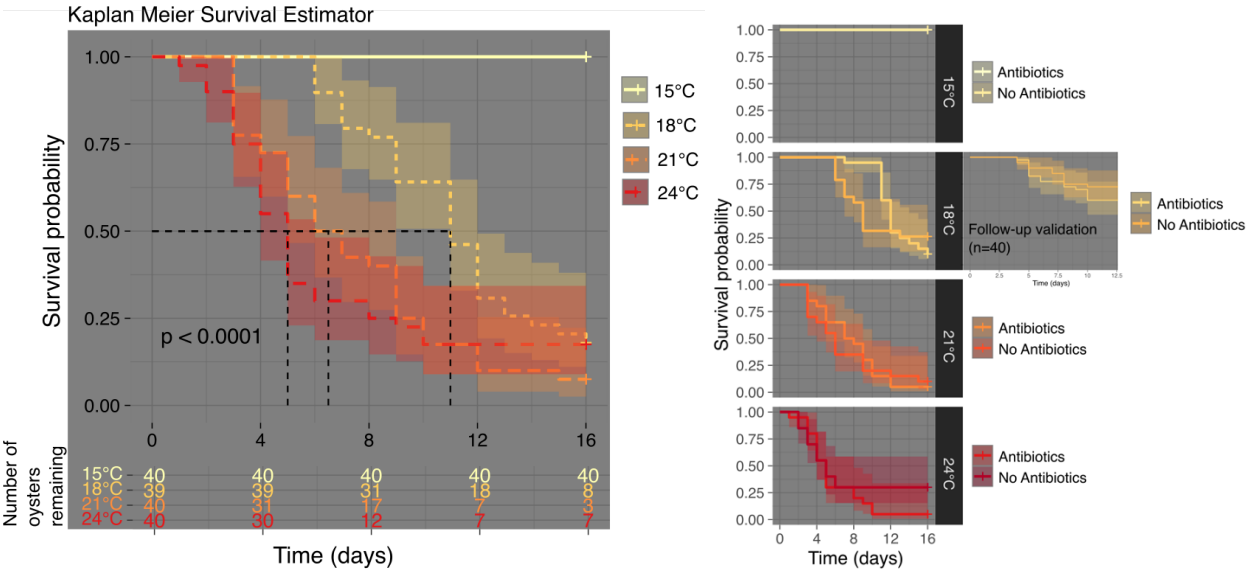

Figure 8. Kaplan Meier mortality curves displaying the proportion of oysters dead in each condition each day and estimated probability of survival with 95% confidence intervals. Top panel displays survival curves by temperature with an x axis of time in days. Significance of the statistical difference between temperatures is exhibited with p value < 0.0001. The number of oysters remaining at given time points is displayed below the Kaplan Meier plot, where the initial sample size of oysters is the first number listed (n = 40 for 15, 21 and 24°C, n = 39 for 18°C). Bottom panel displays survival curves by antibiotic exposure, faceted into one plot per temperature. For 18°C, the follow-up validation experiment with 40 oysters is coupled with the original experiment to show trends from the duplicated experiments.

Mortality varied significantly by temperature but did not vary with antibiotic treatment. No oysters in the control group, at any temperature with or without antibiotic treatment died, thus only OsHV-1 exposed oysters were plotted for mortality. At 15°C, no oysters died in any of the temperatures either with or without antibiotic treatment (Figure 8). In all other temperatures, there was no significant difference in mortality between antibiotic treated or untreated oysters (Figure 8). Log rank tests were used to determine whether mortality was significantly different between temperatures. Overall, mortality did significantly vary between temperatures ($p < 0.0001$*) (Figure 8). Mortality at 18°C was significantly different from that of 15°C ($p < 0.0001$*), 21°C ($p = 0.00065$*) and 24°C ($p = 0.00227$*). However, mortality at 21°C did not

vary from 24°C (p = 0.66852). Over 75% of oysters died in all temperatures 18°C and higher, but oysters at 21°C and 24°C started dying sooner after OsHV-1 exposure than oysters at 18°C (Figure 8). At 18°C, antibiotic treated oysters appear to start dying later than untreated oysters, but this difference was not statistically significant in either the initial or the follow-up experiment (Figure 8).

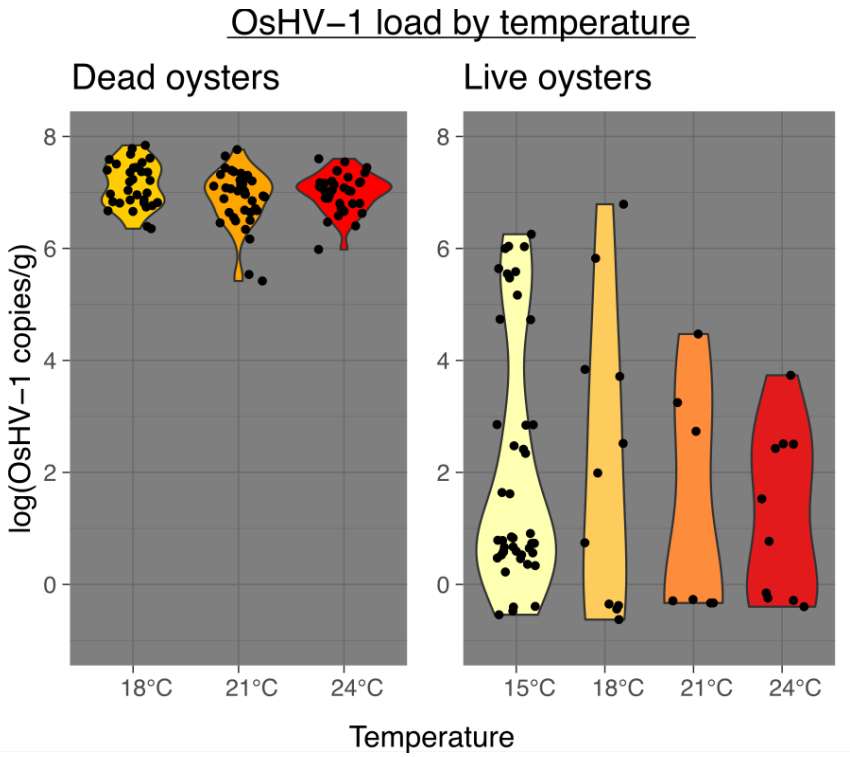

Figure 9. Viral load of OsHV-1 copies normalized by weight across temperatures faceted by mortality. Copy numbers were determined by qPCR and each individual dot represents one sample. Violin plots are used to summarize density distribution of values across temperatures. Left panel displays normalized qPCR values for dead oysters sampled throughout the experiment, while the right panel displays values for remaining live oysters collected only at the end of the experiment. 15°C is not included in the left panel as no oysters died at this temperature.

OsHV-1 load was much higher in dead oysters compared to remaining live oysters but did not vary by temperature. Kruskal Wallis tests were conducted separately for live and dead oysters. Within the dead oysters, OsHV-1 normalized qPCR values did not significantly differ

between temperatures (p = 0.168) (Figure 9). Similarly, OsHV-1 load did not significantly differ between temperatures within remaining live oysters (p = 0.7112) (Figure 9). A Wilcoxon test (or Mann Whitney test) was conducted to determine whether OsHV-1 load varied between dead and live oysters across all temperatures combined. OsHV-1 load was significantly higher in dead oysters compared to live oysters (p < 0.001*) (Figure 9). The variability of normalized qPCR values was much higher in remaining alive oysters, while values for dead oysters were all very similar (Figure 9).

Oyster Infection Experiment #2 - Microbiome:

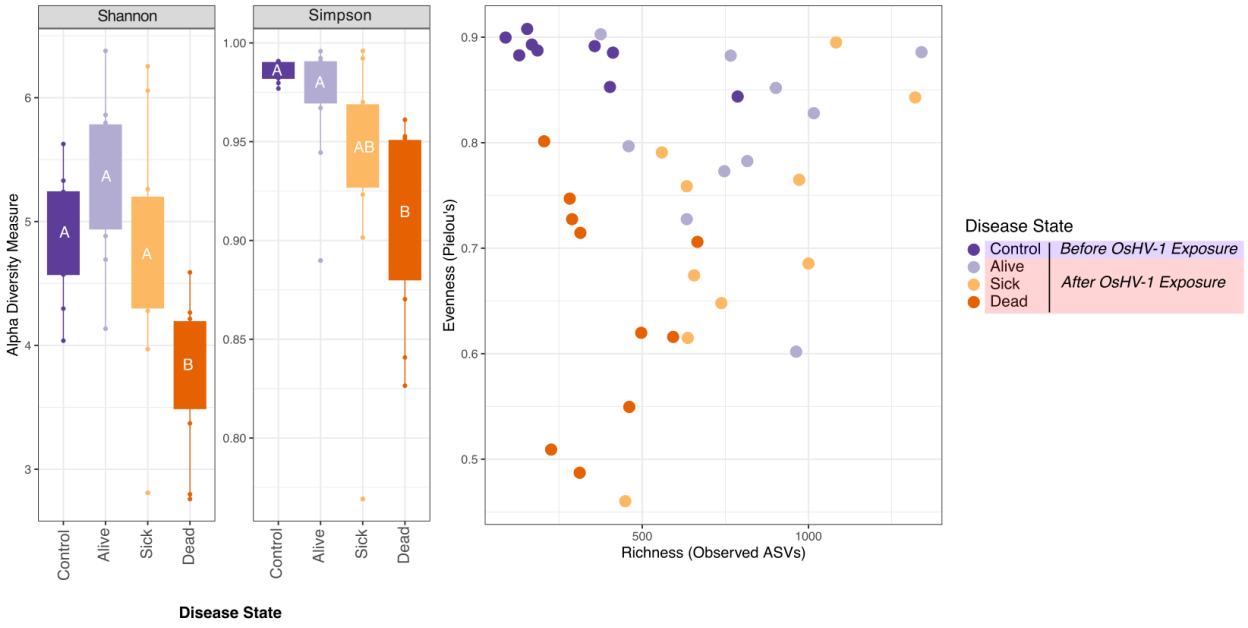

Figure 10. Alpha Diversity of oysters before and after exposure to OsHV-1. Left displays Shannon and Simpson diversity with boxplots corresponding to 4 different disease states: 1: before OsHV-1 exposure, 2: after exposure but still alive, 3: after exposure and showing signs of sickness and 4: completely dead. Statistically significant difference (p < 0.05) between groups is denoted by "A", "AB", and "B", with "AB" suggesting overlap with both "A" and "B". Right displays the richness in number of observed ASVs versus the evenness as measured by Pielou's index as a dotplot. Dots are colored by their respective disease states.

Following infection, the tissue-associated microbial alpha diversity decreased over the spectrum of mortality (alive>sick>dead; Figure 10). Figure 10 demonstrates two alpha diversity

measures across oyster disease states (Shannon's and Simpson's) and then breaks down these metrics into their components by plotting Richness against Evenness. Richness and Evenness are both components of Shannon's and Simpson's index, with richness having more weight in Shannon's index and evenness having more weight in Simpson's index. After exposure to OsHV-1, but while oysters were still alive or sick, Shannon's and Simpson's overall diversity measures were unchanged (Kruskal Wallis (KW) & Dunn's test(D)/ $p > 0.05$*)(Figure 10). However, Richness increased significantly from before exposure to after (Control – Alive/ KW&D/ $p = 0.0012$*; Control – Sick/ KW&D/ $p = 0.0012$*)(Figure 10). Evenness only started to decrease once oysters show signs of sickness (Control – Sick/ KW&D/ $p = 0.0026$*)(Figure 10). Once oysters were found dead, Shannon's and Simpson's diversity decreased significantly (Figure 10). In dead oysters, Richness returned to a similar level to before OsHV-1 exposure (Control – Dead/ KW&D/ $p = 0.4515$) and was significantly lower than remaining sick and alive exposed oysters (Alive – Dead/ KW&D/ $p = 0.0086$*; Sick – Dead/ KW&D/ $p = 0.0073$*)(Figure 10). However, Evenness decreases in dead oysters and was significantly lower than oysters before exposure and oysters that were still alive without signs of sickness (Control – Dead/ KW&D/ $p = 0.001$*; Alive – Dead/ KW&D/ $p = 0.0228$*)(Figure 10). Evenness was also significantly negatively correlated with viral load. As OsHV-1 load (log(copies/g)) increased, evenness decreased (alpha correlation, $r = -0.7318$, $p < 0.0001$*).

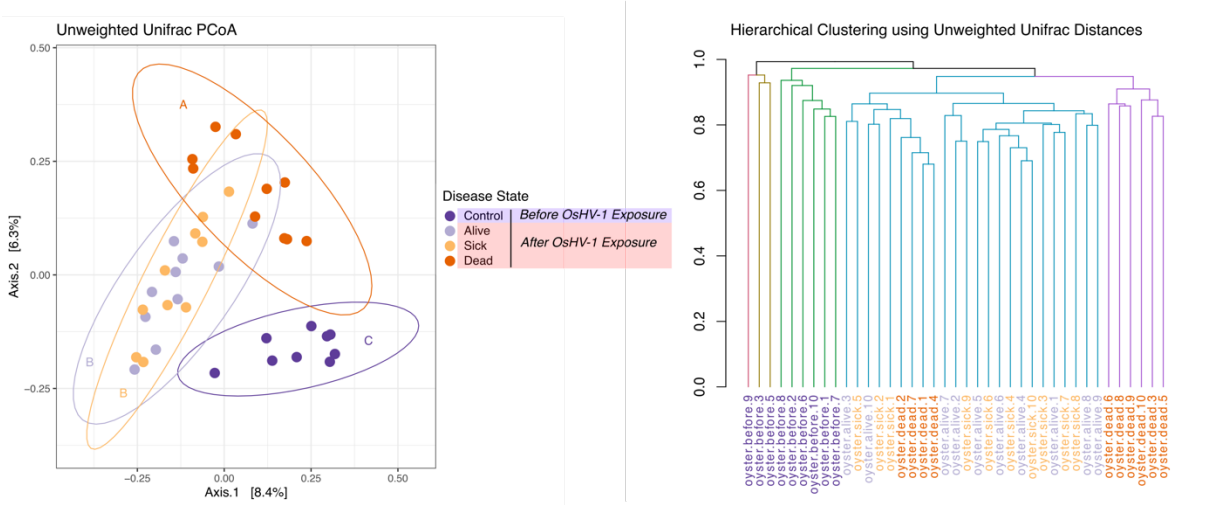

Figure 11. Beta Diversity Distances between Disease States. Left displays a Principal Coordinate Analysis of the Unweighted UniFrac distances between samples. Dots are each a single sample color-coded by Disease State and ellipses are added around the groups to demonstrate overlap. Significant differences are denoted by groups "A", "B", and "C". Right displays hierarchical clustering of samples based on the Unweighted Unifrac dissimilarity matrix using the complete linkage method. Sample names are listed along the bottom and color-coded by Disease State. The colors of the lines indicate the 5 most prevalent clustering groups.

The microbial composition of oyster tissues changes after OsHV-1 exposure and shifts again once the oyster has died. Figure 11 demonstrates the clustering of similar samples based on their microbial communities. Unweighted UniFrac (beta diversity metric) looks at ASVs present but not their abundance. UniFrac also accounts for phylogenetic similarity based on the SEPP fragment insertion phylogenetic tree. Unweighted UniFrac shows significant difference between the microbial constituents of control oysters and alive oysters (adonis, p = 0.006*), as well as control oysters and sick oysters (adonis, p = 0.006*), but not between alive and sick oysters (adonis, p = 0.906) (Figure 11). Dead oysters also have a significantly different beta diversity compared to control, alive and sick oysters (adonis, all pairwise comparisons p = 0.006*)(Figure 11). Unweighted and weighted Unifrac distances are also significantly associated with viral load (adonis, Unweighted: R2 = 0.064, p = 0.001*, Weighted: R2 = 0.224, p = 0.001*). Hierarchical

clustering breaks the oyster samples into 5 distinct clusters (Figure 11). Three clusters are composed of only control oysters, and control oysters are not found in either of the other two clusters (Figure 11). One cluster contains a mix of alive and sick oysters with a few dead oysters (Figure 11). The final cluster contains only dead oysters (Figure 11). The oysters which cluster into groups together are most likely to be found in close positions on the Unweighted UniFrac plot as well, suggesting some overlap in the ASVs found in these samples. Most notable is the clear separation between unexposed and OsHV-1-exposed oysters in terms of both Unweighted UniFrac ordination and Hierarchical clustering (Figure 11).

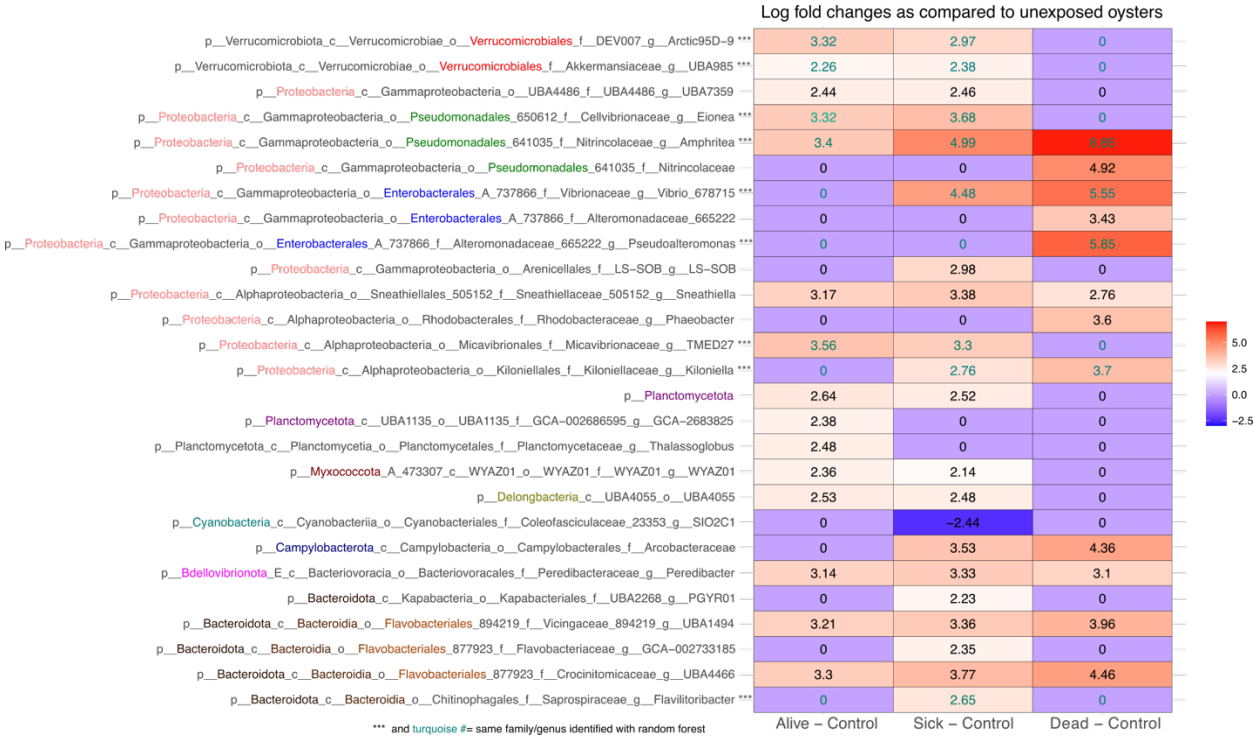

Figure 12. Differential abundance analysis of taxa changing significantly from before to after OsHV-1 exposure. Taxonomic classification down to genus level is provided on the left side of the plot, with distinct levels or groups of levels separated by text color. The log fold change of the taxa from A: Control to Alive, B: Control to Sick, and C: Control to Dead is listed in order from left to right. The value of log fold change is written in its respective box for each comparison and taxa, and the box is colored along a gradient scale from negative to positive values, with a center around 2. Numbers in the blue-green color and taxa names ending with 3 asterisks *** indicate that this genus was also identified as one of the top 20 most important in Random Forest analysis for predicting disease state, which are listed in Table 1.

There were 27 genera found to be differentially relatively abundant after conducting pairwise comparisons between control oysters and alive, sick or dead oysters with ANCOM-BC. The heatmap in Figure 12 displays significant log fold change values (Holm-adjusted p value < 0.05) for each genus for each pairwise comparison. Only one genus was found to significantly decrease in abundance from the control group (Figure 12). The Cyanobacteria Family Coleofasciculaceae was a significantly lower proportion of the community in the sick oysters (Figure 12). Many genera were more abundant in both alive and sick oysters compared to control oysters, but not in dead oysters (Figure 12). These include 2 genera from Verrucomicrobiales (one of which is from the family Akkermansiaceae), the Proteobacterial groups Eionea and Micavibrionaceae, a Planctomycetota, a Myxococcota group, and a Delongbacteria group (Figure 12). There were also groups that were more abundant in both sick and dead compare to control, but not alive oysters (Figure 12). These are Vibrio, Kiloniella and Arcobacteraceae (Figure 12). No genera were found to be more abundant in both alive and dead, but not sick oysters (Figure 12). Two Planctomycetota groups (GCA−2683825 and Thalassoglobus) were only more abundant in alive oysters post-OsHV-1 exposure. (Figure 12) Various groups were only more abundant in sick oysters, such as Arenicellales, Kapabacteriales, Flavobacteriaceae, and Flavilitoribacter (Figure 12). Four groups were only more abundant in dead oysters; an unknown genus of Nitrincolaceae, 2 Alteromonadaceae, one of which was Pseudoalteromonas, and Phaeobacter (Figure 12). Finally, various taxa were found to be more abundant in all oyster disease states after OsHV-1 exposure, including Amphritea (which increases in log fold change with increasing severity of disease state), Sneathiella, Peredibacter, Vicingaceae, and Crocinitomicaceae (Figure 12).

Of the genera found to be differentially abundant by ANCOM-BC, 9 were also identified to be predictive of disease state using Random Forest analysis (Figure 12, Table 1). These are both Verrucomicrobiales genera, Eionea, Amphritea, Vibrio, Pseudoalteromonas, Micavibrionaceae TMED27, Kiloniella, and Flavilitoribacter (Figure 12, Table 1). These taxa were most important based on the greatest mean decrease in the Gini coefficient, which means that these taxa increased the ability of the model to predict which group the sample was from. Random Forest models were run on two different subsets of the samples. One model was run on control oysters (n = 9) versus alive and sick oysters grouped together (n = 20), which was "Before versus After OsHV-1 Infection" (Table 1). Dead oysters were removed from this model because dead oyster tissue likely contains many bacteria involved in decomposition, but not directly associated with OsHV-1 infection. This model had an out of bag error rate of 3.45%. The second model was run on alive (n = 10) versus dead (n = 10) oysters to determine which bacteria were responsible for moving between disease states once the oyster was already exposed to the virus (Table 1). This model had an out of bag error rate of 10%. Some taxa were found to be important for model prediction in both "Before versus After OsHV-1 infection" and "Alive versus Dead oysters" (Table 1). These include Akkermansiaceae, Roseovarius, and Amphritea spongicola (Table 1).

Taken together, ANCOM-BC and Random Forest results can be more robustly assessed. For example, Akkermansiaceae, Flavilitoribacter, Vibrio, Kiloniella, Amphritea, Verrucomicrobiales genus Arctic95d-9, Eionea, and Micavibrionaceae TMED27 were all found to be important for predicting whether oysters had been exposed to OsHV-1 or not (Table 1). In ANCOM-BC, these genera were also significantly different between exposed and unexposed oysters, with all groups having increased in the exposed oysters (Figure 12). In predicting

whether oyster samples came from surviving or dead oysters under OsHV-1 exposure, Pseudoalteromonas, Vibrio, Amphritea, and Akkermansiaceae were all found to be important (Table 1). In differential abundance analysis, Pseudoalteromonas, Vibrio and Amphritea all increased as a proportion of the microbiome in dead oysters (Figure 12). Akkermansiaceae is significantly increased in surviving oysters, but not in dead oysters (Figure 12).

Table 1. Top 20 most important ASVs for classifying oyster samples in Random Forest analysis. ASVs are listed in order of increasing importance. Genus and Species are italicized. Red lettering denotes the same ASV in both "Before versus After" and "Alive versus Dead" lists. The three asterisks *** indicates that the Genus was identified in both Random Forest and ANCOM-BC analysis.

Top 20 ASV Predictors for Before versus After OsHV-1 Infection	
Predictor Classification	**Mean Decrease Gini**
Bacteroidota|Bacteroidia|Flavobacteriales_877923|Flavobacteriaceae|*Tenacibaculum_A_805184*	0.1641
Verrucomicrobiota|Verrucomicrobiae|Verrucomicrobiales|Akkermansiaceae|*Uba985* ***	0.1734
Bacteroidota|Bacteroidia|Chitinophagales|Saprospiraceae|*Lewinella_A*	0.1774
Planctomycetota|B15-G4|B15-G4|B15-G4|*B15-G4*|*Sp003644265*	0.1788
Bacteroidota|Bacteroidia|Flavobacteriales_877923|Flavobacteriaceae|*Patiriisocius Sp000170815*	0.1891
Proteobacteria|Alphaproteobacteria|Rhodobacterales|Rhodobacteraceae|*Roseovarius_489432*	0.2040
Campylobacterota|Campylobacteria|Campylobacterales|Arcobacteraceae|*Arcobacter_474983*	0.2098
Bacteroidota|Bacteroidia|Chitinophagales|Saprospiraceae|*Flavilitoribacter* ***| *Nigricans*	0.2135
Planctomycetota|B15-G4|B15-G4|B15-G4|*B15-G4*| *Sp003644265*	0.2186
Planctomycetota|Planctomycetia|Pirellulales|Pirellulaceae|*Mariniblastus*| *Sp011087765*	0.2268
Bacteroidota|Bacteroidia|Flavobacteriales_877923|Flavobacteriaceae	0.2348
Proteobacteria|Gammaproteobacteria|Enterobacterales_A_737866|Vibrionaceae|*Vibrio_678715* ***	0.2404
Proteobacteria|Alphaproteobacteria|Rhizobiales_A_501396|Rhizobiaceae_A_499470	0.2571
Proteobacteria|Alphaproteobacteria|Kiloniellales|Kiloniellaceae|*Kiloniella* ***	0.2871
Proteobacteria|Gammaproteobacteria|Pseudomonadales_641035|Nitrincolaceae|*Amphritea* ***| *Spongicola*	0.2910
Verrucomicrobiota|Verrucomicrobiae|Verrucomicrobiales|Dev007|*Arctic95d-9* ***	0.2994
Proteobacteria|Alphaproteobacteria|Sphingomonadales|Emcibacteraceae|*Paremcibacter*| *Congregatus*	0.3072
Proteobacteria|Gammaproteobacteria|Pseudomonadales_650612|Cellvibrionaceae|*Eionea* ***	0.3570
Proteobacteria|Alphaproteobacteria|Micavibrionales|Micavibrionaceae|*Tmed27* ***|*Sp002167715*	0.3641
Proteobacteria|Gammaproteobacteria|Enterobacterales_A_737866|Kangiellaceae|*Aliikangiella_737838*| *Coralliicola*	0.4182

Table 1. Top 20 most important ASVs for classifying oyster samples in Random Forest analysis. ASVs are listed in order of increasing importance. Genus and Species are italicized. Red lettering denotes the same ASV in both "Before versus After" and "Alive versus Dead" lists. The three asterisks *** indicates that the Genus was identified in both Random Forest and ANCOM-BC analysis. (Continued)

Top 20 ASV Predictors for Alive versus Dead oysters (following OsHV-1 infection)	
Predictor Classification	**Mean Decrease Gini**
Proteobacteria|Gammaproteobacteria|Enterobacterales_A_737866|Alteromonadaceae_665222	0.0990
Proteobacteria|Gammaproteobacteria|Enterobacterales_A_737866|Alteromonadaceae_665222|*Paraglaciecola*	0.1000
Bacteroidota|Bacteroidia|Chitinophagales|Saprospiraceae|*Jaautg01*|*Sp012031785*	0.1145
Bacteroidota|Bacteroidia|Flavobacteriales_877923|Cryomorphaceae	0.1274
Planctomycetota|Brocadiae|Brocadiales	0.1400
Proteobacteria|Gammaproteobacteria|Enterobacterales_A_737866|Alteromonadaceae_665222|*Pseudoalteromonas****|*Phenolica*	0.1417
Proteobacteria|Gammaproteobacteria|Enterobacterales_A_737866|Shewanellaceae_666538|*Shewanella* | *Colwelliana*	0.1442
Campylobacterota|Campylobacteria|Campylobacterales|Arcobacteraceae	0.1450
Proteobacteria|Alphaproteobacteria|Rhodobacterales|Rhodobacteraceae|*Roseovarius_489432*	0.1543
Bacteroidota|Bacteroidia|Flavobacteriales_877923|Flavobacteriaceae	0.1583
Proteobacteria|Alphaproteobacteria|Rhodobacterales|Rhodobacteraceae	0.1720
Calditrichota|Calditrichia|Rbg-13-44-9|J042|*J075*|*Sp003695285*	0.1742
Proteobacteria|Gammaproteobacteria|Enterobacterales_A_737866|Vibrionaceae|*Vibrio_678715* ***|*Hanmi*	0.1763
Planctomycetota|Gca-002687715|Gca-002687715|Gca-002687715|*Gca-2683135*| *Sp002683135*	0.1772
Proteobacteria|Gammaproteobacteria|Xanthomonadales_616050|Marinicellaceae|*Marinicella*| *Sediminis*	0.1829
Proteobacteria|Gammaproteobacteria|Pseudomodales_641035|Nitrincolaceae|*Amphritea* ***|*Spongicola*	0.1980
Verrucomicrobiota|Verrucomicrobiae|Verrucomicrobiales|Akkermansiaceae|*Uba985* ***	0.1990
Proteobacteria|Gammaproteobacteria|Pseudomonadales_650612|Pseudohongiellaceae|*Uba9145*	0.2765
Bacteroidota|Bacteroidia|Flavobacteriales_877923|Flavobacteriaceae|*Maritimimonas*|*Rapae*	0.3192
Proteobacteria|Gammaproteobacteria|Pseudomonadales_650612|Porticoccaceae|*Porticoccus*	0.4142

Discussion:

Oyster Infection Experiment #1 - Mortality:

Mortality in this experiment is due to the interaction between temperature and OsHV-1. Temperature alone was not responsible for killing oysters, because no control oysters died during experimentation. Marine diseases are tightly linked with temperature. This has been especially well documented in corals, which have been monitored for disease for decades [139–141]. Exposure of pathogens to new hosts via range expansion of either the host or the pathogen is in part driven by changes in ocean heat content making new areas suitable for invasion [139,140]. This may be exacerbated by human-mitigated introduction of new species or populations [140]. Spread of Dermo and MSX in eastern oysters (*Crassostrea virginica*) on the East Coast of the United States was likely driven by warming ocean temperatures [139–141]. Temperature can also impact virulence of pathogens in their current ranges and alter host susceptibility through physiological stress [140,141]. There may also be overlap in the optimal growth temperature of known pathogens with other opportunistic bacteria, fungi and viruses which creates conditions for polymicrobial infections [141].

Colder temperatures have previously been shown to decrease mortality in OsHV-1 exposed oysters [113–115]. For the French microvariant, oyster survival is highest at 13°C or lower [113,115]. For the Australian microvariant, OsHV-1 was not capable of killing oysters when the temperature was dropped to 14°C, and a threshold for productive viral infection and mortality is likely between 14°C and 18°C [114]. Low temperature likely permits more effective antiviral response by oysters hosts, allowing oysters to survive by limiting viral replication [119]. In the case of the San Diego Bay microvariant assessed in this study, temperatures of 15°C or lower are likely to confer 100% survival against OsHV-1 infection. While quantification of viral

copies showed that the virus was able to replicate in at least some oysters at the low temperature, this did not lead to mortality. Therefore, in San Diego Bay, naïve juvenile oysters are unlikely to become lethally infected with OsHV-1 at these low temperatures.

As temperatures increase, the ability of OsHV-1 to infect oysters increases. In this experiment, the optimal temperature for the San Diego Bay OsHV-1 microvariant was 21 to 24°C. Oysters died faster at these temperatures than at 18°C, which may be due to increased metabolism at higher temperatures promoting increased viral replication [142]. Mortality after just 2 days of bath exposure has been documented previously [110]. However, overall survival was very low at temperatures above 18°C, making any temperature that is permissive to the virus a big risk for juvenile oysters. In other OsHV-1 variants and microvariants, mortality also increases with temperature [113,116,143]. The Tomales Bay, CA variant causes outbreaks during the summer which are primarily associated with temperature extremes above 24°C [93,143]. The French microvariant tends to be most virulent at temperatures between 16 and 26°C [113,116]. Above this temperature range, oyster mortality is decreased, potentially due to altered oyster physiology and more efficient immune response [113,116,144]. The highest temperature tested in this study was 24°C, but it is possible that higher temperatures could inactivate and limit replication of the San Diego Bay microvariant. For the Australian microvariant, mortality increases severely at 22 and 26°C, with 26°C likely being the optimal temperature for inducing mortality [114]. The San Diego microvariant likely has a similar temperature threshold to other OsHV-1 microvariants, but viral copies are still found in oysters at 15°C after 14 days, suggesting infection is still possible at these lower temperatures if the virus is introduced.

All dead oysters had very similar viral loads regardless of temperature, while remaining alive oysters had highly dispersed viral loads at all temperatures. These dispersed viral loads suggest that individual oysters were at various stages of infection. The viral load and likelihood of mortality also depend highly on genotype, as some families could be more resistant to OsHV-1 infection than others [89]. Burge and Friedman 2012 suggests that viral gene expression is highest in the first few days after infection [111]. Infection may be occurring at different times for each individual oyster, as 10 oysters are housed together, and they may be feeding at different times and rates. Low viral load below 10^6 copies/mg [94] suggests that the oyster was tolerant of the viral infection or was able to slow infection from bath exposure and from viral shedding of other oysters throughout the experiment. Higher viral loads in live oysters may be predictive of further mortality, had the oysters been monitored for longer. Oysters may be able to tolerate high viral loads without succumbing to death, which was demonstrated by high viral loads (10^8 copies) in surviving oysters infected with the French and Australian microvariants [109]. Some viral loads in alive oysters overlapped with dead, further suggesting that surpassing a threshold of viral copies may not be the only predictor of death. Although many oysters exposed to OsHV-1 at low temp were able to clear the virus, another study showed that OsHV-1 load increased again when moved to warmer temperatures [115]. Once the virus is present in an oyster, it is likely latent and can persist until warmer temperatures are able to re-activate it [145]. This is likely part of the cause for reactivation during 2020 In San Diego. Outbreaks have only occurred in San Diego Bay in 2018 and 2020, despite temperatures rising well above 18°C every summer. Infected oysters were entirely removed from San Diego following OsHV-1 detection, but OsHV-1 may survive latently in wild oysters or other unknown sources [93]. OsHV-1 has never been detected in wild oysters in San Diego Bay, but these oysters may be tolerant of the virus and

keep viral copies below the limit of detection. Temperature is likely not the only reason for OsHV-1 activation, but additional factors leading to OsHV-1 dispersal are unknown.

Antibiotics had no effect on mortality rates in this experiment. Therefore, the OsHV-1 San Diego Bay microvariant is capable of killing oysters even with a suppressed bacterial community, which differs from other microvariants where *Vibrio* colonization is essential to full disease expression [145]. As was used in a prior study, Chloramphenicol was utilized as an antibiotic to limit bacterial colonization of oysters during OsHV-1 infection [89]. The study by de Lorgeril et al found that antibiotic treatment significantly reduced mortality in OsHV-1 challenged oysters [89]. Based on gene expression analysis, OsHV-1 infection places oysters in an immunocompromised state, allowing pathogenic bacteria to overcome host immune defenses and leading to lethal bacterial infection [89]. However, the present study did not inoculate *Vibrio* pathogens into the seawater alongside OsHV-1, which would have ensured the presence of a bacterial pathogen with capacity to kill oysters. It is possible that the oysters used in this study did not contain any known pathogenic bacteria from the start of the experiment, which would have been necessary to see the difference between antibiotic treated versus untreated oysters. Alternatively, the viral infection may have been highly potent and efficient in dampening oyster immune response in the specific experimental setting used, whereas a weaker viral infection would have permitted a stronger effect of the antibiotics on survival. Therefore, antibiotics did not offer any additional survival benefit, even if they altered activity of opportunistic bacteria within the oyster microbiome. In other words, the OsHV-1 San Diego Bay microvariant can kill oysters independently of other infections under the right conditions. This experiment focused on juvenile stage oysters, but age has been found to play an important role in

OsHV-1 susceptibility [146]. As such, these results may not directly apply to other age groups, such as oyster seed or adults.

Oyster Infection Experiment #2 - Microbiome:

Bacterial community diversity deteriorates as OsHV-1 induced disease progresses to mortality. Microbial alpha diversity metrics, such as Shannon's and Simpson's indices, remain unchanged following exposure of Pacific oyster spat to an OsHV-1 microvariant in New Zealand [126], but these metrics do not portray specific changes in either richness or evenness, which can change in themselves without impacting Shannon's or Simpson's diversity. Microbe richness increases after OsHV-1 exposure but decreases as the oysters display illness symptoms, and then die. Based on previous studies, both absolute abundance of bacteria and number of different bacterial species commonly increase during OsHV-1 infection [89,125,147]. De Lorgeril et al 2018 refers to this period as a destabilization of the bacterial community, which coincides with a decrease in antimicrobial products [89]. Oyster defenses against bacteria are likely suppressed by viral infection and this disturbance likely promotes the growth of bacteria which were previously susceptible to host immune responses. Once the oyster has died, there is no more host immune response to bacterial invaders and no control over the bacterial community within the tissue. This allows for the bacteria community to shift based on environmental controls and competition for resources rather than host mitigation. At this point, the community has likely shifted to a state of decomposition favoring oyster spoilage bacteria [148] and appears to select for dominance of fewer bacterial groups. This is further reflected by the paired drop in evenness when oysters become visibly sick. Bacteria previously promoted by the oyster immune system have likely lost protection with a deficient immune response. As the oysters immune system is weakened by viral proliferation, microbes are also able to proliferate [147], but competition between bacteria

leads to winners and losers in the oyster microbiome. Certain taxa outcompete others and grow in abundance, while many other taxa die out, leaving an uneven distribution of bacterial abundances. In other studies, evenness was found to predict oyster survival against OsHV-1, as resistant oyster families started off with higher bacterial evenness measurements and maintained high evenness during infection [87]. Evenness is an important measure to consider with OsHV-1 infection because the imbalance of bacteria in susceptible oysters is likely an additional stress to the host. Taken together, the changes in richness and evenness are likely due to a weakening immune system brought on by viral infection, which leads to a re-assembling of the bacterial community and a transition towards an opportunist-dominated microbiome and eventually mortality.

Community composition is significantly impacted by OsHV-1 exposure. After OsHV-1 exposure, there is a significant shift towards a new community of bacteria. This community is highly similar between alive and sick oysters (Fig. 11). Multiple studies show a strong shift in the microbiome from before to after OsHV-1 exposure [87,126], with the greatest change occurring after 24 hours of exposure [89,125]. This change likely occurs alongside exponential viral replication and dysfunction of hemocytes [89,125]. Although oysters were not sampled until at least 4 days after exposure in this study, the shift in the microbiome likely occurred after just 24 hours if the disease behaves similarly to prior studies [89,125]. There is strong overlap between alive and sick oysters in hierarchical clustering analysis. Some of the dead oysters are also close in microbial composition to alive and sick oysters, one explanation for which is that they died more recently and are yet to decompose. Disease states were subjectively assigned based on behavior and appearance, but microbial composition may do a better job at suggesting disease stage than visual appearance and could even provide an estimation of time since death

[149]. Another shift in composition happens once oysters die. Similar to alpha diversity, this likely results from a lack of host control over the microbial community, causing exclusion of certain bacteria and favoring decomposing bacteria. The timing of viral replication is likely the most important factor dictating microbial community composition, as demonstrated in previous studies [89,125], as opposed to visual characteristics of exposed oysters. Therefore, the taxa responsible for these shifts in composition may be closely linked to OsHV-1 replication and altered hemocyte function.

Certain bacterial taxa were significantly associated with the transition between disease states. The only bacteria group found to significantly decrease in any comparison was cyanobacterial family Coleofasciculaceae, which was far less represented in sick oysters compared to pre-exposure oysters. This family of cyanobacteria has not been reported in oyster tissue before, preventing a thorough assessment of whether the loss of the bacteria is a sign of declining oyster health. Taxa found in mostly live and sick oysters that were exposed to OsHV-1 may take advantage of the host's compromised state. In this study, these taxa include Akkermansiaceae, *Flavilitoribacter*, *Vibrio*, *Kiloniella*, *Amphritea*, Verrucomicrobiales genus Arctic95d-9, *Eionea*, and Micavibrionaceae TMED2. Each of these taxa were also important for predicting whether oysters fit into pre- or post-OsHV-1 exposure status. *Vibrio* and *Amphritea* specifically have been identified in association with OsHV-1 infected oysters across many studies [89,117,125,126] and increased in this study with increasing severity of disease state. Additionally, *Arcobacter* was found to be important for distinguishing between exposed and unexposed oyster samples, although the genus itself was not identified in the differential abundance analysis between disease states. Of all these taxa, *Arcobacter*, *Vibrio* and *Amphritea* were found to have significantly higher transcriptional activity than other bacteria during OsHV-

1 infection in Clerissi et al 2023. Some of these bacteria may be functionally complementary and take advantage of the weakened host state [125]. On the other hand, certain *Vibrio* species are known to act synergistically with OsHV-1 to accelerate the disease, working in tandem to cause hemocyte damage and impair immune defenses [127]. *Peredibacter* is another bacteria overrepresented in exposed oysters of all states which has been seen with OsHV-1 infection before but only early on in infection [125]. Other bacteria in this study were found to be primarily associated with mortality or predictive of whether oysters were alive or dead, such as *Pseudoaltermononas*, *Phaeobacter* and Cryomorphaceae. *Pseudaltermonoas* and *Phaeobacter* were also found to be associated with OsHV-1 in Clerissi et al 2023, but only *Pseudaltermonoas* demonstrated high transcriptomic activity during infection [125]. Cryomorphaceae was overrepresented in OsHV-1 infected oysters in both Clerissi et al 2023 and de Lorgeril 2018 [89,125]. In this study, *Pseudalteromonas* and *Phaeobacter* are more unique to dead oyster samples, which may either suggest that they have an important role in the disease progression, alongside *Arcobacter*, *Vibrio* and *Amphritea*, or they are just coincidental with dying tissue. *Arcobacter* and *Pseudoalteromonas* were found to be some of predominant spoilage or decomposing bacteria in oyster gills [148], but this does not rule out their potential to be opportunistic oyster pathogens. In conclusion, despite differences in OsHV-1 microvariant and temperature thresholds, similar bacteria are found to associate with OsHV-1 induced disease across many studies. *Arcobacter*, *Vibrio* and *Amphritea* and *Pseudoalteromonas* are most likely to be interconnected with OsHV-1 induced disease and further research should follow up on their potential to work in concert with OsHV-1 to kill oysters.

Conclusion:

In the present study, mortality of oysters was significantly impacted by the interaction between temperature and OsHV-1 exposure. The San Diego Bay OsHV-1 microvariant can infect, but not kill, oysters when temperatures are 15°C or below. OsHV-1 can kill oysters faster at 21 and 24°C, which are typical summer temperatures experienced in San Diego Bay. Bacterial communities are significantly altered by OsHV-1 exposure but suppression of bacteria did not significantly lower mortality rates. OsHV-1 may shape bacterial community structure by altering host immune response, leading to an initial increase in bacterial richness followed by a dominance of a few bacteria. The microbiome composition is predictive of disease status, likely more so than visual observation of slow valve closing symptoms. Similar bacteria (Arcobacter, Vibrio and Amphritea and Pseudoalteromonas) were found to associate with OsHV-1 induced disease across this and multiple other studies despite differences in OsHV-1 microvariants and temperature thresholds. Overall, this study determined that temperature is important for predicting OsHV-1 San Diego Bay microvariant induced mortality, but it is unknown which factors instigate a transmission to previously unexposed oysters in natural conditions in San Diego Bay. This study also importantly recognized a high abundance of 4 conserved taxa which are almost always detected in OsHV-1 exposed oysters but had not previously been demonstrated for the San Diego microvariant and oysters from California. Future research should further investigate the interactions between these bacterial taxa and OsHV-1 to better understand their roles in oyster mortality and disease progression.

Data Availability:

All 16S rRNA amplicon DNA sequences are deposited publicly in the European Nucleotide Archive at study accession PRJEB72643. The scripts for analyzing data generated in this study are publicly available at https://github.com/ekunselman/OsHV-1.

Acknowledgements

Chapter 2, in full, has been submitted for publication at the Applied Microbiology International Journal of Sustainable Microbiology as of April 15th, 2024. Emily Kunselman, Daysi Manrique, Colleen Burge, Sarah Allard, Zachary Daniel, Guillaume Mitta, Bruno Petton, Jack A. Gilbert. Temperature and microbe mediated impacts of the San Diego Bay ostreid herpesvirus (OsHV-1) microvariant on juvenile Pacific oysters. The dissertation author was the primary investigator and author of this paper. Thank you to the Hog Island Oyster Company for donating the oysters used in this study. Thank you to Darren de Silva at the USDA Pacific Oyster Genome Selection Project (POGS) for preparing and sending the algal cultures used in this study. Thank you to the UCSD Microbiome Core for quality library preparation and sequencing to generate the 16S rRNA amplicon data analyzed in this study. This research was funded by the American Malacological Society, Conchologists of America and the Western Society of Malacologists.

Chapter 3 ABALONE WITHERING SYNDROME

Chapter 3.1 METAGENOME-ASSEMBLED GENOME OF WITHERING SYNDROME CAUSATIVE AGENT, '*CANDIDATUS* XENOHALIOTIS CALIFORNIENSIS', FROM ENDANGERED WHITE ABALONE (*HALIOTIS SORENSENI*)

Abstract:

The genome of '*Candidatus* Xenohaliotis californiensis' was assembled from shotgun metagenomic sequencing of experimentally infected white abalone. 91% genome completeness was achieved with low contamination. This provides further insight to an uncultured bacterial pathogen and opportunity to further investigate its functionality.

Announcement:

White Abalone (*Haliotis sorenseni*) in the Captive Breeding Program at UC Davis Bodega Marine Lab were experimentally infected with the intracellular bacterial pathogen, '*Candidatus* Xenohaliotis californiensis' (*Ca*Xc) using header tanks with infected abalone. *Ca*Xc is uncultured and falls in the order Rickettsiales. *CaXc* presence and quantification was determined using *CaXc*-specific quantitative PCR [150] and 16S rRNA amplicon sequencing of the V4 region using primer pair 515F–806R [129]. Post esophagus, digestive gland tissue and fecal matter were all sampled, with some containing over 99% of *Candidatus* Xenohaliotis reads. One post-esophagus and one digestive gland sample from different abalone were chosen for shotgun metagenomic sequencing due to dominance of pathogen DNA. A fecal sample with 20% of *Candidatus* Xenohaliotis reads was also sequenced due to an expectation of lower host DNA contamination. The goal of shotgun metagenomic sequencing was to obtain a genome for the abalone pathogen, *Ca*Xc, which causes withering syndrome in many abalone species.

DNA was extracted by the UCSD Microbiome Core using the Applied Biosystems MagMax Ultra Nucleic Acid Isolation Kit (cat #A52358). Library preparation was conducted by the UCSD Microbiome Core using the KAPA Hyper Plus Kit (Roche Diagnostics, USA).

Sequencing was conducted by the UCSD IGM Genomics Center on the Illumina NovaSeq 6000 platform with paired-end 150 base pair cycles.

A protocol for assembling draft genomes from metagenomic sequencing reads was followed in KBase [151]. Read quality was assessed with FastQC v0.12.1. 18,524,162 sequences were obtained across all 3 samples and sequence quality remained above 30 for all bases. Trimmomatic v0.36 was used to trim adapters and pair forward and reverse reads [152]. Following this, 12,667,415 paired sequences were retained. metaSPAdes v3.15.3 was chosen for assembly based on best contig length, high N50 and low L50 [153]. Contigs were binned using MaxBin2 v2.2.4, MetaBAT2 v1.7, and CONCOCT v1.1 and DAS tool v1.1.2 was used to optimize bins from all outputs combined [154–157]. 3 bins were generated, one of which had 83 genomes, was from the order Rickettsiales and was suspected to be the *Ca*Xc genome.

To confirm the identity of the assembly as *CaXc*, the 16S rRNA gene sequence was extracted using ConTest16S [158] and compared to reference genomes using NCBI's BLASTn. The sequence shared 99% similarity across 99% of the query with 'abalone withering syndrome agent' and 100% similarity across 88% of the query with '*Candidatus* Xenohaliotis californiensis'. This confirmed that the genome assembly is that of *Ca*Xc, the abalone pathogen in our experiment.

N's in the *Ca*Xc assembly were removed before it was uploaded to MicroScope Microbial Genome Annotation and Analysis Platform v3.16.2 [159]. This platform identified 1,054 coding sequences in the 1,095,060 base pair long genome. CheckM [160] determined that the assembly had 91.1369% completeness and 1.18% contamination with 25 marker genes missing and 3 markers duplicated. *Ca*Xc is a gram-negative bacterium and the genome has a GC content of 30.99%. A majority of genes were unknown (40.61%) or unclassified (59.39%).

Data Availability:

The *Ca*Xc genome is publicly available through ENA project accession PRJEB68339 and sample accession ERS17938213.

Acknowledgements

Chapter 3.1, in full, has been accepted for publication by ASM Microbial Resource Announcements. Emily Kunselman, Sarah Allard, Colleen Burge, Blythe Marshman, Alyssa Frederick, Jack Gilbert. This work was funded in part through contract P1970003 from CDFW to UC Davis, through a federal NOAA Section 6 Grant NA19NMF4720103 to CDFW. All work with white abalone was performed under the Endangered Species Act (ESA) permit for white abalone (Invertebrate Enhancement Permit 14344-2R) held by UC Davis. This publication includes data generated at the UC San Diego IGM Genomics Center utilizing an Illumina NovaSeq 6000 that was purchased with funding from a National Institutes of Health SIG grant (#S10 OD026929). The LABGeM (CEA/Genoscope & CNRS UMR8030), the France Génomique and French Bioinformatics Institute national infrastructures (funded as part of Investissement d'Avenir program managed by Agence Nationale pour la Recherche, contracts ANR-10-INBS-09 and ANR-11-INBS-0013) are acknowledged for support within the MicroScope annotation platform.

Chapter 3.2 ABALONE WITHERING SYNDROME: THE CASCADING MICROBIAL IMPACTS OF ONE BACTERIAL INVADER.

Abstract:

Candidatus Xenohaliotis californiensis (*Ca*Xc) is an intracellular pathogen that infects abalone gastrointestinal tract tissue, causing Withering Syndrome, characterized by starvation and mortality. While previous research highlights *Ca*Xc's impact on gut morphology, its effects on the abalone microbiome, host gene expression, and consequently the overall impact on abalone health remain poorly understood in stages prior to clinical symptoms appearing. White abalone are highly susceptible to Withering Syndrome and are severely endangered. To better understand how this pathogen impacts white abalone, this study characterizes the microbiome of abalone gastrointestinal tract tissues (post esophagus, digestive gland, distal intestine), gut contents, and feces under pathogen exposure compared to baseline conditions. An 11-month time series was carried out to examine trends in pathogen load, fecal microbiome diversity and composition post *Ca*Xc exposure via fecal transmission. At the end of the 11-month exposure period, white abalone tissues were assessed for microbiome diversity, composition, and gene expression patterns. Results show the volatile nature of the white abalone fecal microbiome over time and a small but significant impact of *Ca*Xc exposure on the fecal microbiome. Differential infection, impacting early digestive tract greater than late digestive tract, leads to a drop in microbial evenness and loss of many taxa (including *Mycoplasma*, *Vibrio* and *Psychrilyobacter*). Transcriptional responses to *Ca*Xc vary between post esophagus and digestive gland tissue. All results are taken in the context of a phage infected *Ca*Xc, which likely reduced pathogenicity and explains a lack of visible withering symptoms in the white abalone used in this study.

Introduction:

Withering Syndrome in abalone is caused by a Rickettsiales-like prokaryote which infects the digestive or gastrointestinal tract [161]. The unique name of the pathogen is *Candidatus* Xenohaliotis californiensis (*Ca*Xc) [161]. This pathogen is obligately intracellular [162], dividing in the cytoplasm of host cells [161] like many Rikettsiales bacteria [163]. They are able to cause significant damage to cell structure and move between adjacent cells via adhesion and direct cell-cell contact as they are non-motile but able to bind to host cells and manipulate host gene expression [163]. Infection leads to disruption of gut morphology, starvation, shrinking of the foot tissue and mortality [162]. Infection and mortality rates may increase exponentially although this takes place over long periods of time, typically around 6 months [162]. More clinical signs of withering occur at warmer temperatures [162]. *Ca*Xc has been documented in wild black, white and red abalone on the North American coast [162] (personal communication with J Moore and B Marshman). A phage has evolved to infect *Ca*Xc and can induce morphological changes of the *Ca*Xc bacteria [162,164]. The phage delays and reduces *Ca*Xc load and mortality of abalone [162,165]. Infected abalone can be treated and completely clear the infection with oxytetracycline baths [166]. Of utmost concern are captive abalone because of the proximity of the animals, but proper husbandry practices can minimize this risk [162].

White abalone (*Haliotis sorenseni*) are a critically endangered species of abalone along the west coast of North America. Overfishing decimated the white abalone population before Withering Syndrome started appearing [167]. White abalone were the first ever invertebrate to be listed as an endangered species (Federal Register 66 (103), 29046-29055, 29 May 2001). There are too few white abalone in the wild to reproduce on their own, thus a captive breeding program was established and is now centered at the University of California Davis Bodega Marine

Laboratory. White abalone are one of the abalone species that is highly susceptible to Withering Syndrome [162,168]. Few studies to date have looked at the impact of Withering Syndrome in white abalone, but published work focuses on the response of the microbiome and treatment by oxytetracycline [23,169]. While antibiotic treatment temporarily reduces bacterial alpha diversity in the gut of white abalone, it does not cause negative long term impacts and is a useful tool for preventing reinfection [23]. Withering Syndrome has been documented in captive white abalone but not wild white abalone, despite the presence of *Ca*Xc in wild broodstock (unpublished). Hence the use of antibiotic treatment to eliminate *Ca*Xc infections is practical specifically in captive settings.

Other bacteria within abalone are likely to experience effects of *Ca*Xc infection due to bacterial interactions and impacts on host gene expression. However, gene expression in *Ca*Xc-infected abalone is severely understudied and the only results, which come from pinto abalone, found no significant change in expression of immune genes in response to infection [170]. It is expected that phagocytosis, apoptosis and antimicrobial production would be some primary methods of immune defense, similar to other abalone species and other mollusks [171–173]. However, without any immune expression data, it is unclear how the pathogen may be impacting abalone immune function. Therefore, it is also unclear how host immune response to a pathogen would impact other bacteria within the digestive tract. On the other hand, *Ca*Xc-exposed pinto abalone did show upregulation of receptors involved in feeding signaling, which demonstrates stress related to feeding [170]. It is possible that this stress would cause dampened immune function and led to a reduction of immune system expression [172]. Bacteria are important for both digestion and defense and could contribute to both the nutritional health and pathogen defense within abalone. Bacteria may be used as probiotics for abalone to support disease

resistance [46] and may assist in seaweed digestion [47]. It has previously been shown that overall bacterial community diversity is reduced during *Ca*Xc infection [23]. Instead of defending against the pathogen, it is possible that the bacterial community turns dysbiotic with infection [41]. Discovery of new or existing multiple pathogen infections are becoming more common in marine organisms and this could be the case in abalone [162]. Maintaining bacterial diversity may be a critical component of abalone resistance or tolerance to *Ca*Xc [41].

As *Ca*Xc primarily infects the gastrointestinal tract, starting at the post-esophagus, 3 different gastrointestinal tract tissues as well as feces were targeted for response to *Ca*Xc in this study. *Ca*Xc can transfer via feces into a new abalone, and this was used to both experimentally infect naïve abalone and as a reason to assess the fecal microbiome after exposure to *Ca*Xc. Feces are also the only non-invasive sample collected in this study and allowed an extraordinarily long time series of fecal pathogen load monitoring and microbial response. At the end of the study, abalone were sacrificed to obtain gastrointestinal tract tissues from the post-esophagus, digestive gland and distal intestine. These samples were analyzed for both microbiome characterization and abalone gene expression. The goal of this study was to determine how *Ca*Xc exposure impacts both the white abalone and its microbiome.

Methods:

Pathogen-free recipient white abalone were available on site at the UC Davis Bodega Marine Laboratory. Seven days prior to the start of the experiment, abalone were placed into individual tanks with flow-through seawater and aeration and acclimated in these conditions. Four days prior to the start of the experiment, abalone were fed with a local batch of local kelp (*Macrocystis pyrifera*). At the start of the experiment (day 0), fecal samples were collected from abalone tanks using transfer pipettes. In addition to fecal samples, 5 acclimated abalone were

sacrificed and dissected for post-esophagus, digestive gland, distal intestine and gut contents. Gut contents were collected by pinching the distal intestine with a sterile blunt tool and pushing its contents out the end. These tissues were split in 2, with one half placed in RNAlater and the other immediately frozen at -80°C. After the first round of fecal and tissue samples were taken, a few *Ca*Xc-positive or negative abalone were placed in the respective header tanks. Fecal samples were spun down, and the supernatant was discarded. The pellet was resuspended for transfer into a 1.5 mL cryogenic tube, spun down again and the supernatant was discarded. These pellets were frozen at -80°C and shipped to the Scripps Institution of Oceanography for extraction. Fecal samples were taken once a month for the next 10 months following the same procedure. Abalone were fed a combination of kelp (*Macrocystis pyrifera*) and dulse (*Palmaira mollis*) ad libitum as each species was available. On the final day of collection at 11 months, fecal samples were collected and then all remaining abalone were sacrificed and dissected for post-esophagus, digestive gland, distal intestine and gut contents. Any animals that became moribund prior to the end of the experiment were sacrificed and dissected for their digestive gland only, because other tissues were too decomposed to retrieve.

Extraction and Sequencing:

Fecal matter and tissue samples were transferred to an extraction tube using a sterile swab. The UC San Diego Microbiome Core performed nucleic acid extractions utilizing previously published protocols [174]. Briefly, samples were purified using the MagMAX Microbiome Ultra Nucleic Acid Isolation Kit (Thermo Fisher Scientific, USA) and automated on KingFisher Flex^{T} robots (Thermo Fisher Scientific, USA). Some of the fecal sample extracts were additionally cleaned with AMPure XP magnetic beads (Beckman Coulter). Blank controls and mock communities (Zymo Research Corporation, USA) were included and carried through

all downstream processing steps. 16S rRNA gene amplification was performed according to the Earth Microbiome Project protocol [175]. Briefly, Illumina primers with unique forward primer barcodes were used to amplify the V4 region of the 16S rRNA gene (515F-806R, [62,129]. Amplification was performed as single reactions per sample [176], then equal volumes of each amplicon were pooled and the libraries sequenced on the Illumina NovaSeq 6000 sequencing platform with paired-end 150 bp cycles at the Institute for Genomic Medicine (IGM), UC San Diego.

RNA extraction was performed on tissue samples preserved in RNA later, which were shipped over dry ice to Scripps Institution of Oceanography. RNA was extracted using the Qiagen RNeasy mini kit (cat. #74004). Quantification and quality checks were performed by submitting the RNA for a Bioanalyzer run through UCSD IGM. Five randomly selected abalone each from both the exposed and control groups were submitted to UC Davis Genome Center for Poly-A depletion, library prep, and RNA sequencing. The sequencing was carried out at the DNA Technologies and Expression Analysis Core at the UC Davis Genome Center. Each abalone had two different tissue types (post-esophagus and digestive gland) which were sequenced.

qPCR:

Extracted DNA was sent back to the Bodega Marine Lab in plates over dry ice. Quantitative PCR of the *Ca*Xc pathogen was conducted using primers and a custom Taqman probe designed by Friedman et al 2014 [150]. 96-well plates were set up with 10 uL of Applied Biosystems Taqman Gene Expression Master Mix (cat #4369016), 0.26 uL of each 25 uM primer (WSN1-F/WSN1-R), 0.04 uL of the 100 uM stock probe, 0.6 uL of BSA and 6.84 uL of nuclease-free water in each well. A plasmid stock of the WSN1 gene was run in duplicate with 1

to 10 dilutions from 3 million down to 3 copies. Negative controls of nuclease-free water were run in duplicate on every plate. DNA template was run in duplicate and absolute quantity was determined by using the equation of the standard curve to convert the fluorescence value to the copy number per ng of genomic DNA and then taking the average between the two duplicates. Values below 3 copies were converted to 0 because 3 is the limit of detection for this qPCR assay. To address zeros in the qPCR data, a pseudo count of 1 was added to the average copy number of every sample. Pathogen load was then normalized by dividing the copy number by the concentration of input DNA per sample. Values are either reported in $\log_{10}$ of the normalized copy number or the axis is adjusted as a log scale.

Sequence Analysis:

Paired end sequences were demultiplexed in qiime2 [65] and denoised by DADA2 [133], which produced exact amplicon sequence variants (ASVs) for analysis. In qiime2 [65], data was cross-checked with controls using Bray Curtis beta diversity PCoA plot assessment. Four samples were closely clustered with controls, so these samples were removed from the analysis. Sequences were re-clustered after filtering out errant samples and all positive and negative controls. Sequences were trimmed to a length of 150 base pairs, forward and reverse reads were merged with vsearch [177], and filtered by Q score using qiime2 quality filter to remove low quality sequences. Clustering was re-performed with the Deblur program [64], which removes probable artifact sequences produced by the sequencing machine. Sequences were aligned with the Silva 16S database [73]. Any sequences matching to chloroplast or mitochondria were filtered out. A phylogenetic tree was built using SEPP fragment insertion [71]. Alpha rarefaction curves were created to determine the number of observed ASVs at which observed richness and

diversity plateaued. Rarefaction depths for diversity analyses were informed by the number of observed ASVs per depth and the number of samples retained at each sampling depth.

The first analysis focused on changes in fecal microbiome with time and across conditions. The Deblur table was filtered to retain only fecal samples from animals which remained alive for the entire experiment and was rarefied at 58,660 sequences per sample. Longitudinal Weighted UniFrac volatility between conditions was plotted with the q2 longitudinal plug in [68,69,178]. Pairwise distance from time point zero (prior to exposure) to 11 months post-exposure was compared between the control and *Ca*Xc-exposed treatments with a Kruskal Wallis test to determine if there was a larger change in the microbiome in one treatment compared to the other. Fecal samples were then subset by time of collection and analyzed for their Weighted UniFrac distances and the control and exposed treatments were statistically compared with a PERMANOVA test using the adonis command in qiime2. The qiime2 deblur table subset by fecal samples was imported into R as a phyloseq object using the Qiime2R package [179] and converted into a Tree Summarized Experiment (tse) object using the mia package. Maaslin2 [180] was run on fecal samples with a fixed effect of time (reference = Time, 0) and random effect of tube id to account for repeated sampling of the same animals. A linear model was used in Maaslin2 after TSS normalization and an 85% prevalence filter to focus on the most common features, corresponding to the use of weighted UniFrac to display sample distances. The top 4 most significant features changing over time are plotted in Figure 13, Panel D. Next, the phyloseq [135] object was subset to only look at the final collection time point and compare the most differentially abundant features between the control and exposed condition. Maaslin2 was run with a fixed effect of treatment (reference = Treatment, Control) and the same

parameters as listed prior. The top 4 most significant features differing between control and exposed abalone fecal samples are displayed in Figure 13, Panel E.

The second analysis focused on differences between sample types and the impact of *Ca*Xc exposure on the typical microbiome differentiation between tissue types and feces. In qiime2, the Deblur table was filtered to retain only samples from the final collection time point (all sample types included). Tables were subset into either control (n=44) or exposed (n=44) abalone samples from the final collection. The control table was rarefied at 43,246 sequences while the exposed table was rarefied at 28,738 sequences to accommodate the maximum number of observed ASVs while retaining most of the samples. Alpha diversity focused on measurements of evenness and beta diversity focused on weighted UniFrac distances to display differences in microbiome by sample type (Figure 13, Panels B & C). Alpha diversity plots were constructed in R using the microbiome package to estimate evenness and ggplot2 [181] to create figures. Beta diversity plots were constructed in Emperor from qiime2 distance matrices [182]. A Kruskal Wallis test was used to statistically compare evenness across sample types while a PERMANOVA was used for weighted UniFrac distances. Maaslin2 was utilized again to model differentially abundant features between fecal samples and tissue samples, and between exposed and control abalone. Fixed effects of both sample type (reference = Fecal) and treatment (reference = Control) were used with the same parameters as described previously. The top 50 most significant features identified in either comparison (Tissue/ Fecal or Exposed/ Control) is plotted in the heatmap from Maaslin2 in Panel D of Figure 13. Values were log transformed to demonstrate whether there was a positive or negative change from one sample set to the other.

The third analysis focused on different levels of impact from *Ca*Xc exposure in each tissue type. The deblur table with only samples from the final collection point was subset again

to remove fecal samples. The table was converted to a phyloseq object in R and samples were merged by either (1) tissue type or (2) treatment using summation of all features into one representative sample per tissue type. The microViz package [183] was used to generate taxonomic bar plot visualizations shown in Figure 15, Panel A. The top 10 most abundant features are listed by name, while the remaining portion of features is compiled as "other". In qiime2, samples from each tissue type were subset into their own tables for core diversity metrics analysis. To compare pathogen load to microbial richness, Faith's Phylogenetic diversity [184] was calculated and plotted against the $\log_{10}$ transformed, normalized copy number of *Ca*Xc in the sample (Figure 15, Panel B). Points are also colored by treatment, but statistical analysis of correlation was performed on normalized copy numbers versus Faith's PD values. To compare presence and absence of bacteria between exposed and control abalone, unweighted UniFrac distances were generated and plotted in PCoA plots in Figure 15, Panel C. Statistical comparisons of beta diversity were performed between control and exposed abalone using PERMANOVA tests. Finally, in Panel D of Figure 15, ANCOM-BC [137] was run in R on tables with either post esophagus or distal intestine samples individually. In R, either table was converted to a tse object and differential abundance between treatments was analyzed with ANCOM-BC, using a prevalence cutoff of 0.1 to include potentially rarer bacterial species, in line with the use of unweighted UniFrac beta diversity analyses. ASVs were grouped at the genus level. The ANCOM-BC output was filtered to a table containing only significantly different features (alpha < 0.05). The plots in Panel D of Figure 15 display $\log_{10}$ fold changes from the control to the exposed groups. Features are colored according to the group in which they are overrepresented.

Two tissue samples were also sent for shotgun metagenomic sequencing as described in Kunselman et al 2024 (Chapter 3.1). Each sample was from a different abalone, one digestive gland sample and one post esophagus sample, but both were from the *Ca*Xc-exposed condition on the final collection in April 2022. Both abalone tested positive for *Ca*Xc by qPCR with a high pathogen load and contained over 99% relative abundance of *Candidatus* Xenohaliotis 16S rRNA sequence reads. The DNA in these samples was used to build a draft genome of the *Candidatus* Xenohaliotis californiensis pathogen. In addition to the methods described in the genome announcement (Chapter 3.1), Kaiju [185] taxonomic classification was run on the raw metagenomic reads to search for presence of the *Ca*Xc phage [164,165].

The final analysis focused on the gene expression patterns between control and exposed abalone. RNA sequences were trimmed to remove adaptors, polyX sequences and polyA tails using fastp [186]. Reads were also quality filtered with fastp to remove sequences below 50 base pairs, with low quality scores, and with unmatched forward or reverse reads in the dataset. FastQC was used to confirm the trimming and quality filtering steps were successful [187]. Trinity v2.15.1 was used for de novo assembly of the transcriptome of the white abalone, producing 737,166 genes and 1,137,019 transcripts [188]. Median contig length was 395 base pairs. Transcript abundance was estimated using RSEM [189] and a gene counts matrix was generated for differential expression analysis. Functional annotation of the genes was performed with Trinotate v4.0.2 [190]. Differential expression analysis was run in R using DESeq2 [191]. DESeq2 data sets were subset into either post esophagus or digestive gland samples and filtered to remove low abundance genes (< 10 reads) per group. DESeq2 was run to compare exposed to control abalone. Principal Component Analysis with a variance stabilizing transformation was computed to look at overall differences in gene expression between conditions. The DESeq2

results were filtered to retain only significantly differentially expressed genes with p value less than 0.05 and Log2FoldChange greater than 2. This was performed separately for post esophagus and digestive gland samples and then the differentially expressed genes were compared with a Venn diagram using jvenn [192].

Results:

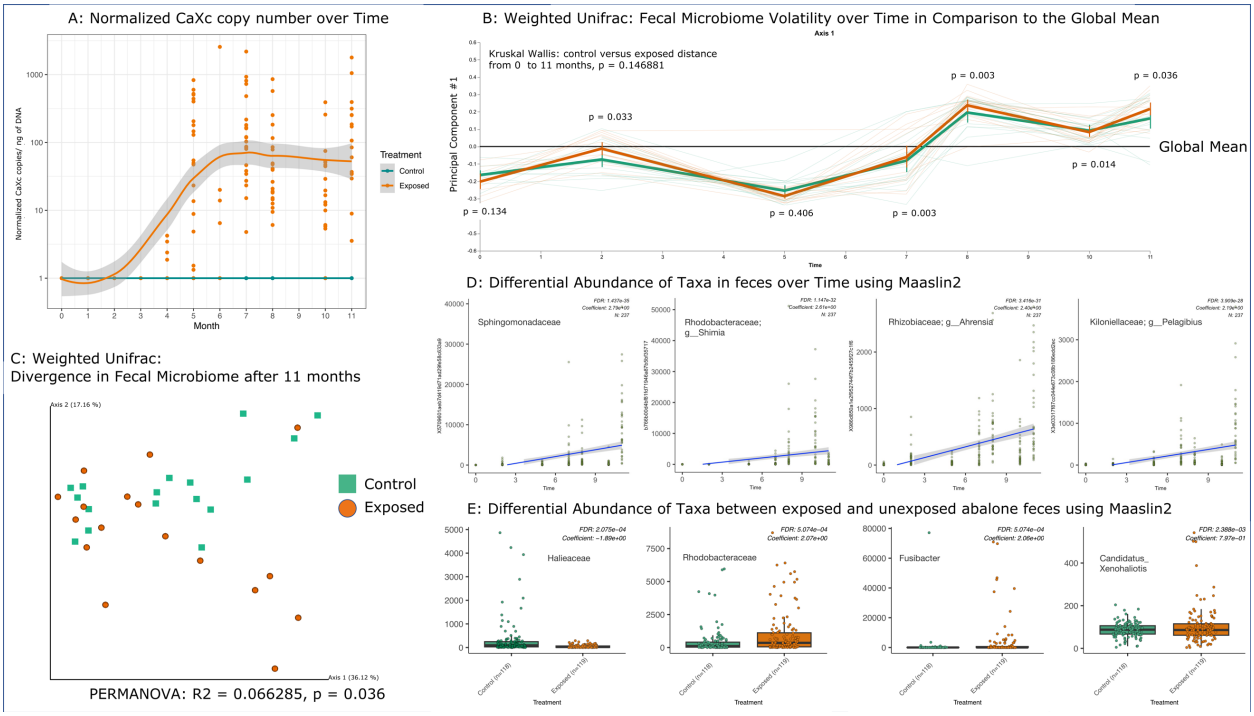

Figure 13. Abalone fecal microbiome is volatile over time and impacted by exposure to *Ca*Xc.

A) qPCR quantification of the pathogen, *Ca*Xc, normalized by DNA concentration, in fecal samples over time from pre-exposure to 11 months post-exposure. None of the control fecal samples were positive for the pathogen. Trend lines were fit with locally estimated scatterplot smoothing.

B) Microbiome Volatility analysis using q2-longitudinal. This plot shows average distance between fecal samples over time from pre-exposure to 11 months post-exposure. Each line is an individual animal tracked over time, with the bold lines demonstrating the mean value on Principal Component 1 for either the control or exposed group of animals. Principal Component 1 is shown because it was the top explanatory axis, explaining 30.49% of Weighted UniFrac distance between samples. Kruskal Wallis test compares whether the distances from 0 to 11 months post exposure were different between control and exposed groups. p values over each bend indicate whether control was different from exposed at that time point using a PERMANOVA test.

C) Weighted UniFrac beta diversity PCoA plot demonstrating quantitative and compositional differences in fecal microbiomes between Exposed and Control abalone after 11 months. A PERMANOVA test accompanies these results to demonstrate the percent of variation in the microbiome explained by treatment (6.6%) and its significance (p = 0.036).

D) Maaslin2 regression and boxplots showing ASVs responsible for differences over time and between treatments at 11 months. The top 4 explanatory ASVs are shown for both change over time and difference between treatments. Only the ASVs present in at least 85% of samples were considered for analysis. FDR is the adjusted p value of the statistical comparison, and the coefficient can be interpreted as the log fold change from the left to the right side of any plot.

Part 1: Abalone fecal microbiome is volatile over time and impacted by exposure to CaXc

All abalone which were exposed to Candidatus Xenohaliotis californiensis by infected animals in header tanks eventually tested positive (n=17). In fecal samples, the first detection of CaXc occurred at 4 months after the start of exposure (Fig13A). Copies of CaXc per ng of DNA peaked at approximately 6 months post-exposure and leveled out in consecutive months to an average of less than 100 copies (Fig13A). Copies of CaXc per ng of DNA served as a proxy for level of infection, which varied greatly across individual abalone (Fig13A). Although CaXc infection did not present its signal in the fecal samples until 4 months post exposure, the beta diversity (Weighted UniFrac principal complaint 1) of the fecal microbiota already significantly varied between exposed and control conditions after 2 months (adonis permanova, $R2 = 0.05$, $F = 2.35$, $p = 0.033$) (Fig13B). However, the beta diversity between exposed and control was again indistinguishable at 5 months post-exposure (adonis permanova, $p = 0.406$) (Fig13B). For the remainder of the experiment, the beta diversity of the fecal microbiomes significantly varied between exposed and control abalone (adonis permanova; Time = 7, $R2 = 0.08$, $F = 3.40$, $p = 0.003$; Time = 8, $R2 = 0.10$, $F = 4.15$, $p = 0.003$; Time = 10, $R2 = 0.098$, $F = 3.70$, $p = 0.014$; Time = 11, $R2 = 0.066$, $F = 2.27$, $p = 0.36$)(Fig 13B). Abalone fecal microbial community structure experienced large divergences from the global mean of the first principal component of the weighted UniFrac distance as it changed over time (Fig 13B). Beta diversity distances from the pre-exposure collection timepoint to 11 months post-exposure were not significantly different between control and exposed abalone (Kruskal Wallis, $H = 2.1$, $p = 0.146881$). In other words, the fecal microbial composition changed at the same magnitude whether abalone are exposed to the pathogen or not. Differential abundance analysis within each abalone over time revealed that the topmost explanatory features for this variation included the Sphingomonadaceae family, the

Shimia genus, the Ahrensia genus, or the Pelagibius genus (Fig 13D). The 4 most abundant ASVs explaining the variation through time tended to increase over time and their spikes in relative abundance coincided with principal component 1 values close to or above the global mean. These spikes occurred at 2, 7, 8, 10 or 11 months after the start of the experiment. Even though abalone fecal microbiomes were consistently volatile through time, some weighted compositional differences in the microbiome could be attributed to exposure by CaXc (Fig13C). Zooming in on the final collection time point, around 7% of the variation in the microbiome at this instance could be explained by exposure to the pathogen (adonis permanova, $R2 = 0.066285$, $F = 2.27$, $p = 0.036$)(Fig13C). These variations were primarily explained by the top 4 most proportional abundant ASVs in Figure 13E. From control to exposed abalone, an ASV from the Halieaceae family was largely lost (Fig 13E). Meanwhile, ASVs associated with Rhodobacteraceae, Fusibacter and Candidatus_Xenohaliotis (the pathogen itself) were overrepresented in the exposed abalone microbiomes. In conclusion, while the abalone microbiome showed significant changes over time, CaXc exposure and infection had a limited impact on community structure and the relative proportions of specific taxa.

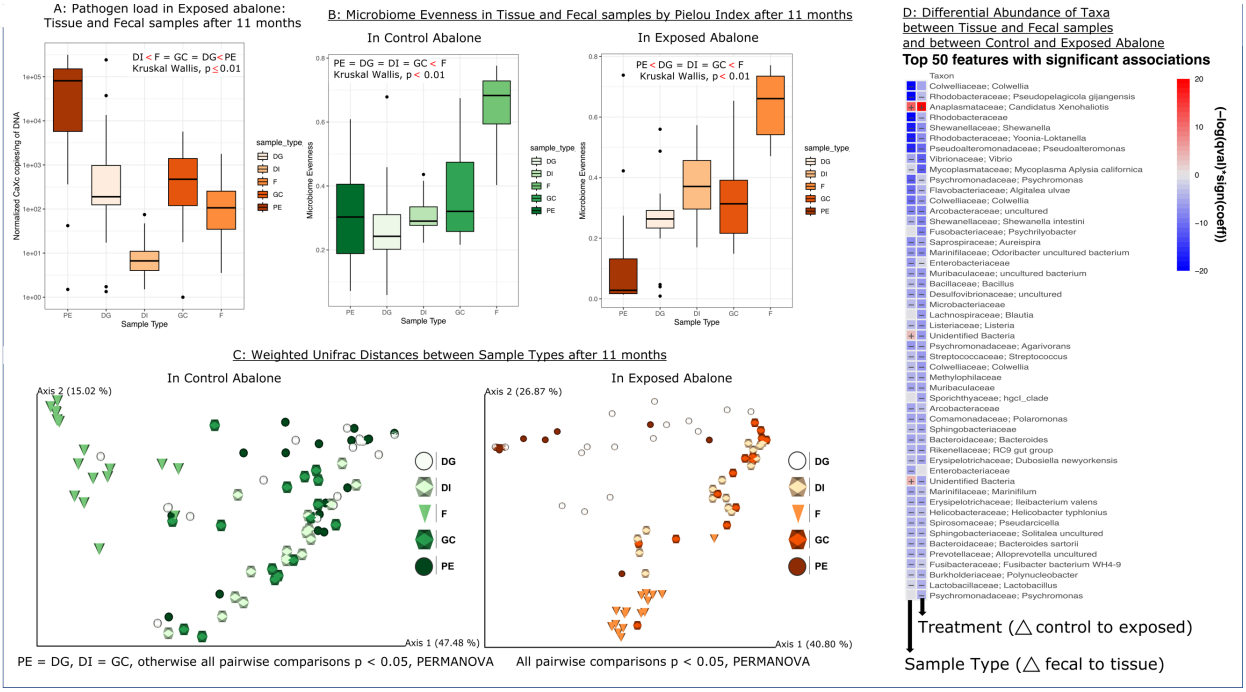

Figure 14. *Ca*Xc differentially infects early digestive tract (PE) more than late digestive tract (DI, GC, F) and this contributes to a drop in microbial evenness of the early digestive tract.

A) qPCR quantification of the pathogen, *Ca*Xc, normalized by DNA concentration in tissue and fecal samples from exposed abalone only. Kruskal Wallis and Pairwise Wilcoxon tests were performed to demonstrate whether pathogen load varied by sample type and which sample types had significantly different pathogen load, respectively.

B) Microbiome evenness by sample type, measured by Pielou's evenness metric. Kruskal Wallis and Pairwise Wilcoxon tests were performed to demonstrate whether evenness varied by sample type and which sample types had significantly different evenness, respectively. All boxplots demonstrate average value for the group, spread of data, and outliers as shown by separate dots.

C) Weighted UniFrac beta diversity PCoA plot demonstrating abundance and compositional differences in the microbiome between sample types in either control or exposed treatments. A PERMANOVA test accompanies these results to demonstrate which sample types were significantly different from one another. Similarity in microbiome of different sample types is denoted by the '=' sign.

D) Maaslin 2 heatmap for two fixed effects: sample type and treatment. ASVs are organized by row, with the family and genus (if known) indicated on the right. Differential abundance of ASVs between sample types is shown in the left column, with a red '+' indicating an increase in representation of that ASV from fecal to tissue samples, and a blue '-' indicating a decrease from fecal to tissue samples. Differential Abundance of ASVs between treatments is shown in the right column, with a red '+' indicating an increase in representation of that ASV from control to exposed samples, and a blue '-' indicating a decrease from control to exposed samples. The top 50 features with significant associations to either effect are shown ($p < 0.05$) Only the ASVs present in at least 85% of samples were considered for analysis.

Part 2: *Ca*Xc differentially infects early digestive tract (PE) more than late digestive tract (DI, GC, F) and this contributes to a drop in microbial evenness of the early digestive tract.

Pathogen load and microbial diversity varied across the sample types. The final time point was selected to assess differences in pathogen load, alpha and beta diversity between sample types in either condition, as well as the features responsible for distinguishing tissue from fecal samples and exposed from control abalone. Within exposed abalone, pathogen load was greatest in post esophagus samples and least in distal intestine samples (Fig. 14A). A few outliers existed in different tissues, demonstrating the different levels of infection between individual abalone. Although not pictured in Figure 14, the trend from greatest *Ca*Xc copies in the PE to least in the DI was consistent within individual animals as well, suggesting that the overall trend mimicked infection levels within an individual abalone. Digestive gland pathogen load was at a similar level to gut contents and fecal pathogen load, suggesting that these non-invasive samples were a proxy for digestive gland infection rate. Alpha diversity, by comparison, did not follow the same trend as pathogen load in exposed abalone (Fig 14B). In exposed abalone, the microbial evenness (Pielou's evenness metric) was inversely correlated with pathogen load in the post esophagus (Fig. 14A&B). Yet, without exposure to *Ca*Xc, evenness in the post esophagus tissue was not significantly different from other internal abalone tissues and gut contents (Fig 14B). Overall, feces has the greatest evenness (Pielou's J; Kruskal Wallis, $p < 0.01$ for Fecal-PE, Fecal – DG, Fecal – DI, and Fecal – GC; Fig. 14B). Beta diversity (Weighted UniFrac) was significantly different between feces and other sample types (adonis permanova on control abalone, F – PE $p = 0.0025$, F – DG $p = 0.0025$, F – DI $p = 0.0025$, F – GC $p = 0.0025$; Fig. 14C). In control abalone, which captured typical beta diversity trends across sample types, post esophagus and digestive gland tissue (both in the anterior portion of the digestive tract)

shared similar microbial community structure (adonis permanova on control abalone, PE – DG, p = 0.617; Fig. 14C). Gut contents which were squeezed out of the distal intestine tissue shared a similar microbial composition to the distal intestine (adonis permanova on control abalone, F – GC, p = 0.293; Fig. 14C). In exposed abalone, all sample types significantly varied in beta diversity (Fig. 14C). In pairwise comparisons, post esophagus samples were closest to digestive gland samples, followed by distal intestine, gut contents, and finally feces (adonis permanova on exposed abalone; PE – DG pseudo F = 7.385460, p = 0.002; PE – DI pseudo F = 32.977724, p = 0.001; PE – GC pseudo F = 38.012759, p = 0.001; PE – F pseudo F = 53.016694, p = 0.001). Weighted UniFrac was used as the beta diversity metric to encapsulate differences in composition and relative abundance of ASVs within each sample. This was paired with evenness data for each sample type to demonstrate that decline in evenness in the post esophagus was caused by dominance of a few ASVs, which shifted beta distances further from other sample types. The observed trends in specific features were further examined by differential abundance analysis of abundant ASVs between sample types and treatments (Fig. 14D). *Candidatus* Xenohalitois and two unidentified bacteria had a significantly greater proportion in tissue samples, while most other taxa were at a significantly greater proportion in feces (Fig. 14D). One of the unidentified bacteria was most closely related to Spirochaetaceae, but the other could not be identified further. *Candidatus* Xenohalitois was the only ASV significantly enriched in exposed samples (Fig. 14D). The strong log fold increase of *Ca*Xc in the post esophagus samples was the most likely culprit for the decrease in evenness and the divergence in beta diversity observed in exposed PE samples.

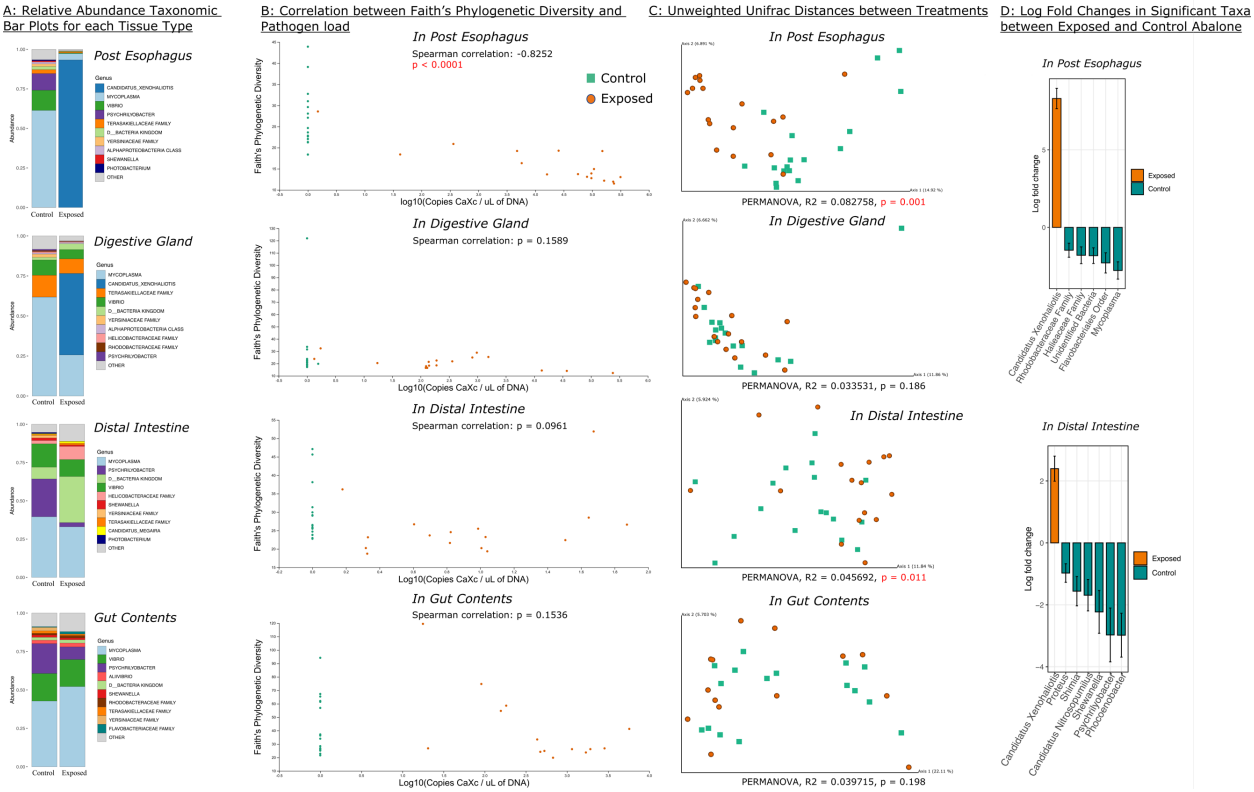

Figure 15. Changes to the exposed abalone microbiome are primarily related to replacement of key taxa by *Ca*Xc in the Post Esophagus and Distal Intestine, and to a minor extent, presence or absence of rarer ASVs.

(A) Summed Taxonomic Bar Plots demonstrate composition of each sample type across treatments. Samples of the same category were merged with Phyloseq using summation. Genus or Family are written in the legend to identify bars by color. "Other" category includes remaining, lower abundance ASVs.

(B) Scatterplots demonstrate the correlation between Faith's Phylogenetic diversity and the pathogen load of each individual animal, organized by sample type. A spearman correlation test was run to determine the significance of the correlation between diversity and *Ca*Xc copies. The correlation coefficient is included for the post esophagus samples, which were the only sample type that had a correlation between diversity and pathogen load.

(C) Unweighted UniFrac beta diversity PCoA plot demonstrating compositional differences (presence or absence and phylogenetic relatedness) between control and exposed abalone, organized by sample type. A PERMANOVA test was run to determine whether the control and exposed conditions significantly varied in their microbiome composition, and if significant ($p < 0.05$), what percentage of the variation was explained by whether they were exposed or not (R2 x 100).

(D) ANCOMBC differential abundance analysis between control and exposed abalone, within either the post esophagus or distal intestine tissues. Log fold change indicates change from control to exposed abalone. A significance cutoff of 0.05 was used to select taxa. Any taxa present in less than 10% of samples were dropped.

Part 3: Changes to the exposed abalone microbiome are primarily related to replacement of both core and rare taxa by *Ca*Xc in the Post Esophagus and Distal Intestine.

Considering the microbial compositional divergence between abalone tissues after 11 months, each tissue was analyzed separately. First, taxonomic bar plots show the summed composition of the top 10 most abundant ASVs across all control or exposed abalone for each tissue type (Fig. 15A). As suspected, post esophagus samples had a greater proportion of the pathogen, outweighing other taxa such as *Mycoplasma*, *Vibrio* and *Psychrilyobacter* (Fig. 15A). Digestive gland samples shared a similar pattern of relative abundance with post esophagus samples but with a greater proportion of Terasakellaceae and slightly lower proportion of the pathogen (Fig. 15A). In contrast to the esophagus and digestive gland, both distal intestine and gut contents samples had an absence of the pathogen in the top ten most abundant ASVs (Fig. 15A). Second, Faith's phylogenetic diversity calculated for each abalone was plotted against the pathogen load, which shows that post esophagus tissues experienced lower alpha diversity as pathogen burden increased (Spearman correlation, $r = -0.8252$, $p < 0.0001$). For all other tissue types, there was no significant correlation between phylogenetic richness and pathogen load (Fig. 15B). One of the control dots falls above zero in the digestive gland plot because this animal tested positive for *Ca*Xc by qPCR at the 11-month mark. We also compared Unweighted UniFrac beta diversity between exposed and control across tissues (Fig. 15C). In the post esophagus and distal intestine, microbial community structure was significantly different upon exposure to *Ca*Xc (Fig. 15C; PE - adonis permanova, $R^2 = 0.082758$, $F = 2.89$, $p = 0.001$; DI - adonis permanova, $R^2 = 0.045692$, $F = 1.48$, $p = 0.011$). However, no significant difference in beta diversity was observed in the digestive gland and gut content samples between treatments ($p > 0.05$; Fig. 15C). ANCOM-BC results demonstrated that in post esophagus and distal intestine

samples, *Ca*Xc dominated the community of exposed abalone with no other significantly differentiated taxa (Fig. 15D). The most significantly reduced taxa in the post esophagus (Rhodobacteraceae, Laiaceae, Flavobacteriales and *Mycoplasma*) were different from those in the distal intestine (*Proteus*, *Shimia* - within the Rhodobacteraceae family, *Candidatus Nitrosopumilis*, *Shewanella*, *Pschrilyobacter* and *Phocoenobacter*) (Fig. 15D). The ASVs with the greatest proportion that were impacted by *Ca*Xc were *Mycoplasma*, *Psychrilyobacter*, and *Shewanella* (Fig15A&D). Other ASVs identified as driving differences between control and exposed abalone were at lower proportions, or at least not included in the top 10 most abundant ASVs displayed in the taxa bar plots (Fig. 15B&D).

Part 4: Detection of *Ca*Xc phage in shotgun metagenomic data

Using metagenomic assembly techniques we assembled a 90% complete metagenome for *Ca*Xc from samples in this study (Chapter 3.1). However, we were also able to assemble two strains of the *Ca*Xc phage using the Kaiju taxonomic classification, Xenohaliotis phage pCXc-HR2015 with taxonomy ID 1933104 and Xenohaliotis phage pCXc-HC2016 with taxonomy ID 1933103. Xenohaliotis phage pCXc-HR2015 was submitted by the Centro de Investigacion Cientifica y de Educacion Superior de Ensenada in 2017. In total, 56,369 reads mapped to pCXc-HR2015 and 21 reads mapped to pCXc-HC2016. This confirmed the presence of a phage targeting *Ca*Xc in this experiment. Only a few samples were tested, so these results do not demonstrate the extent of the phage presence in all samples.

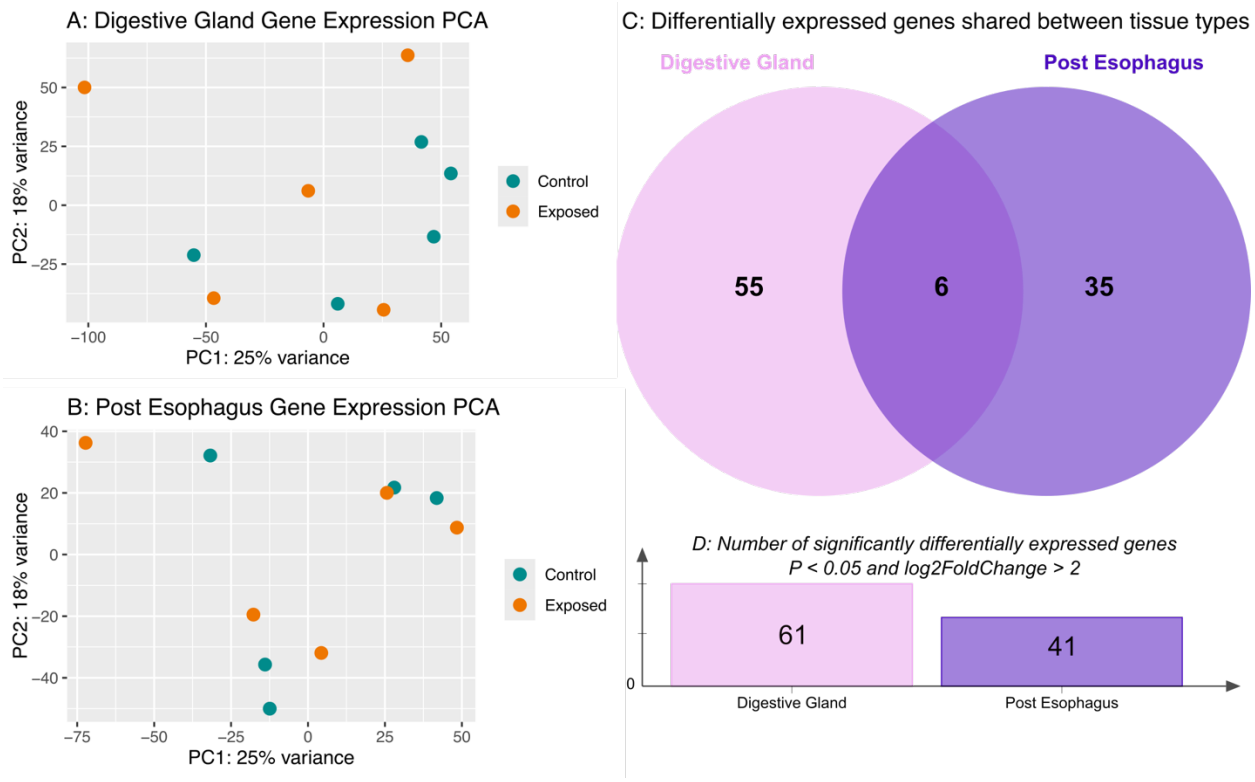

Figure 16. Gene expression in response to *Ca*Xc exposure varies between Post Esophagus and Digestive Gland.

(A) Principal Components Analysis of gene matrix for digestive gland tissue samples only. Color coded by control (n=5) and *Ca*Xc-exposed (n=5) abalone.

(B) Venn diagram produced with jvenn showcasing the number of significant gene IDs shared between digestive gland and post esophagus samples (n = 6), the number of significant gene IDs unique to digestive gland samples (n = 55) and the number of significant gene IDs unique to post esophagus samples (n = 35). Significant gene IDs are those which were found to be differentially expressed between *Ca*Xc-exposed and control abalone with a p value less than 0.05 and a log2FoldChange greater than 2.

(C) Bar plot displaying the total number of significantly differentially expressed genes in *Ca*Xc-exposed versus control abalone for each tissue type.

(D) Principal Components Analysis of gene matrix for post esophagus tissue samples only. Color coded by control and *Ca*Xc-exposed abalone.

Part 5: Differential expression of host genes between *Ca*Xc-exposed and control abalone varies by tissue.

Digestive Gland and Post Esophagus tissues were analyzed separately because the microbial response to *Ca*Xc differed between tissues. Host gene expression overlapped greatly between control and exposed abalone in both digestive gland (Fig. 16A) and post esophagus

(Fig. 16B). There was no clear separation between conditions on the most explanatory axes of the PCA. Of the genes that were significantly differentially expressed with a log fold change greater than 2, only 6 overlapped between digestive gland and post esophagus samples (Fig. 16C). The 6 genes which were significantly expressed in both tissue types were all downregulated in exposed conditions. The majority of significantly differentially expressed genes between exposed and control abalone were unique to specific tissue types. More genes were significantly differentially expressed in digestive gland tissue (n = 61) as compared to post esophagus tissue (n = 41) (Figure 16D). Unfortunately, due to low levels of gene annotation (< 9%) and poor predictive capability, functional responses to *CaXc* in white abalone could not be determined.

Discussion

The white abalone fecal microbiome is volatile over the course of 11 months and differentially impacted by exposure to *Ca*Xc between tissues. This study produced the longest time series analysis of abalone feces from *Ca*Xc-infected abalone. The pathogen *Ca*Xc is intracellular [161,162] but was detected in fecal samples after 4 months of exposure. While the pathogen load initially increased, all samples collected after 6 months remained at a similar pathogen load and no abalone showed symptoms of Withering Syndrome for the entire 11-month time series. This is likely due to the presence of the *Ca*Xc phage, which decreases the virulent impact of the *Ca*Xc pathogen [164,165]. The *Ca*Xc phage pCXc-HR2015 was detected in at least a few of the exposed abalone tanks. As such, the results presented here should be assessed in the context of a less virulent *Ca*Xc infection. In contrast to quantification of *Ca*Xc, disruption of the microbiome initially occurs at 2 months post exposure. This may indicate initial establishment of *Ca*Xc internally in the post esophagus or digestive gland without expulsion by the abalone.

Alternatively, because the microbiome does not significantly vary between control and exposed abalone at 5 months, this signal may not be a result of *Ca*Xc infection. At later time points, the microbiome of exposed abalone differs consistently from that of the control abalone, suggesting some disruption to the internal microbiome that has downstream effects on the fecal microbiome. After all, the fecal microbiome of a mollusk is typically composed of transient or excluded bacteria [193], which may differ depending on the behavior of the host immune system and other bacterial competitors.

The abalone fecal microbiome demonstrated a significant shift over the 11 months of observation regardless of exposure status. This is likely caused by a change in diet over time, because abalone were fed kelp, dulse or a mix of both at any given time, which was solely dependent on availability of either algae and equally changed for both control and exposed abalone. Diet has been previously demonstrated to cause high turnover in the fecal microbiome of oysters [81]. Across all abalone the proportion of Sphingomonadaceae, *Shimia*, *Ahrensia* and *Pelagibius* increased over the experimental period. None of these taxa have been previously found in association with *Ca*Xc [23,41,42]. Their overrepresentation may be due to changes in food over time. In fact, *Ahrensia* has previously been identified as a diet-specific bacteria in abalone, found to be scarce in a *L. japonica* diet compared to a *G. lemaneiformis* diet [194]. Sphingomonadaceae have been detected in abalone guts [22], *Shimia haliotis* was isolated from an abalone gut [195] but *Pelagibius* has yet to be found in abalone. Considering the novelty of abalone microbiome studies, this is not unexpected. There were taxa, in addition to the *Candidatus* Xenohaliotis genus, in the fecal samples which were specifically associated with *Ca*Xc-exposed abalone, including Rhodobacteraceae and *Fusibacter*, but these have also not been documented in previous studies of abalone Withering Syndrome. *Marinomonas* has been

documented to increase in abundance in Withering Syndrome affected abalone, but was not detected in this study [42]. Halieaceae was underrepresented in *Ca*Xc-exposed abalone, which may be a sign that this group is impacted by *Ca*Xc presence. In abalone, Rhodobacteraceae have been correlated with increasing water temperature [196]. Interestingly, *Ca*Xc infection is also correlated to increased water temperatures, and Rhodobacteraceae may favor similar conditions to *Ca*Xc [197]. While there are nuanced differences between exposed and unexposed abalone, the relative impact of *Ca*Xc on the fecal microbiome is minimal compared to the high volatility of the abalone microbiome over time. The fecal microbiome is also highly diverse compared to inner tissue microbiomes and may not be the best proxy for measuring the microbial impacts of *Ca*Xc infection.

*Ca*Xc affects individual tissues quite differently. Along the digestive tract, the post esophagus tissue comes first, followed by the digestive gland, and finally the distal intestine. The earliest tissue in the digestive tract is also the most impacted by *Ca*Xc infection. This is known to be the first site targeted by *Ca*Xc infection [165,197]. Weighted UniFrac was paired with evenness data to demonstrate that decline in evenness in the post esophagus, caused by dominance of few ASVs, contributes greatly to the shift in the microbial community of that tissue. The post esophagus hosts the highest pathogen load after 11 months of exposure and phylogenetic diversity is negatively correlated with pathogen load, suggesting a direct interaction between the pathogen and other resident bacteria that persists in the long term. The post esophagus microbiome closely resembles the digestive gland microbiome in the healthy abalone, but pathogen exposure causes the post esophagus microbiome to diverge significantly from the digestive gland microbiome. Disruption of the microbiome in the gut of *Ca*Xc-exposed abalone has been documented across species of abalone to differing degrees [41,42]. These previous

studies have only focused on one tissue type or homogenized the whole gut of abalone to characterize its microbiota. Therefore, this is the first study to recognize similarity in microbiome of post esophagus and digestive gland tissue. Interestingly, the digestive gland microbiome composition is not significantly altered by *Ca*Xc-exposure. Although the *Ca*Xc pathogen is thought to predominantly infect both the digestive gland and post esophagus tissue [161], the majority of microbial disruption is seen in the post esophagus. Keeping in mind that the virulence of *Ca*Xc is likely reduced in this case due to the *Ca*Xc phage and the abalone showed no visible symptoms of Withering Syndrome, the digestive gland microbiome appears to be more resilient against the pathogen than the post esophagus tissue. This may be important for maintaining abalone health during this study, considering the digestive gland is the primary site of digestive activity and may host bacteria important for aiding in digestion [47,198].

The distal intestine has negligible pathogen load but experiences a significant shift in microbiome composition. *CaXc* is typically found at much lower intensity in the distal intestine, as observed through microscopy [161]. However, the infection and disruption of the microbiome in the early digestive tract appears to have downstream consequences on the intestinal microbiome without leading to visible symptoms of withering. Faith's phylogenetic diversity was not correlated to distal intestine pathogen load because it was too low, but a significant shift was seen in the distal intestinal microbial composition. Exposed abalone have a distal intestine microbiome which is very different from the gut contents which moved through it. This is not necessarily due to a change in the gut contents, but rather by a change in the distal intestine microbiome (Fig 15D). The distal intestine of abalone contains enzymes for terminal digestion [199], but is proposed to have a minor role in overall nutrient absorption [197]. Similar to the post esophagus, the microbiome of the intestine may not be as resilient against pathogens

because of different interactions between intestinal tissue cells and bacterial adhesion. The digestive gland, on the other hand, is a critical site of nutrient absorption and may host highly dependent and strongly associated bacteria. Therefore, if the abalone had succumbed to Withering Syndrome, this likely would have been reflected by an alteration in the digestive gland microbiota and this would equate with signs of poor health.

The shift in microbiome diversity and composition in infected abalone was due to a dominance of the *Ca*Xc bacterial pathogen, but no other bacteria increased in coordination with *Ca*Xc. Although polymicrobial infections are possible with a weakened host immune system, this did not appear to be the case in this experiment because other bacteria were greatly outweighed in relative abundance by *Ca*Xc. Since the data produced in this study are relative abundances, the dominance of *Ca*Xc reads may be due to either replacement of other bacteria or an overall increase in bacterial biomass favoring *Ca*Xc. This can be seen in both Figures 14D and 15C, where *Candidatus* Xenohaliotis is the only taxa overrepresented in exposed abalone, yet many other taxa were underrepresented. This poses alternative concerns for the health of the abalone because beneficial bacteria are typically involved in the digestive process and contribute to the nutrition of the abalone [47]. Many bacteria found in the abalone gut are capable of degrading algal polysaccharides and other compounds, which is important for an organism with an algal-based diet [199]. In healthy control abalone, *Mycoplasma, Psychrilyobacter*, and *Shewanella* were all proportionally abundant, but were dramatically outweighed by *Ca*Xc in exposed abalone, specifically in post esophagus and distal intestine samples. The decreased ratio of *Mycoplasma* to *Candidatus* Xenohaliotis under exposure conditions has also been noted in red abalone experiencing Withering Syndrome [41,42]. *Mycoplasma* have the potential to be highly metabolically active in abalone with the capability of breaking down complex compounds and

are likely to directly interact with *Ca*Xc at the host cell interface [17,41]. Cicala et al 2022 presented a great overview of some of the functional potential of *Mycoplasma* and their specificity within abalone. The loss of *Mycoplasma* is a warning for the loss of potential core microbiota, which has also been reported by this author previously in oysters [200]. *Psychrilyobacter* are typically found in high abundance in abalone guts, enriched in abalone compared to the surrounding environment and stable across changing environmental conditions and diets [194,196]. This also supports some potential selection for this species within the abalone microbiome and importance of its metabolic function within the abalone gut [196]. *Shewanella* species are proposed as potential probiotics for disease resistance in abalone [46]. The loss of all these bacteria may present a sign of dysbiosis within the infected abalone tissue and suggests that there are hidden yet considerable effects of *Ca*Xc on the abalone without visible symptoms and even with the *Ca*Xc phage present.

The signal of *Ca*Xc is strongest within gastrointestinal tissue, even without visible symptoms of Withering Syndrome. Rhodobacteraceae and Haliaeaceae were found to be underrepresented in both post esophagus and fecal samples from exposed abalone. However, this is the only common trend in bacteria between tissue and feces, suggesting that feces are not a good indicator of internal changes, as previously mentioned and showcased in other mollusks [193]. *Ca*Xc was also overrepresented in tissue samples compared to fecal samples, further supporting this conclusion. With the presence of the *Ca*Xc phage, some microbial impacts of *Ca*Xc infection may be dampened [165]. Nonetheless, there are clear internal disruptions to the core microbiome of abalone following *Ca*Xc exposure and infection which do not appear to affect the abalone health visually but may still induce stress and alter gene expression.

Gene expression of white abalone varied only minimally with *Ca*Xc exposure. Despite significant microbial disruption to the post esophagus samples following *Ca*Xc exposure, the patterns of genes expressed overlapped between control and exposed post esophagus tissue. Yet, 41 genes were significantly up or downregulated in response to *Ca*Xc exposure. Interestingly, more genes were significantly altered in response to *Ca*Xc exposure in the digestive gland, which experienced less microbiome disruption. However, digestive gland gene expression also overlapped greatly between control and exposed abalone. The low variability in gene expression between exposed and control abalone may be due to the presence of the *Ca*Xc phage, which would reduce the virulence of the pathogen and reduce host recognition of pathogenic activity. However, a previous study on Pinto abalone found no significant immune gene expression in response to *CaXc* infection, and rather the pathogen impacted hunger and metabolic pathways [170]. This study also experienced difficulty with gene annotation, which could explain the lack of immune response detected [170]. Considering the abalone in the current study also showed no visible signs of withering, it is reasonable not to see a broad genetic response, whether it was immune response or metabolic pathway signals. The most interesting result from this analysis of gene expression is the unique genetic responses of each tissue type. Post esophagus and digestive gland tissue only share only a minority of similar genes expressed, suggesting a difference in cellular response and function. These differences may also play into the response to *Ca*Xc and the ability of *Ca*Xc to invade post esophagus tissue before entering the digestive gland. These questions should be explored further once greater resolution of white abalone gene annotation is achieved. White abalone are one of the more susceptible species to Withering Syndrome and they need to be better understood to ensure successful captive breeding and restoration in the wild.

Conclusion

White abalone are a critically endangered species and highly susceptible to Withering Syndrome. This study demonstrated the cascading impacts of *Ca*Xc exposure on the abalone digestive tract microbiome. The early digestive tract, the post esophagus, was most impacted by *Ca*Xc exposure, with *Ca*Xc outweighing all other bacteria and the highest quantification of pathogen load of all tissue and fecal samples. The digestive gland microbiome was more resilient against *Ca*Xc infection, and this maintenance of bacterial diversity in the region of digestion may be critical to abalone health through protection of gut tissue. Both the post esophagus and the digestive gland had some differential gene expression following *Ca*Xc infection, but the overall response was not at an intensity expected for a severely diseased animal. While the distal intestine microbiome was also significantly impacted by *Ca*Xc exposure, it likely plays less of a role in nutrient absorption and the microbiome may be less specialized and less resilient than the digestive gland. The stabilization of infection and lack of withering signs may be more due to the presence of the *Ca*Xc phage, which would reduce its virulence and minimize its ability to damage host tissue. While fecal samples may be used to detect *Ca*Xc, the changes in the microbiome of the feces vary more with time than with *Ca*Xc exposure. The abalone fecal microbiome does not reflect the internal tissue microbiome of the abalone, which is specific to each tissue in the digestive tract. The internal host response to *Ca*Xc also varied between tissues in the digestive tract, suggesting a unique role of each abalone tissue in infection, immunity and microbial activity.

Data Availability:

Raw 16S V4 reads for microbial DNA are available at NCBI BioProject accession PRJNA1079384. Raw RNA Sequences for abalone genes are available at NCBI BioProject

accession PRJNA1090106. Scripts for data processing are available at https://github.com/ekunselman/AbaloneCaXc

Acknowledgements

Chapter 3.2 is in preparation for submission to the Animal Microbiome Journal. Emily Kunselman, Blythe Marshman, Chelsey Souza, James Moore, Colleen Burge, Sarah Allard, Jack A. Gilbert. Abalone Withering Syndrome: The cascading microbial impacts of one bacterial invader. The dissertation author was the primary researcher and author of this paper. This work was funded through contract P1970003 from CDFW to UC Davis, through a federal NOAA Section 6 Grant NA19NMF4720103 to CDFW. The DNA Sequencing was carried out by the UCSD Microbiome Core. This publication includes data generated at the UC San Diego IGM Genomics Center utilizing an Illumina NovaSeq 6000 that was purchased with funding from a National Institutes of Health SIG grant (#S10 OD026929). The RNA sequencing was carried out at the DNA Technologies and Expression Analysis Core at the UC Davis Genome Center, supported by NIH Shared Instrumentation Grant 1S10OD010786-01. Thank you to the UC Davis Bodega Marine Laboratory White Abalone Captive Breeding Program and the California Department of Fish and Wildlife Shellfish Health Laboratory for providing facilities and resources to support this study. All work with white abalone was performed under the Endangered Species Act (ESA) permit for white abalone (Invertebrate Enhancement Permit 14344-2R) held by UC Davis.

CONCLUSION

This dissertation has discussed microbiome dynamics under both environmental and pathogen-driven disturbances for Olympia oysters, Pacific oysters, and white abalone.

The microbiome is important in mollusks for digestion and pathogen defense, but mollusk microbiomes experience a high level of exposure to the environment and the microbes in that environment. Microbial communities are unique to tissues and may be highly specialized. This is important for digestion of different algal diets for both oysters and abalone. Pathogens are also specialized based on their evolved route of infection, and this creates dysbiosis in infected tissue, as seen in oysters' infection with OsHV-1 and abalone infected with *C*aXc. Disruption to one tissue may spread to other tissues during severe disease progression. Large disturbances such as pathogens or increasingly stressful environments can lead to a reassembly of the mollusk microbiome which is not favorable to its health or recovery from infection. For example, low oxygen as demonstrated in Chapter 1, viral infection as demonstrated in Chapter 2, or pathogenic bacterial exposure as demonstrated in Chapter 3.

The study of microbiomes in mollusks is highly relevant to aquaculture. One form of aquaculture is for restoration, such as for the native Olympia oyster or the endangered white abalone, both found on the West Coast of the United States. The microbiome may be influenced by the environmental characteristics of a specific restoration site, including physical parameters such as temperature and oxygen, environmental microbial communities, presence of pathogens, and food sources and the microbes that may be associated with them. These all impact the suitability of restorations sites and the suitability of an animal for a restoration site. Both the environment and the outplanted mollusk should be assessed prior to enacting restoration strategies due to the potential risks which may jeopardize the health of new mollusks, their

establishment success, and the organisms around them which may be susceptible to infections. Although abalone Withering Syndrome can be detected by fecal samples, it takes a long time to present and other invasive methods cannot be used to test infection before outplanting abalone in wild, which may make the assessment process more difficult. Commercial aquaculture must also consider microbiomes, especially regarding disease because it may impact profit, food safety and environmental impact assessments. Oyster herpesvirus is a serious threat to aquaculture because its onset is rapid and mortality rates are high in oysters, which leads to reduced supply and shifts in the microbial community in response to OsHV-1 could negatively impact surrounding ecosystems. The microbiome is altered when the oyster dies, and these microbes may be expelled into the environment and exposed to nearby susceptible hosts. Similar microbes have been found across mollusks species, such as *Vibrio* and *Mycoplasma* which were seen in all chapters in this dissertation, which alludes to that fact that they can positively or negatively impact multiple mollusks in the same way.

Many commonalities have been found across the mollusk species assessed in this dissertation. For example, *Vibrio* species are a common member of the microbiome of both oysters and abalone. However, their presence can be a positive or negative indicator of mollusk health depending on species. Unfortunately, species-level resolution of *Vibrio* bacteria is very hard to accomplish with 16S rRNA sequencing data. *Mycoplasma* species are also found to be core members in the guts of most mollusk species, but this genus also has different species which may fall into either commensal or pathogenic categories. Again, without species resolution and without knowledge of species characteristics within the Mycoplasma genus, it is difficult to confirm whether a high relative abundance of *Mycoplasma* is a sign of a healthy or dysbiotic mollusk gut. Yet, there are multiple cases documented where *Mycoplasma* bacteria decrease

relative to invaders, such as a decreased ratio of *Mycoplasma* to *Candidatus* Xenohaliotis californiensis in infected abalone. A final commonality described in this dissertation is the phenomenon of decreased bacterial evenness in stressed and pathogen-infected mollusks. Decrease in evenness flags a decrease in ecosystem health in macro and microscale ecology, because it suggests the dominance of fewer species and therefore a decrease in diversity. A healthy level of disturbance often promotes high diversity in an ecosystem because it lowers the likelihood that one species will outcompete the rest, but too large of a disturbance will knock down beneficial members of the mollusk microbiome and allow for the most opportunistic species or bacterial invaders to take over. While these general conclusions offer insight into the dynamics of mollusk microbiomes and how they are linked to health and disease, future studies should dive deeper into the direct relationships between mollusk pathogens and resident bacteria and the functions being performed by different members of the community to solidify the explanation behind these trends.

While many commonalities do exist across mollusks, there are also many species-specific considerations that must be taken into account. Their response to environmental changes and different types of pathogens may vary from one species to the next. For example, OsHV-1 is hypothesized to be a polymicrobial infection because the infection by the virus leads to a shift in the microbial community and previous studies have demonstrated increased bacterial load and bacterial infestation of tissue. However, abalone Withering Syndrome does not appear to be a polymicrobial infection, because no bacteria were found to increase alongside *Ca*Xc. The differences between these systems are numerous and any one of these differences could explain why the systems do not respond in the same way. *Ca*Xc is a bacterial pathogen while OsHV-1 is a virus, *Ca*Xc is intracellular, *Ca*Xc is specialized to abalone while OsHV-1 is specialized to

Pacific oysters, and *Ca*Xc has a phage which may reduce its pathogenicity. These differences call for adaptive practices to manage and eliminate pathogens of different classes across different species of mollusks.

The main takeaways of this dissertation are 1) a robust microbiome is important in the face of multiple stressors, such as temperature, reduced oxygen, and pathogen exposure, but the definition and characteristics of a robust microbiome may vary based on the host, 2) there is a strong connection between the microbiome and mollusk performance which can be taken advantage of when designing alternative solutions to mollusk aquaculture, such as treatment with probiotics and phage, and 3) changing ocean temperatures and other impacts of climate change pose serious concerns for mollusks due to the increased virulence and spread of marine pathogens and impacts on internal mollusk microbiomes.

REFERENCES

1. King GM, Judd C, Kuske CR, Smith C. Analysis of Stomach and Gut Microbiomes of the Eastern Oyster (Crassostrea virginica) from Coastal Louisiana, USA. Neufeld J, editor. PLoS ONE. 2012 Dec 12;7(12):e51475.

2. Offret C, Paulino S, Gauthier O, Château K, Bidault A, Corporeau C, Miner P, Petton B, Pernet F, Fabioux C, Paillard C, Blay GL. The marine intertidal zone shapes oyster and clam digestive bacterial microbiota. FEMS Microbiology Ecology [Internet]. 2020 Aug 1 [cited 2021 Aug 31];96(8). Available from: https://doi.org/10.1093/femsec/fiaa078

3. Vezzulli L, Stagnaro L, Grande C, Tassistro G, Canesi L, Pruzzo C. Comparative 16SrDNA Gene-Based Microbiota Profiles of the Pacific Oyster (Crassostrea gigas) and the Mediterranean Mussel (Mytilus galloprovincialis) from a Shellfish Farm (Ligurian Sea, Italy). Microb Ecol. 2018 Feb;75(2):495–504.

4. Pierce ML, Ward JE. Gut Microbiomes of the Eastern Oyster (*Crassostrea virginica*) and the Blue Mussel (*Mytilus edulis*): Temporal Variation and the Influence of Marine Aggregate-Associated Microbial Communities. McMahon K, editor. mSphere [Internet]. 2019 Dec 18 [cited 2021 Aug 31];4(6). Available from: https://journals.asm.org/doi/10.1128/mSphere.00730-19

5. King WL, Siboni N, Williams NLR, Kahlke T, Nguyen KV, Jenkins C, Dove M, O'Connor W, Seymour JR, Labbate M. Variability in the Composition of Pacific Oyster Microbiomes Across Oyster Families Exhibiting Different Levels of Susceptibility to OsHV-1 µvar Disease. Front Microbiol. 2019 Mar 11;10:473.

6. Dubé CE, Ky CL, Planes S. Microbiome of the Black-Lipped Pearl Oyster Pinctada margaritifera, a Multi-Tissue Description With Functional Profiling. Front Microbiol. 2019 Jul 5;10:1548.

7. Wegner K, Volkenborn N, Peter H, Eiler A. Disturbance induced decoupling between host genetics and composition of the associated microbiome. BMC Microbiol. 2013;13(1):252.

8. Green TJ, Siboni N, King WL, Labbate M, Seymour JR, Raftos D. Simulated Marine Heat Wave Alters Abundance and Structure of Vibrio Populations Associated with the Pacific Oyster Resulting in a Mass Mortality Event. Microb Ecol. 2019 Apr;77(3):736–47.

9. Lasa A, di Cesare A, Tassistro G, Borello A, Gualdi S, Furones D, Carrasco N, Cheslett D, Brechon A, Paillard C, Bidault A, Pernet F, Canesi L, Edomi P, Pallavicini A, Pruzzo C, Vezzulli L. Dynamics of the Pacific oyster pathobiota during mortality episodes in Europe assessed by 16S rRNA gene profiling and a new target enrichment next-generation sequencing strategy. Environ Microbiol. 2019 Dec;21(12):4548–62.

10. Silva Neta MT, Maciel BM, Lopes ATS, Marques ELS, Rezende RP, Boehs G. Microbiological quality and bacterial diversity of the tropical oyster Crassostrea rhizophorae in a monitored farming system and from natural stocks. Genet Mol Res. 2015;14(4):15754–68.

11. King WL, Siboni N, Kahlke T, Dove M, O'Connor W, Mahbub KR, Jenkins C, Seymour JR, Labbate M. Regional and oyster microenvironmental scale heterogeneity in the Pacific oyster bacterial community. FEMS Microbiology Ecology. 2020 May 1;96(5):fiaa054.

12. Pierce ML, Ward JE. Microbial Ecology of the Bivalvia, with an Emphasis on the Family Ostreidae. Journal of Shellfish Research. 2018 Oct;37(4):793–806.

13. Lokmer A, Kuenzel S, Baines JF, Wegner KM. The role of tissue-specific microbiota in initial establishment success of Pacific oysters: Microbiota and oyster establishment. Environ Microbiol. 2016 Mar;18(3):970–87.

14. Hernandez-Zarate G, Olmos-Soto J. Identification of bacterial diversity in the oyster Crassostrea gigas by fluorescent in situ hybridization and polymerase chain reaction. J Appl Microbiol. 2006 Apr;100(4):664–72.

15. Pathirana E, McPherson A, Whittington R, Hick P. The role of tissue type, sampling and nucleic acid purification methodology on the inferred composition of Pacific oyster (*Crassostrea gigas*) microbiome. J of Applied Microbiology. 2019 Aug;127(2):429–44.

16. Wang X, Tang B, Luo X, Ke C, Huang M, You W, Wang Y. Effects of temperature, diet and genotype-induced variations on the gut microbiota of abalone. Aquaculture. 2020 Jul;524:735269.

17. Cicala F, Cisterna-Céliz JA, Moore JD, Rocha-Olivares A. Structure, dynamics and predicted functional role of the gut microbiota of the blue (*Haliotis fulgens*) and yellow (*H. corrugata*) abalone from Baja California Sur, Mexico. PeerJ. 2018 Nov 2;6:e5830.

18. Danckert NP, Wilson N, Phan-Thien KY, Stone DAJ. The intestinal microbiome of Australian abalone, Haliotis laevigata and Haliotis laevigata × Haliotis rubra, over a 1-year period in aquaculture. Aquaculture. 2021 Mar;534:736245.

19. Gobet A, Mest L, Perennou M, Dittami SM, Caralp C, Coulombet C, Huchette S, Roussel S, Michel G, Leblanc C. Seasonal and algal diet-driven patterns of the digestive microbiota of the European abalone Haliotis tuberculata, a generalist marine herbivore. Microbiome. 2018 Dec;6(1):60.

20. Trabal N, Mazón-Suástegui JM, Vázquez-Juárez R, Asencio-Valle F, Morales-Bojórquez E, Romero J. Molecular Analysis of Bacterial Microbiota Associated with Oysters (Crassostrea gigas and Crassostrea corteziensis) in Different Growth Phases at Two Cultivation Sites. Microb Ecol. 2012 Aug;64(2):555–69.

21. Zurel D, Benayahu Y, Or A, Kovacs A, Gophna U. Composition and dynamics of the gill microbiota of an invasive Indo-Pacific oyster in the eastern Mediterranean Sea. Environmental Microbiology. 2011 Jun;13(6):1467–76.

22. Tanaka R, Ootsubo M, Sawabe T, Ezura Y, Tajima K. Biodiversity and in situ abundance of gut microflora of abalone (Haliotis discus hannai) determined by culture-independent techniques. Aquaculture. 2004 Nov;241(1–4):453–63.

23. Parker-Graham CA, Eetemadi A, Yazdi Z, Marshman BC, Loeher M, Richey CA, Barnum S, Moore JD, Soto E. Effect of oxytetracycline treatment on the gastrointestinal microbiome of critically endangered white abalone (Haliotis sorenseni) treated for withering syndrome. Aquaculture. 2020 Sep;526:735411.

24. Wu Z, Yu X, Guo J, Fu Y, Guo Y, Pan M, Zhang W, Mai K. Effects of replacing fish meal with corn gluten meal on growth performance, intestinal microbiota, mTOR pathway and immune response of abalone Haliotis discus hannai. Aquaculture Reports. 2022 Apr;23:101007.

25. Yu W, Lu Y, Shen Y, Liu J, Gong S, Yu F, Huang Z, Zou W, Zhou M, Luo X, You W, Ke C. Exploring the Intestinal Microbiota and Metabolome Profiles Associated With Feed Efficiency in Pacific Abalone (Haliotis discus hannai). Front Microbiol. 2022 Mar 17;13:852460.

26. Mizutani Y, Mori T, Miyazaki T, Fukuzaki S, Tanaka R. Microbial community analysis in the gills of abalones suggested possible dominance of epsilonproteobacterium in *Haliotis gigantea*. PeerJ. 2020 Jun 30;8:e9326.

27. Roterman YR, Benayahu Y, Reshef L, Gophna U. The gill microbiota of invasive and indigenous *Spondylus* oysters from the Mediterranean Sea and northern Red Sea. Environ Microbiol Rep. 2015 Dec;7(6):860–7.

28. Lokmer A, Goedknegt MA, Thieltges DW, Fiorentino D, Kuenzel S, Baines JF, Wegner KM. Spatial and Temporal Dynamics of Pacific Oyster Hemolymph Microbiota across Multiple Scales. Front Microbiol [Internet]. 2016 Aug 31 [cited 2021 Aug 11];7. Available from: http://journal.frontiersin.org/Article/10.3389/fmicb.2016.01367/abstract

29. Segarra A, Pépin JF, Arzul I, Morga B, Faury N, Renault T. Detection and description of a particular Ostreid herpesvirus 1 genotype associated with massive mortality outbreaks of Pacific oysters, Crassostrea gigas, in France in 2008. Virus Research. 2010 Oct;153(1):92–9.

30. García Bernal M, Trabal Fernández N, Saucedo Lastra PE, Medina Marrero R, Mazón-Suástegui JM. *Streptomyces* effect on the bacterial microbiota associated to *Crassostrea sikamea* oyster. J Appl Microbiol. 2017 Mar;122(3):601–14.

31. Laroche O, Symonds JE, Smith KF, Banks JC, Mae H, Bowman JP, Pochon X. Understanding bacterial communities for informed biosecurity and improved larval survival in Pacific oysters. Aquaculture. 2018 Dec;497:164–73.

32. Khan B, Clinton SM, Hamp TJ, Oliver JD, Ringwood AH. Potential impacts of hypoxia and a warming ocean on oyster microbiomes. Marine Environmental Research. 2018 Aug;139:27–34.

33. Pierce ML, Ward JE, Holohan BA, Zhao X, Hicks RE. The influence of site and season on the gut and pallial fluid microbial communities of the eastern oyster, Crassostrea virginica

(Bivalvia, Ostreidae): community-level physiological profiling and genetic structure. Hydrobiologia. 2016 Feb;765(1):97–113.

34. Pujalte MJ, Ortigosa M, Macián MC, Garay E. Aerobic and facultative anaerobic heterotrophic bacteria associated to Mediterranean oysters and seawater. Int Microbiol. 1999 Dec;2(4):259–66.

35. Ossai S, Ramachandran P, Ottesen A, Reed E, DePaola A, Parveen S. Microbiomes of American Oysters (*Crassostrea virginica*) Harvested from Two Sites in the Chesapeake Bay. Genome Announc [Internet]. 2017 Jul 27 [cited 2021 Aug 31];5(30). Available from: https://journals.asm.org/doi/10.1128/genomeA.00729-17

36. Lokmer A, Mathias Wegner K. Hemolymph microbiome of Pacific oysters in response to temperature, temperature stress and infection. ISME J. 2015 Mar;9(3):670–82.

37. King WL, Jenkins C, Go J, Siboni N, Seymour JR, Labbate M. Characterisation of the Pacific Oyster Microbiome During a Summer Mortality Event. Microb Ecol. 2019 Feb;77(2):502–12.

38. Moore JD. Disease and potential disease agents in wild and cultured abalone. In: Developments in Aquaculture and Fisheries Science [Internet]. Elsevier; 2023 [cited 2024 Jan 4]. p. 189–250. Available from: https://linkinghub.elsevier.com/retrieve/pii/B9780128149386000075

39. Pathirana E, Fuhrmann M, Whittington R, Hick P. Influence of environment on the pathogenesis of Ostreid herpesvirus-1 (OsHV-1) infections in Pacific oysters (Crassostrea gigas) through differential microbiome responses. Heliyon. 2019 Jul;5(7):e02101.

40. Green TJ, Barnes AC. Bacterial diversity of the digestive gland of Sydney rock oysters, *Saccostrea glomerata* infected with the paramyxean parasite, *Marteilia sydneyi*. Journal of Applied Microbiology. 2010 Aug;109(2):613–22.

41. Cicala F, Cisterna-Céliz JA, Paolinelli M, Moore JD, Sevigny J, Rocha-Olivares A. The Role of Diversity in Mediating Microbiota Structural and Functional Differences in Two Sympatric Species of Abalone Under Stressed Withering Syndrome Conditions. Microb Ecol [Internet]. 2022 Jan 22 [cited 2022 Jun 20]; Available from: https://link.springer.com/10.1007/s00248-022-01970-5

42. Villasante A, Catalán N, Rojas R, Lohrmann KB, Romero J. Microbiota of the Digestive Gland of Red Abalone (Haliotis rufescens) Is Affected by Withering Syndrome. Microorganisms. 2020 Sep 13;8(9):1411.

43. Desriac F, Le Chevalier P, Brillet B, Leguerinel I, Thuillier B, Paillard C, Fleury Y. Exploring the hologenome concept in marine bivalvia: haemolymph microbiota as a pertinent source of probiotics for aquaculture. FEMS Microbiol Lett. 2014 Jan;350(1):107–16.

44. Defer D, Desriac F, Henry J, Bourgougnon N, Baudy-Floc'h M, Brillet B, Le Chevalier P, Fleury Y. Antimicrobial peptides in oyster hemolymph: The bacterial connection. Fish & Shellfish Immunology. 2013 Jun;34(6):1439–47.

45. Stevick RJ, Sohn S, Modak TH, Nelson DR, Rowley DC, Tammi K, Smolowitz R, Markey Lundgren K, Post AF, Gómez-Chiarri M. Bacterial Community Dynamics in an Oyster Hatchery in Response to Probiotic Treatment. Front Microbiol. 2019 May 15;10:1060.

46. Jiang HF, Liu XL, Chang YQ, Liu MT, Wang GX. Effects of dietary supplementation of probiotic Shewanella colwelliana WA64, Shewanella olleyana WA65 on the innate immunity and disease resistance of abalone, Haliotis discus hannai Ino. Fish & Shellfish Immunology. 2013 Jul;35(1):86–91.

47. Erasmus JH, Cook PA, Coyne VE. The role of bacteria in the digestion of seaweed by the abalone Haliotis midae. Aquaculture. 1997 Sep;155(1–4):377–86.

48. Peter-Contesse T, Peabody B. Reestablishing Olympia Oyster Populations in Puget Sound, Washington. Washington Sea Grant Program; 2005 Jan.

49. Wang C, Bao WY, Gu ZQ, Li YF, Liang X, Ling Y, Cai SL, Shen HD, Yang JL. Larval settlement and metamorphosis of the mussel *Mytilus coruscus* in response to natural biofilms. Biofouling. 2012 Mar;28(3):249–56.

50. Nielsen SJ, Harder T, Steinberg PD. Sea urchin larvae decipher the epiphytic bacterial community composition when selecting sites for attachment and metamorphosis. FEMS Microbiology Ecology. 2015 Jan 1;91(1):1–9.

51. Dobretsov S, Rittschof D. Love at First Taste: Induction of Larval Settlement by Marine Microbes. IJMS. 2020 Jan 22;21(3):731.

52. Burge CA, Judah LR, Conquest LL, Griffin FJ, Cheney DP, Suhrbier A, Vadopalas B, Olin PG, Renault T, Friedman CS. Summer seed mortality of the Pacific Oyster, Crassostrea gigas Thungberg grown in Tomales Bay, CA, USA: The influence of oyster stock, planting time, pathogens, and environmental stressors. Journal of Shellfish Research. 2007 Apr;26(1):163–72.

53. Dickinson GH, Ivanina AV, Matoo OB, Pörtner HO, Lannig G, Bock C, Beniash E, Sokolova IM. Interactive effects of salinity and elevated CO2 levels on juvenile eastern oysters, *Crassostrea virginica*. Journal of Experimental Biology. 2012 Jan 1;215(1):29–43.

54. Keppel AG, Breitburg DL, Burrell RB. Effects of Co-Varying Diel-Cycling Hypoxia and pH on Growth in the Juvenile Eastern Oyster, Crassostrea virginica. Vopel KC, editor. PLoS ONE. 2016 Aug 22;11(8):e0161088.

55. Elizabeth H. Silvy, Frances P. Gelwick, Nova J. Silvy. Factors Affecting Dermo Disease (Perkinsus marinus) in Eastern Oysters (Crassostrea virginica) in Galveston Bay, Texas. JESE-A [Internet]. 2020 Sep 28 [cited 2021 Aug 31];9(6). Available from: http://www.davidpublisher.com/index.php/Home/Article/index?id=44106.html

56. Scanes E, Parker LM, Seymour JR, Siboni N, King WL, Danckert NP, Wegner KM, Dove MC, O'Connor WA, Ross PM. Climate change alters the haemolymph microbiome of oysters. Mar Pollut Bull. 2021 Mar;164:111991.

57. Coffin MRS, Clements JC, Comeau LA, Guyondet T, Maillet M, Steeves L, Winterburn K, Babarro JMF, Mallet MA, Haché R, Poirier LA, Deb S, Filgueira R. The killer within: Endogenous bacteria accelerate oyster mortality during sustained anoxia. Limnol Oceanogr. 2021 Jul;66(7):2885–900.

58. Agamennone V, Le NG, van Straalen NM, Brouwer A, Roelofs D. Antimicrobial activity and carbohydrate metabolism in the bacterial metagenome of the soil-living invertebrate Folsomia candida. Sci Rep. 2019 Dec;9(1):7308.

59. Modak TH, Gomez-Chiarri M. Contrasting Immunomodulatory Effects of Probiotic and Pathogenic Bacteria on Eastern Oyster, Crassostrea Virginica, Larvae. Vaccines. 2020 Oct 6;8(4):588.

60. Chiu CH, Guu YK, Liu CH, Pan TM, Cheng W. Immune responses and gene expression in white shrimp, Litopenaeus vannamei, induced by Lactobacillus plantarum. Fish & Shellfish Immunology. 2007 Aug;23(2):364–77.

61. Minich JJ, Sanders JG, Amir A, Humphrey G, Gilbert JA, Knight R. Quantifying and Understanding Well-to-Well Contamination in Microbiome Research. mSystems. 2019 Jun 25;4(4):e00186-19.

62. Caporaso JG, Lauber CL, Walters WA, Berg-Lyons D, Huntley J, Fierer N, Owens SM, Betley J, Fraser L, Bauer M, Gormley N, Gilbert JA, Smith G, Knight R. Ultra-high-throughput microbial community analysis on the Illumina HiSeq and MiSeq platforms. ISME J. 2012 Aug;6(8):1621–4.

63. Gonzalez A, Navas-Molina JA, Kosciolek T, McDonald D, Vázquez-Baeza Y, Ackermann G, DeReus J, Janssen S, Swafford AD, Orchanian SB, Sanders JG, Shorenstein J, Holste H, Petrus S, Robbins-Pianka A, Brislawn CJ, Wang M, Rideout JR, Bolyen E, Dillon M, Caporaso JG, Dorrestein PC, Knight R. Qiita: rapid, web-enabled microbiome meta-analysis. Nat Methods. 2018 Oct;15(10):796–8.

64. Amir A, McDonald D, Navas-Molina JA, Kopylova E, Morton JT, Zech Xu Z, Kightley EP, Thompson LR, Hyde ER, Gonzalez A, Knight R. Deblur Rapidly Resolves Single-Nucleotide Community Sequence Patterns. Gilbert JA, editor. mSystems [Internet]. 2017 Apr 21 [cited 2021 Aug 31];2(2). Available from: https://journals.asm.org/doi/10.1128/mSystems.00191-16

65. Bolyen E, Rideout JR, Dillon MR, Bokulich NA, Abnet CC, Al-Ghalith GA, Alexander H, Alm EJ, Arumugam M, Asnicar F, Bai Y, Bisanz JE, Bittinger K, Brejnrod A, Brislawn CJ, Brown CT, Callahan BJ, Caraballo-Rodríguez AM, Chase J, Cope EK, Da Silva R, Diener C, Dorrestein PC, Douglas GM, Durall DM, Duvallet C, Edwardson CF, Ernst M, Estaki M, Fouquier J, Gauglitz JM, Gibbons SM, Gibson DL, Gonzalez A, Gorlick K, Guo J, Hillmann B, Holmes S, Holste H, Huttenhower C, Huttley GA, Janssen S, Jarmusch AK,

Jiang L, Kaehler BD, Kang KB, Keefe CR, Keim P, Kelley ST, Knights D, Koester I, Kosciolek T, Kreps J, Langille MGI, Lee J, Ley R, Liu YX, Loftfield E, Lozupone C, Maher M, Marotz C, Martin BD, McDonald D, McIver LJ, Melnik AV, Metcalf JL, Morgan SC, Morton JT, Naimey AT, Navas-Molina JA, Nothias LF, Orchanian SB, Pearson T, Peoples SL, Petras D, Preuss ML, Pruesse E, Rasmussen LB, Rivers A, Robeson MS, Rosenthal P, Segata N, Shaffer M, Shiffer A, Sinha R, Song SJ, Spear JR, Swafford AD, Thompson LR, Torres PJ, Trinh P, Tripathi A, Turnbaugh PJ, Ul-Hasan S, van der Hooft JJJ, Vargas F, Vázquez-Baeza Y, Vogtmann E, von Hippel M, Walters W, Wan Y, Wang M, Warren J, Weber KC, Williamson CHD, Willis AD, Xu ZZ, Zaneveld JR, Zhang Y, Zhu Q, Knight R, Caporaso JG. Reproducible, interactive, scalable and extensible microbiome data science using QIIME 2. Nat Biotechnol. 2019 Aug;37(8):852–7.

66. C. E. Shannon. A mathematical theory of communication. The Bell System Technical Journal. 1948 Jul;27(3):379–423.

67. Bray JR, Curtis JT. An Ordination of the Upland Forest Communities of Southern Wisconsin. Ecological Monographs. 1957 Oct 1;27(4):325–49.

68. Lozupone C, Hamady M, Knight R. UniFrac – An online tool for comparing microbial community diversity in a phylogenetic context. BMC Bioinformatics. 2006;7(1):371.

69. McDonald D, Vázquez-Baeza Y, Koslicki D, McClelland J, Reeve N, Xu Z, Gonzalez A, Knight R. Striped UniFrac: enabling microbiome analysis at unprecedented scale. Nat Methods. 2018 Nov;15(11):847–8.

70. Martino C, Morton JT, Marotz CA, Thompson LR, Tripathi A, Knight R, Zengler K. A Novel Sparse Compositional Technique Reveals Microbial Perturbations. Neufeld JD, editor. mSystems [Internet]. 2019 Feb 26 [cited 2021 Aug 31];4(1). Available from: https://journals.asm.org/doi/10.1128/mSystems.00016-19

71. Janssen S, McDonald D, Gonzalez A, Navas-Molina JA, Jiang L, Xu ZZ, Winker K, Kado DM, Orwoll E, Manary M, Mirarab S, Knight R. Phylogenetic Placement of Exact Amplicon Sequences Improves Associations with Clinical Information. Chia N, editor. mSystems [Internet]. 2018 Jun 26 [cited 2021 Aug 31];3(3). Available from: https://journals.asm.org/doi/10.1128/mSystems.00021-18

72. Anderson MJ. A new method for non-parametric multivariate analysis of variance. Austral Ecology. 2001 Feb 1;26(1):32–46.

73. Quast C, Pruesse E, Yilmaz P, Gerken J, Schweer T, Yarza P, Peplies J, Glöckner FO. The SILVA ribosomal RNA gene database project: improved data processing and web-based tools. Nucleic Acids Research. 2012 Nov 27;41(D1):D590–6.

74. Yilmaz P, Parfrey LW, Yarza P, Gerken J, Pruesse E, Quast C, Schweer T, Peplies J, Ludwig W, Glöckner FO. The SILVA and "All-species Living Tree Project (LTP)" taxonomic frameworks. Nucl Acids Res. 2014 Jan;42(D1):D643–8.

75. Morton JT, Marotz C, Washburne A, Silverman J, Zaramela LS, Edlund A, Zengler K, Knight R. Establishing microbial composition measurement standards with reference frames. Nat Commun. 2019 Dec;10(1):2719.

76. Jacqueline White, Jennifer L. Ruesink, Alan C. Trimble. The Nearly Forgotten Oyster: Ostrea lurida Carpenter 1864 (Olympia Oyster) History and Management in Washington State. Journal of Shellfish Research. 2009 Mar 1;28(1):43–9.

77. Arfken A, Song B, Bowman JS, Piehler M. Denitrification potential of the eastern oyster microbiome using a 16S rRNA gene based metabolic inference approach. Li X, editor. PLoS ONE. 2017 Sep 21;12(9):e0185071.

78. Pimentel ZT, Dufault-Thompson K, Russo KT, Scro AK, Smolowitz RM, Gomez-Chiarri M, Zhang Y. Microbiome Analysis Reveals Diversity and Function of *Mollicutes* Associated with the Eastern Oyster, *Crassostrea virginica*. Campbell BJ, editor. mSphere [Internet]. 2021 Jun 30 [cited 2021 Aug 31];6(3). Available from: https://journals.asm.org/doi/10.1128/mSphere.00227-21

79. Chauhan A, Wafula D, Lewis DE, Pathak A. Metagenomic Assessment of the Eastern Oyster-Associated Microbiota. Genome Announc [Internet]. 2014 Oct 30 [cited 2021 Aug 31];2(5). Available from: https://journals.asm.org/doi/10.1128/genomeA.01083-14

80. King WL, Kaestli M, Siboni N, Padovan A, Christian K, Mills D, Seymour J, Gibb K. Pearl Oyster Bacterial Community Structure Is Governed by Location and Tissue-Type, but Vibrio Species Are Shared Among Oyster Tissues. Front Microbiol. 2021 Aug 9;12:723649.

81. Simons AL, Churches N, Nuzhdin S. High turnover of faecal microbiome from algal feedstock experimental manipulations in the Pacific oyster (*Crassostrea gigas*). Microb Biotechnol. 2018 Sep;11(5):848–58.

82. Li Z, Wang L. Metagenomic 16S rRNA Sequencing Analysis of Pacific Oyster (*Crassostrea gigas*) Microbiota from the Puget Sound Region in the United States. Genome Announc [Internet]. 2017 Jun 8 [cited 2021 Aug 11];5(23). Available from: https://journals.asm.org/doi/10.1128/genomeA.00468-17

83. Destoumieux-Garzón D, Canesi L, Oyanedel D, Travers M, Charrière GM, Pruzzo C, Vezzulli L. *Vibrio* –bivalve interactions in health and disease. Environ Microbiol. 2020 Oct;22(10):4323–41.

84. Avila-Poveda OH, Torres-Ariño A, Girón-Cruz DA, Cuevas-Aguirre A. Evidence for accumulation of Synechococcus elongatus (Cyanobacteria: Cyanophyceae) in the tissues of the oyster Crassostrea gigas (Mollusca: Bivalvia). Tissue and Cell. 2014 Oct;46(5):379–87.

85. Lasa A, Avendaño-Herrera R, Estrada JM, Romalde JL. Isolation and identification of Vibrio toranzoniae associated with diseased red conger eel (Genypterus chilensis) farmed in Chile. Veterinary Microbiology. 2015 Sep;179(3–4):327–31.

86. Huang B, Zhang X, Wang C, Bai C, Li C, Li C, Xin L. Isolation and Characterization of Vibrio kanaloae as a Major Pathogen Associated with Mass Mortalities of Ark Clam, Scapharca broughtonii, in Cold Season. Microorganisms. 2021 Oct 16;9(10):2161.

87. Clerissi C, de Lorgeril J, Petton B, Lucasson A, Escoubas JM, Gueguen Y, Dégremont L, Mitta G, Toulza E. Microbiota Composition and Evenness Predict Survival Rate of Oysters Confronted to Pacific Oyster Mortality Syndrome. Front Microbiol. 2020 Feb 27;11:311.

88. Dinnel P. Restoration of the Native Oyster, Ostrea lurida, in Fidalgo Bay, Padilla Bay and Cypress Island. 2016;56.

89. de Lorgeril J, Lucasson A, Petton B, Toulza E, Montagnani C, Clerissi C, Vidal-Dupiol J, Chaparro C, Galinier R, Escoubas JM, Haffner P, Dégremont L, Charrière GM, Lafont M, Delort A, Vergnes A, Chiarello M, Faury N, Rubio T, Leroy MA, Pérignon A, Régler D, Morga B, Alunno-Bruscia M, Boudry P, Le Roux F, Destoumieux-Garzón D, Gueguen Y, Mitta G. Immune-suppression by OsHV-1 viral infection causes fatal bacteraemia in Pacific oysters. Nat Commun. 2018 Dec;9(1):4215.

90. Britt A, Bernini M, McSweeney B, Dalapati S, Duchin S, Cavanna K, Santos N, Donovan G, O'Byrne K, Noyes S, Romero M, Poonacha KNT, Scully T. The effects of atrazine on the microbiome of the eastern oyster: Crassostrea virginica. Sci Rep. 2020 Dec;10(1):11088.

91. Stevick RJ, Post AF, Gómez-Chiarri M. Functional plasticity in oyster gut microbiomes along a eutrophication gradient in an urbanized estuary. anim microbiome. 2021 Dec;3(1):5.

92. Abbadi M, Zamperin G, Gastaldelli M, Pascoli F, Rosani U, Milani A, Schivo A, Rossetti E, Turolla E, Gennari L, Toffan A, Arcangeli G, Venier P. Identification of a newly described OsHV-1 µvar from the North Adriatic Sea (Italy). Journal of General Virology. 2018 May 1;99(5):693–703.

93. Burge C, Griffin F, Friedman C. Mortality and herpesvirus infections of the Pacific oyster Crassostrea gigas in Tomales Bay, California, USA. Dis Aquat Org. 2006 Sep 14;72:31–43.

94. Burge CA, Friedman CS, Kachmar ML, Humphrey KL, Moore JD, Elston RA. The first detection of a novel OsHV-1 microvariant in San Diego, California, USA. Journal of Invertebrate Pathology. 2021 Sep;184:107636.

95. Burioli EAV, Prearo M, Riina MV, Bona MC, Fioravanti ML, Arcangeli G, Houssin M. Ostreid herpesvirus type 1 genomic diversity in wild populations of Pacific oyster Crassostrea gigas from Italian coasts. Journal of Invertebrate Pathology. 2016 Jun;137:71–83.

96. Burioli EAV, Prearo M, Houssin M. Complete genome sequence of Ostreid herpesvirus type 1 µVar isolated during mortality events in the Pacific oyster Crassostrea gigas in France and Ireland. Virology. 2017 Sep;509:239–51.

97. Jenkins C, Hick P, Gabor M, Spiers Z, Fell S, Gu X, Read A, Go J, Dove M, O'Connor W, Kirkland P, Frances J. Identification and characterisation of an ostreid herpesvirus-1 microvariant (OsHV-1 µ-var) in Crassostrea gigas (Pacific oysters) in Australia. Dis Aquat Org. 2013 Jul 22;105(2):109–26.

98. Keeling S, Brosnahan C, Williams R, Gias E, Hannah M, Bueno R, McDonald W, Johnston C. New Zealand juvenile oyster mortality associated with ostreid herpesvirus 1—an opportunistic longitudinal study. Dis Aquat Org. 2014 Jul 3;109(3):231–9.

99. Lynch SA, Carlsson J, Reilly AO, Cotter E, Culloty SC. A previously undescribed ostreid herpes virus 1 (OsHV-1) genotype detected in the pacific oyster, Crassostrea gigas, in Ireland. Parasitology. 2012 Oct;139(12):1526–32.

100. Martenot C, Fourour S, Oden E, Jouaux A, Travaillé E, Malas JP, Houssin M. Detection of the OsHV-1 µVar in the Pacific oyster Crassostrea gigas before 2008 in France and description of two new microvariants of the Ostreid Herpesvirus 1 (OsHV-1). Aquaculture. 2012 Mar;338–341:293–6.

101. Peeler EJ, Allan Reese R, Cheslett DL, Geoghegan F, Power A, Thrush MA. Investigation of mortality in Pacific oysters associated with Ostreid herpesvirus-1µVar in the Republic of Ireland in 2009. Preventive Veterinary Medicine. 2012 Jun;105(1–2):136–43.

102. Davison AJ, Trus BL, Cheng N, Steven AC, Watson MS, Cunningham C, Deuff RML, Renault T. A novel class of herpesvirus with bivalve hosts. Journal of General Virology. 2005 Jan 1;86(1):41–53.

103. Mazaleyrat A, Normand J, Dubroca L, Fleury E. A 26-year time series of mortality and growth of the Pacific oyster C. gigas recorded along French coasts. Sci Data. 2022 Dec;9(1):392.

104. Martenot C, Gervais O, Chollet B, Houssin M, Renault T. Haemocytes collected from experimentally infected Pacific oysters, Crassostrea gigas: Detection of ostreid herpesvirus 1 DNA, RNA, and proteins in relation with inhibition of apoptosis. Fernández Robledo JA, editor. PLoS ONE. 2017 May 18;12(5):e0177448.

105. Schikorski D, Renault T, Saulnier D, Faury N, Moreau P, Pépin JF. Experimental infection of Pacific oyster Crassostrea gigas spat by ostreid herpesvirus 1: demonstration of oyster spat susceptibility. Vet Res. 2011;42(1):27.

106. Martenot C, Faury N, Morga B, Degremont L, Lamy JB, Houssin M, Renault T. Exploring First Interactions Between Ostreid Herpesvirus 1 (OsHV-1) and Its Host, Crassostrea gigas: Effects of Specific Antiviral Antibodies and Dextran Sulfate. Front Microbiol. 2019 May 24;10:1128.

107. Green TJ, Vergnes A, Montagnani C, de Lorgeril J. Distinct immune responses of juvenile and adult oysters (Crassostrea gigas) to viral and bacterial infections. Vet Res. 2016 Dec;47(1):72.

108. Picot S, Faury N, Pelletier C, Arzul I, Chollet B, Dégremont L, Renault T, Morga B. Monitoring Autophagy at Cellular and Molecular Level in Crassostrea gigas During an Experimental Ostreid Herpesvirus 1 (OsHV-1) Infection. Front Cell Infect Microbiol. 2022 Apr 4;12:858311.

109. Agnew MV, Friedman CS, Langdon C, Divilov K, Schoolfield B, Morga B, Degremont L, Dhar AK, Kirkland P, Dumbauld B, Burge CA. Differential Mortality and High Viral Load in Naive Pacific Oyster Families Exposed to OsHV-1 Suggests Tolerance Rather than Resistance to Infection. Pathogens. 2020 Dec 17;9(12):1057.

110. Burge C, Reece K, Dhar A, Kirkland P, Morga B, Dégremont L, Faury N, Wippel B, MacIntyre A, Friedman C. First comparison of French and Australian OsHV-1 µvars by bath exposure. Dis Aquat Org. 2020 Mar 12;138:137–44.

111. Burge CA, Friedman CS. Quantifying Ostreid Herpesvirus (OsHV-1) Genome Copies and Expression during Transmission. Microb Ecol. 2012 Apr;63(3):596–604.

112. Martenot C, Oden E, Travaillé E, Malas JP, Houssin M. Comparison of two real-time PCR methods for detection of ostreid herpesvirus 1 in the Pacific oyster Crassostrea gigas. Journal of Virological Methods. 2010 Dec;170(1–2):86–9.

113. Petton B, Pernet F, Robert R, Boudry P. Temperature influence on pathogen transmission and subsequent mortalities in juvenile Pacific oysters Crassostrea gigas. Aquacult Environ Interact. 2013 Jun 4;3(3):257–73.

114. de Kantzow M, Hick P, Becker J, Whittington R. Effect of water temperature on mortality of Pacific oysters Crassostrea gigas associated with microvariant ostreid herpesvirus 1 (OsHV-1 µVar). Aquacult Environ Interact. 2016 Aug 3;8:419–28.

115. Pernet F, Tamayo D, Petton B. Influence of low temperatures on the survival of the Pacific oyster (Crassostrea gigas) infected with ostreid herpes virus type 1. Aquaculture. 2015 Aug;445:57–62.

116. Delisle L, Petton B, Burguin JF, Morga B, Corporeau C, Pernet F. Temperature modulate disease susceptibility of the Pacific oyster Crassostrea gigas and virulence of the Ostreid herpesvirus type 1. Fish & Shellfish Immunology. 2018 Sep;80:71–9.

117. Pathirana E, Whittington RJ, Hick PM. Impact of seawater temperature on the Pacific oyster (Crassostrea gigas) microbiome and susceptibility to disease associated with Ostreid herpesvirus-1 (OsHV-1). Watt L, editor. Anim Prod Sci. 2022 May 26;62(11):1040–54.

118. Wiltshire KH. Ecophysiological tolerances of the Pacific oyster, Crassostreagigas, with regard to the potential spread of populations in South Australian waters. South Australian Research and Development Institute (Aquatic Sciences); 2007 p. 29. (SARDI Research Report Series Number 222). Report No.: F2007/000499-1.

119. Green TJ, Montagnani C, Benkendorff K, Robinson N, Speck P. Ontogeny and water temperature influences the antiviral response of the Pacific oyster, Crassostrea gigas. Fish & Shellfish Immunology. 2014 Jan;36(1):151–7.

120. Burge CA, Shore-Maggio A, Rivlin ND. Ecology of Emerging Infectious Diseases of Invertebrates. In: Hajek AE, editor. Ecology of Invertebrate Diseases [Internet]. Dordrecht: Springer Netherlands; 2017 [cited 2023 May 30]. p. 587–625. Available from: https://link.springer.com/10.1007/978-94-017-3284-0

121. Dégremont L, Garcia C, Allen SK. Genetic improvement for disease resistance in oysters: A review. Journal of Invertebrate Pathology. 2015 Oct;131:226–41.

122. Divilov K, Schoolfield B, Morga B, Dégremont L, Burge CA, Mancilla Cortez D, Friedman CS, Fleener GB, Dumbauld BR, Langdon C. First evaluation of resistance to both a California OsHV-1 variant and a French OsHV-1 microvariant in Pacific oysters. BMC Genet. 2019 Dec;20(1):96.

123. Divilov K, Schoolfield B, Mancilla Cortez D, Wang X, Fleener GB, Jin L, Dumbauld BR, Langdon C. Genetic improvement of survival in Pacific oysters to the Tomales Bay strain of OsHV-1 over two cycles of selection. Aquaculture. 2021 Oct;543:737020.

124. Rodgers C, Arzul I, Carrasco N, Furones Nozal D. A literature review as an aid to identify strategies for mitigating ostreid herpesvirus 1 in *Crassostrea gigas* hatchery and nursery systems. Reviews in Aquaculture. 2019 Aug;11(3):565–85.

125. Clerissi C, Luo X, Lucasson A, Mortaza S, De Lorgeril J, Toulza E, Petton B, Escoubas JM, Dégremont L, Gueguen Y, Destoumieux-Garzón D, Jacq A, Mitta G. A core of functional complementary bacteria infects oysters in Pacific Oyster Mortality Syndrome. anim microbiome. 2023 May 3;5(1):26.

126. Delisle L, Laroche O, Hilton Z, Burguin JF, Rolton A, Berry J, Pochon X, Boudry P, Vignier J. Understanding the dynamic of POMS infection and the role of microbiota composition in the survival of Pacific oysters, Crassostrea gigas. [Internet]. 2022 [cited 2022 Jun 16]. Available from: https://www.researchsquare.com

127. Oyanedel D, Lagorce A, Bruto M, Haffner P, Morot A, Labreuche Y, Dorant Y, De La Forest Divonne S, Delavat F, Inguimbert N, Montagnani C, Morga B, Toulza E, Chaparro C, Escoubas JM, Gueguen Y, Vidal-Dupiol J, De Lorgeril J, Petton B, Degremont L, Tourbiez D, Pimparé LL, Leroy M, Romatif O, Pouzadoux J, Mitta G, Le Roux F, Charrière GM, Travers MA, Destoumieux-Garzón D. Cooperation and cheating orchestrate Vibrio assemblages and polymicrobial synergy in oysters infected with OsHV-1 virus. Proc Natl Acad Sci USA. 2023 Oct 3;120(40):e2305195120.

128. Petton B, de Lorgeril J, Mitta G, Daigle G, Pernet F, Alunno-Bruscia M. Fine-scale temporal dynamics of herpes virus and vibrios in seawater during a polymicrobial infection in the Pacific oyster Crassostrea gigas. Dis Aquat Org. 2019 Jul 25;135(2):97–106.

129. Apprill A, McNally S, Parsons R, Weber L. Minor revision to V4 region SSU rRNA 806R gene primer greatly increases detection of SAR11 bacterioplankton. Aquat Microb Ecol. 2015 Jun 4;75(2):129–37.

130. Kaplan EL, Meier P. Nonparametric Estimation from Incomplete Observations. Journal of the American Statistical Association. 1958;53(282):26.

131. Therneau TM. _A Package for Survival Analysis in R_ [Internet]. 2023. Available from: <https://CRAN.R-project.org/package=survival>

132. Therneau TM, Grambsch PM. _Modeling Survival Data: Extending the Cox Model_. New York: Springer; 2000.

133. Callahan BJ, McMurdie PJ, Rosen MJ, Han AW, Johnson AJA, Holmes SP. DADA2: High-resolution sample inference from Illumina amplicon data. Nat Methods. 2016 Jul;13(7):581–3.

134. McDonald D, Jiang Y, Balaban M, Cantrell K, Zhu Q, Gonzalez A, Morton JT, Nicolaou G, Parks DH, Karst SM, Albertsen M, Hugenholtz P, DeSantis T, Song SJ, Bartko A, Havulinna AS, Jousilahti P, Cheng S, Inouye M, Niiranen T, Jain M, Salomaa V, Lahti L, Mirarab S, Knight R. Greengenes2 unifies microbial data in a single reference tree. Nat Biotechnol [Internet]. 2023 Jul 27 [cited 2024 Jan 19]; Available from: https://www.nature.com/articles/s41587-023-01845-1

135. McMurdie PJ, Holmes S. phyloseq: An R Package for Reproducible Interactive Analysis and Graphics of Microbiome Census Data. Watson M, editor. PLoS ONE. 2013 Apr 22;8(4):e61217.

136. Gauthier J, Derome N. Evenness-Richness Scatter Plots: a Visual and Insightful Representation of Shannon Entropy Measurements for Ecological Community Analysis. Rodrigues JM, editor. mSphere. 2021 Apr 28;6(2):e01019-20.

137. Lin H, Peddada SD. Analysis of compositions of microbiomes with bias correction. Nat Commun. 2020 Jul 14;11(1):3514.

138. Liaw A, Wiener M. Classification and Regression by randomForest. R News. 2002;2(3):18–22.

139. Burge CA, Mark Eakin C, Friedman CS, Froelich B, Hershberger PK, Hofmann EE, Petes LE, Prager KC, Weil E, Willis BL, Ford SE, Harvell CD. Climate Change Influences on Marine Infectious Diseases: Implications for Management and Society. Annu Rev Mar Sci. 2014 Jan 3;6(1):249–77.

140. Harvell CD, Kim K, Burkholder JM, Colwell RR, Epstein PR, Grimes DJ, Hofmann EE, Lipp EK, Osterhaus ADME, Overstreet RM, Porter JW, Smith GW, Vasta GR. Emerging Marine Diseases--Climate Links and Anthropogenic Factors. Science. 1999 Sep 3;285(5433):1505–10.

141. Harvell CD, Mitchell CE, Ward JR, Altizer S, Dobson AP, Ostfeld RS, Samuel MD. Climate Warming and Disease Risks for Terrestrial and Marine Biota. Science. 2002 Jun 21;296(5576):2158–62.

142. Petton B, Alunno-Bruscia M, Mitta G, Pernet F. Increased growth metabolism promotes viral infection in a susceptible oyster population. Aquacult Environ Interact. 2023 Feb 2;15:19–33.

143. Friedman C, Estes R, Stokes N, Burge C, Hargove J, Barber B, Elston R, Burreson E, Reece K. Herpes virus in juvenile Pacific oysters Crassostrea gigas from Tomales Bay, California, coincides with summer mortality episodes. Dis Aquat Org. 2005;63:33–41.

144. Delisle L, Pauletto M, Vidal-Dupiol J, Petton B, Bargelloni L, Montagnani C, Pernet F, Corporeau C, Fleury E. High temperature induces transcriptomic changes in *Crassostrea gigas* that hinders progress of Ostreid herpesvirus (OsHV-1) and promotes survival. Journal of Experimental Biology. 2020 Jan 1;jeb.226233.

145. Petton B, Bruto M, James A, Labreuche Y, Alunno-Bruscia M, Le Roux F. Crassostrea gigas mortality in France: the usual suspect, a herpes virus, may not be the killer in this polymicrobial opportunistic disease. Front Microbiol [Internet]. 2015 Jul 6 [cited 2024 Feb 26];6. Available from: http://journal.frontiersin.org/Article/10.3389/fmicb.2015.00686/abstract

146. Hick PM, Evans O, Rubio A, Dhand NK, Whittington RJ. Both age and size influence susceptibility of Pacific oysters (Crassostrea gigas) to disease caused by Ostreid herpesvirus -1 (OsHV-1) in replicated field and laboratory experiments. Aquaculture. 2018 Mar;489:110–20.

147. de Lorgeril J, Escoubas JM, Loubiere V, Pernet F, Le Gall P, Vergnes A, Aujoulat F, Jeannot JL, Jumas-Bilak E, Got P, Gueguen Y, Destoumieux-Garzón D, Bachère E. Inefficient immune response is associated with microbial permissiveness in juvenile oysters affected by mass mortalities on field. Fish & Shellfish Immunology. 2018 Jun;77:156–63.

148. Chen H, Wang M, Yang C, Wan X, Ding HH, Shi Y, Zhao C. Bacterial spoilage profiles in the gills of Pacific oysters (Crassostrea gigas) and Eastern oysters (C. virginica) during refrigerated storage. Food Microbiology. 2019 Sep;82:209–17.

149. Metcalf JL, Xu ZZ, Weiss S, Lax S, Van Treuren W, Hyde ER, Song SJ, Amir A, Larsen P, Sangwan N, Haarmann D, Humphrey GC, Ackermann G, Thompson LR, Lauber C, Bibat A, Nicholas C, Gebert MJ, Petrosino JF, Reed SC, Gilbert JA, Lynne AM, Bucheli SR, Carter DO, Knight R. Microbial community assembly and metabolic function during mammalian corpse decomposition. Science. 2016 Jan 8;351(6269):158–62.

150. Friedman C, Wight N, Crosson L, White S, Strenge R. Validation of a quantitative PCR assay for detection and quantification of ‘Candidatus Xenohaliotis californiensis.’ Dis Aquat Org. 2014 Apr 3;108(3):251–9.

151. Chivian D, Jungbluth SP, Dehal PS, Wood-Charlson EM, Canon RS, Allen BH, Clark MM, Gu T, Land ML, Price GA, Riehl WJ, Sneddon MW, Sutormin R, Zhang Q, Cottingham RW, Henry CS, Arkin AP. Metagenome-assembled genome extraction and analysis from microbiomes using KBase. Nat Protoc. 2023 Jan;18(1):208–38.

152. Bolger AM, Lohse M, Usadel B. Trimmomatic: a flexible trimmer for Illumina sequence data. Bioinformatics. 2014 Aug 1;30(15):2114–20.

153. Nurk S, Meleshko D, Korobeynikov A, Pevzner PA. metaSPAdes: a new versatile metagenomic assembler. Genome Res. 2017 May;27(5):824–34.

154. Wu YW, Simmons BA, Singer SW. MaxBin 2.0: an automated binning algorithm to recover genomes from multiple metagenomic datasets. Bioinformatics. 2016 Feb 15;32(4):605–7.

155. Kang DD, Li F, Kirton E, Thomas A, Egan R, An H, Wang Z. MetaBAT 2: an adaptive binning algorithm for robust and efficient genome reconstruction from metagenome assemblies. PeerJ. 2019 Jul 26;7:e7359.

156. Alneberg J, Bjarnason BS, De Bruijn I, Schirmer M, Quick J, Ijaz UZ, Lahti L, Loman NJ, Andersson AF, Quince C. Binning metagenomic contigs by coverage and composition. Nat Methods. 2014 Nov;11(11):1144–6.

157. Sieber CMK, Probst AJ, Sharrar A, Thomas BC, Hess M, Tringe SG, Banfield JF. Recovery of genomes from metagenomes via a dereplication, aggregation and scoring strategy. Nat Microbiol. 2018 May 28;3(7):836–43.

158. Lee I, Chalita M, Ha SM, Na SI, Yoon SH, Chun J. ContEst16S: an algorithm that identifies contaminated prokaryotic genomes using 16S RNA gene sequences. International Journal of Systematic and Evolutionary Microbiology. 2017 Jun 1;67(6):2053–7.

159. Vallenet D, Calteau A, Dubois M, Amours P, Bazin A, Beuvin M, Burlot L, Bussell X, Fouteau S, Gautreau G, Lajus A, Langlois J, Planel R, Roche D, Rollin J, Rouy Z, Sabatet V, Médigue C. MicroScope: an integrated platform for the annotation and exploration of microbial gene functions through genomic, pangenomic and metabolic comparative analysis. Nucleic Acids Research. 2019 Oct 24;gkz926.

160. Parks DH, Imelfort M, Skennerton CT, Hugenholtz P, Tyson GW. CheckM: assessing the quality of microbial genomes recovered from isolates, single cells, and metagenomes. Genome Res. 2015 Jul;25(7):1043–55.

161. Friedman CS, Andree KB, Beauchamp KA, Moore JD, Robbins TT, Shields JD, Hedrick RP. “Candidatus Xenohaliotis californiensis”, a newly described pathogen of abalone, Haliotis spp., along the west coast of North America. International Journal of Systematic and Evolutionary Microbiology. 2000 Mar 1;50(2):847–55.

162. Crosson L, Wight N, VanBlaricom G, Kiryu I, Moore J, Friedman C. Abalone withering syndrome: distribution, impacts, current diagnostic methods and new findings. Dis Aquat Org. 2014 Apr 3;108(3):261–70.

163. Salje J. Cells within cells: Rickettsiales and the obligate intracellular bacterial lifestyle. Nat Rev Microbiol. 2021 Jun;19(6):375–90.

164. Cruz-Flores R, Cáceres-Martínez J, Del Río-Portilla MÁ, Licea-Navarro AF, Gonzales-Sánchez R, Guerrero A. Complete genome sequence of a phage hyperparasite of Candidatus Xenohaliotis californiensis (Rickettsiales) – a pathogen of Haliotis spp (Gasteropoda). Arch Virol. 2018 Apr;163(4):1101–4.

165. Friedman CS, Wight N, Crosson LM, VanBlaricom GR, Lafferty KD. Reduced disease in black abalone following mass mortality: phage therapy and natural selection. Front Microbiol [Internet]. 2014 Mar 18 [cited 2023 Dec 1];5. Available from: http://journal.frontiersin.org/article/10.3389/fmicb.2014.00078/abstract

166. Moore JD, Byron SN, Marshman BC, Snider JP. An oxytetracycline bath protocol to eliminate the agent of withering syndrome, Candidatus Xenohaliotis californiensis, in captive abalone populations. Aquaculture. 2019 Mar;503:267–74.

167. Davis GE, Haaker PL, Richards DV. The perilous condition of white abalone Haliotis sorenseni, Bartsch, 1940. J Shellfish Res. 1998;(17):871–5.

168. Vater A, Byrne BA, Marshman BC, Ashlock LW, Moore JD. Differing responses of red abalone (*Haliotis rufescens*) and white abalone (*H. sorenseni*) to infection with phage-associated *Candidatus* Xenohaliotis californiensis. PeerJ. 2018 Jun 25;6:e5104.

169. Friedman CS, Scott BB, Strenge RE, Vadopalas B, Mccormick TB. Oxytetracycline as a tool to manage and prevent losses of the endangered white abalone, Haliotis sorenseni, caused by withering syndrome. Journal of Shellfish Research. 2007 Sep;26(3):877–85.

170. Frederick AR, Heras J, Friedman CS, German DP. Withering syndrome induced gene expression changes and a de-novo transcriptome for the Pinto abalone, Haliotis kamtschatkana. Comparative Biochemistry and Physiology Part D: Genomics and Proteomics. 2022 Mar;41:100930.

171. Fang Y, Yang X, Zhang S, Chen X, Lin G, Zhang Y, Wang M, Li M. Transcriptome study on immune response against Vibrio parahaemolyticus challenge in gill of abalone Haliotis discus hannai Ino. Front Mar Sci. 2022 Jul 27;9:956317.

172. Hooper C, Day R, Slocombe R, Handlinger J, Benkendorff K. Stress and immune responses in abalone: Limitations in current knowledge and investigative methods based on other models. Fish & Shellfish Immunology. 2007 Apr;22(4):363–79.

173. Yao T, Lu J, Bai C, Xie Z, Ye L. The Enhanced Immune Protection in Small Abalone Haliotis diversicolor Against a Secondary Infection With Vibrio harveyi. Front Immunol. 2021 Jul 6;12:685896.

174. Marotz C, Belda-Ferre P, Ali F, Das P, Huang S, Cantrell K, Jiang L, Martino C, Diner RE, Rahman G, McDonald D, Armstrong G, Kodera S, Donato S, Ecklu-Mensah G, Gottel N, Salas Garcia MC, Chiang LY, Salido RA, Shaffer JP, Bryant MK, Sanders K, Humphrey G, Ackermann G, Haiminen N, Beck KL, Kim HC, Carrieri AP, Parida L, Vázquez-Baeza Y, Torriani FJ, Knight R, Gilbert J, Sweeney DA, Allard SM. SARS-CoV-2 detection status associates with bacterial community composition in patients and the hospital environment. Microbiome. 2021 Dec;9(1):132.

175. Thompson LR, Sanders JG, McDonald D, Amir A, Ladau J, Locey KJ, Prill RJ, Tripathi A, Gibbons SM, Ackermann G, Navas-Molina JA, Janssen S, Kopylova E, Vázquez-Baeza Y, González A, Morton JT, Mirarab S, Zech Xu Z, Jiang L, Haroon MF, Kanbar J, Zhu Q, Jin Song S, Kosciolek T, Bokulich NA, Lefler J, Brislawn CJ, Humphrey G, Owens SM, Hampton-Marcell J, Berg-Lyons D, McKenzie V, Fierer N, Fuhrman JA, Clauset A, Stevens RL, Shade A, Pollard KS, Goodwin KD, Jansson JK, Gilbert JA, Knight R, The Earth Microbiome Project Consortium, Rivera JLA, Al-Moosawi L, Alverdy J, Amato KR, Andras J, Angenent LT, Antonopoulos DA, Apprill A, Armitage D, Ballantine K, Bárta J, Baum JK, Berry A, Bhatnagar A, Bhatnagar M, Biddle JF, Bittner L, Boldgiv B, Bottos E, Boyer DM, Braun J, Brazelton W, Brearley FQ, Campbell AH, Caporaso JG, Cardona C, Carroll J, Cary SC, Casper BB, Charles TC, Chu H, Claar DC, Clark RG, Clayton JB, Clemente JC, Cochran A, Coleman ML, Collins G, Colwell RR, Contreras M, Crary BB, Creer S, Cristol DA, Crump BC, Cui D, Daly SE, Davalos L, Dawson RD, Defazio J, Delsuc F, Dionisi HM, Dominguez-Bello MG, Dowell R, Dubinsky EA, Dunn PO, Ercolini D, Espinoza RE, Ezenwa V, Fenner N, Findlay HS, Fleming ID, Fogliano V, Forsman A, Freeman C, Friedman ES, Galindo G, Garcia L, Garcia-Amado MA, Garshelis D, Gasser RB, Gerdts G, Gibson MK, Gifford I, Gill RT, Giray T, Gittel A, Golyshin P, Gong D, Grossart HP, Guyton K, Haig SJ, Hale V, Hall RS, Hallam SJ, Handley KM, Hasan NA, Haydon SR, Hickman JE, Hidalgo G, Hofmockel KS, Hooker J, Hulth S, Hultman J, Hyde E, Ibáñez-Álamo JD, Jastrow JD, Jex AR, Johnson LS, Johnston ER, Joseph S, Jurburg SD, Jurelevicius D, Karlsson A, Karlsson R, Kauppinen S, Kellogg CTE, Kennedy SJ, Kerkhof LJ, King GM, Kling GW, Koehler AV, Krezalek M, Kueneman J, Lamendella R, Landon EM, Lane-deGraaf K, LaRoche J, Larsen P, Laverock B, Lax S, Lentino M, Levin II, Liancourt P, Liang W, Linz AM, Lipson DA, Liu Y, Lladser ME, Lozada M, Spirito CM, MacCormack WP, MacRae-Crerar A, Magris M, Martín-Platero AM, Martín-Vivaldi M, Martínez LM, Martínez-Bueno M, Marzinelli EM, Mason OU, Mayer GD, McDevitt-Irwin JM, McDonald JE, McGuire KL, McMahon KD, McMinds R, Medina M, Mendelson JR, Metcalf JL, Meyer F, Michelangeli F, Miller K, Mills DA, Minich J, Mocali S, Moitinho-Silva L, Moore A, Morgan-Kiss RM, Munroe P, Myrold D, Neufeld JD, Ni Y, Nicol GW, Nielsen S, Nissimov JI, Niu K, Nolan MJ, Noyce K, O'Brien SL, Okamoto N, Orlando L, Castellano YO, Osuolale O, Oswald W, Parnell J, Peralta-Sánchez JM, Petraitis P, Pfister C, Pilon-Smits E, Piombino P, Pointing SB, Pollock FJ, Potter C, Prithiviraj B, Quince C, Rani A, Ranjan R, Rao S, Rees AP, Richardson M, Riebesell U, Robinson C, Rockne KJ, Rodriguezl SM, Rohwer F, Roundstone W, Safran RJ, Sangwan N, Sanz V, Schrenk M, Schrenzel MD, Scott NM, Seger RL, Seguin-Orlando A, Seldin L, Seyler LM, Shakhsheer B, Sheets GM, Shen C, Shi Y, Shin H, Shogan BD, Shutler D, Siegel J, Simmons S, Sjöling S, Smith DP, Soler JJ, Sperling M, Steinberg PD, Stephens B, Stevens MA, Taghavi S, Tai V, Tait K, Tan CL, Tas¸ N, Taylor DL, Thomas T, Timling I, Turner BL, Urich T, Ursell LK, Van Der Lelie D, Van Treuren W, Van Zwieten L, Vargas-Robles D, Thurber RV,

Vitaglione P, Walker DA, Walters WA, Wang S, Wang T, Weaver T, Webster NS, Wehrle B, Weisenhorn P, Weiss S, Werner JJ, West K, Whitehead A, Whitehead SR, Whittingham LA, Willerslev E, Williams AE, Wood SA, Woodhams DC, Yang Y, Zaneveld J, Zarraonaindia I, Zhang Q, Zhao H. A communal catalogue reveals Earth's multiscale microbial diversity. Nature. 2017 Nov 23;551(7681):457–63.

176. Marotz C, Sharma A, Humphrey G, Gottel N, Daum C, Gilbert JA, Eloe-Fadrosh E, Knight R. Triplicate PCR reactions for 16S rRNA gene amplicon sequencing are unnecessary. BioTechniques. 2019 Jul;67(1):29–32.

177. Rognes T, Flouri T, Nichols B, Quince C, Mahé F. VSEARCH: a versatile open source tool for metagenomics. PeerJ. 2016 Oct 18;4:e2584.

178. Lozupone C, Lladser ME, Knights D, Stombaugh J, Knight R. UniFrac: an effective distance metric for microbial community comparison. The ISME Journal. 2011 Feb 1;5(2):169–72.

179. Bisanz JE. qiime2R: Importing QIIME2 artifacts and associated data into R sessions. unpublished [Internet]. 2018; Available from: https://github.com/jbisanz/qiime2R

180. Mallick H, Rahnavard A, McIver LJ, Ma S, Zhang Y, Nguyen LH, Tickle TL, Weingart G, Ren B, Schwager EH, Chatterjee S, Thompson KN, Wilkinson JE, Subramanian A, Lu Y, Waldron L, Paulson JN, Franzosa EA, Bravo HC, Huttenhower C. Multivariable association discovery in population-scale meta-omics studies. Coelho LP, editor. PLoS Comput Biol. 2021 Nov 16;17(11):e1009442.

181. Wickham H. ggplot2: Elegant Graphics for Data Analysis. Springer-Verlag New York ISBN 978-3-319-24277-4, [Internet]. 2016; Available from: https://ggplot2.tidyverse.org

182. Vázquez-Baeza Y, Pirrung M, Gonzalez A, Knight R. EMPeror: a tool for visualizing high-throughput microbial community data. GigaSci. 2013 Dec;2(1):16.

183. Barnett D, Arts I, Penders J. microViz: an R package for microbiome data visualization and statistics. JOSS. 2021 Jul 10;6(63):3201.

184. Faith DP. Conservation evaluation and phylogenetic diversity. Biological Conservation. 1992;61(1):1–10.

185. Menzel P, Ng KL, Krogh A. Fast and sensitive taxonomic classification for metagenomics with Kaiju. Nat Commun. 2016 Apr 13;7(1):11257.

186. Chen S, Zhou Y, Chen Y, Gu J. fastp: an ultra-fast all-in-one FASTQ preprocessor. Bioinformatics. 2018 Sep 1;34(17):i884–90.

187. Andrews S. FastQC: a quality control tool for high throughput sequence data [Internet]. 2010. Available from: Available online at: http://www.bioinformatics.babraham.ac.uk/projects/fastqc

188. Grabherr MG, Haas BJ, Yassour M, Levin JZ, Thompson DA, Amit I, Adiconis X, Fan L, Raychowdhury R, Zeng Q, Chen Z, Mauceli E, Hacohen N, Gnirke A, Rhind N, Di Palma F, Birren BW, Nusbaum C, Lindblad-Toh K, Friedman N, Regev A. Full-length transcriptome assembly from RNA-Seq data without a reference genome. Nat Biotechnol. 2011 Jul;29(7):644–52.

189. Li B, Dewey CN. RSEM: accurate transcript quantification from RNA-Seq data with or without a reference genome. 2011;

190. Bryant DM, Johnson K, DiTommaso T, Tickle T, Couger MB, Payzin-Dogru D, Lee TJ, Leigh ND, Kuo TH, Davis FG, Bateman J, Bryant S, Guzikowski AR, Tsai SL, Coyne S, Ye WW, Freeman RM, Peshkin L, Tabin CJ, Regev A, Haas BJ, Whited JL. A Tissue-Mapped Axolotl De Novo Transcriptome Enables Identification of Limb Regeneration Factors. Cell Reports. 2017 Jan;18(3):762–76.

191. Love MI, Huber W, Anders S. Moderated estimation of fold change and dispersion for RNA-seq data with DESeq2. Genome Biol. 2014 Dec;15(12):550.

192. Bardou P, Mariette J, Escudié F, Djemiel C, Klopp C. jvenn: an interactive Venn diagram viewer. BMC Bioinformatics. 2014 Dec;15(1):293.

193. Griffin TW, Baer JG, Ward JE. Direct Comparison of Fecal and Gut Microbiota in the Blue Mussel (Mytilus edulis) Discourages Fecal Sampling as a Proxy for Resident Gut Community. Microb Ecol. 2021 Jan;81(1):180–92.

194. Wang X, Tang B, Luo X, Ke C, Huang M, You W, Wang Y. Effects of temperature, diet and genotype-induced variations on the gut microbiota of abalone. Aquaculture. 2020 Jul;524:735269.

195. Hyun DW, Kim MS, Shin NR, Kim JY, Kim PS, Whon TW, Yun JH, Bae JW. Shimia haliotis sp. nov., a bacterium isolated from the gut of an abalone, Haliotis discus hannai. International Journal of Systematic and Evolutionary Microbiology. 2013 Nov 1;63(Pt_11):4248–53.

196. Gobet A, Mest L, Perennou M, Dittami SM, Caralp C, Coulombet C, Huchette S, Roussel S, Michel G, Leblanc C. Seasonal and algal diet-driven patterns of the digestive microbiota of the European abalone Haliotis tuberculata, a generalist marine herbivore. Microbiome. 2018 Dec;6(1):60.

197. Moore JD, Robbins TT, Friedman CS. Withering Syndrome in Farmed Red Abalone Haliotis rufescens: Thermal Induction and Association with a Gastrointestinal Rickettsiales-like Prokaryote. 2000 Jun;9.

198. Garcia-Esquivel Z, Felbeck H. Activity of digestive enzymes along the gut of juvenile red abalone, Haliotis rufescens, fed natural and balanced diets. Aquaculture. 2006 Nov;261(2):615–25.

199. Kemp R. The effect of diet on intestinal structure and function in the abalone (Haliotis laevegata). University of Adelaide; 2001.

200. Kunselman E, Minich JJ, Horwith M, Gilbert JA, Allen EE. Variation in Survival and Gut Microbiome Composition of Hatchery-Grown Native Oysters at Various Locations within the Puget Sound. Kormas KA, editor. Microbiol Spectr. 2022 Jun 29;10(3):e01982-21.